Male Pregnancy in the Seahorse (*Hippocampus abdominalis*): Investigating the Genetic Regulation of a Complex Reproductive Trait

---

Dissertation

zur

Erlangung der naturwissenschaftlichen Doktorwürde
(Dr. sc. nat.)

vorgelegt der

Mathematisch-naturwissenschaftlichen Fakultät

der

Universität Zürich

von

Kai Nikolas Stölting

aus

Deutschland

Promotionskomitee

Prof. Dr. Anthony B. Wilson (Vorsitz und Leitung der Promotion)

Prof. Dr. Andreas Wagner

Prof. Dr. Tadeusz Kawecki

Zürich, 2010

TABLE OF CONTENTS

SUMMARY

Seahorses and pipefish are characterized by different forms of male pregnancy, a complex morphological and physiological process akin a mammalian pregnancy. The genetic regulation of this complex trait, however, is unknown, complicating our efforts to understand how this trait has evolved. To permit such studies, the processes of male pregnancy have been reviewed, and the genes of male pregnancy have been identified using cDNA-AFLP based differential displays and next generation sequencing technology. Initial efforts to identify gene expression differences during male pregnancy using a novel cDNA-AFLP endlabelling protocol proved unsuccessful, and an extensive eukaryote-wide computer-based optimization study was undertaken to optimize the cDNA-AFLP methodology for species in which genome data are unavailable. Next generation sequencing was ultimately used to identify the genes of male pregnancy. More than 38,000 cDNA fragments have been sequenced and annotated wherever possible. Hundreds of genes up- and downregulated during male pregnancy were identified, and major gene functions have been associated with these genes. As a result, a more circumspect picture of both processes and the genes involved in male pregnancy in the seahorse is available.

This thesis is structured into four chapters. Chapters I and III have been published in peer reviewed international journals. Chapters II and IV are being prepared for submission.

Chapter I

We reviewed the processes of mammalian pregnancy and the male pregnancy of seahorses and pipefish (syngnathid fishes) as a basis for further studies on the evolution of male pregnancy. During male pregnancy, syngnathid males incubate developing embryos in a specialized brooding structure, the brood pouch, in which they are aerated, osmoregulated, protected and likely also provisioned during development. Direct comparisons of the syngnathid male pregnancy with other forms of viviparity strongly suggests parallels in physiology, morphology and genetic changes, and a review of recent advances on syngnathid pregnancy highlights similarities and differences between seahorse and

mammalian pregnancy. This comparison is the foundation to further studies on the evolution of a complex trait, the male pregnancy.

Chapter II

Amplified fragment length polymorphisms (AFLP) are a widely used fingerprinting tool, which can be used in high-throughput AFLP protocols which require the incorporation of fluorescently-labelled oligonucleotides. Large numbers of fragments can thus be rapidly screened on automated DNA sequencing machines. The per-marker costs are comparably low for AFLPs, but the key element for high-throughput approaches, the fluorescently-labelled oligonucleotide, remain costly. In reducing this fraction of the experimental setup by implementing fluorescent endlabelling of AFLPs, this tool will be even more accessible for laboratories with reduced budgets. The endlabelling alternative presented here benefits from statistical analyses which indicate that the standard fluorescent AFLPs and the novel endlabelled alternatives produce comparable results. However, given the differences in the size and numbers of fragments generated with the two methods, we do not recommend to combine partial data generated with both approaches. Given the considerably reduced setup costs and comparable performance, we suggest that researchers commencing a new AFLP project use endlabelled AFLPs instead of traditional fluorescent AFLPs.

Chapter III

Differentially expressed genes can be detected using the AFLP methodology on complementary DNA through the correlation of trait expression with cDNA expression profiles. However, given the methodological complexity of the AFLP approach and the taxonomic diversity of organisms typically studied with AFLPs, the optimal design of such approaches can vary from species to species. In modeling and optimizing the cDNA-AFLP assay design for all eukaryotic species, we identify factors which can substantially increase the quality of cDNA-AFLP experiments in any eukaryotic species. Factors revealed by *in silico* simulations on 92 species covering most major eukaryotic group include the choice of individual restriction enzymes substantially affecting screen quality. While some evidence of phylogenetic signal in the cDNA-pool coverage is present, this signal is largely mediated by organismal GC content, a second key factor

affecting the quality of a screen. In optimizing cDNA-AFLP on a broad sample, a strict linear relationship between the number of fragments screened per selective AFLP-PCR reaction and the size of the underlying cDNA pool is detected. This allows to estimate the number of genes expressed in a target tissue, an application that should be invaluable as next-generation sequencing technologies are adapted for differential display.

Chapter IV

Studies on the evolution of reproductive complexity have been complicated by an absence of transitional forms. Syngnathid fishes are an ideal model for such investigations, as extant species exhibit a wide diversity of rudimentary and more complex form of male pregnancy. Unfortunately, little is known about the genetic regulation of male pregnancy in syngnathid fishes, and knowledge on the genes associated with pregnancy is key to undertaking comparative evolutionary studies investigating the origins of this mode of reproduction. We assembled the first reference transcriptome for the seahorse, consisting of 38,419 contigs representing more than 30,000 different cDNAs. Functional annotations of approximately 27% of these contigs allow the first comprehensive view of seahorse gene functions, biological processes and cellular localizations during the pregnancy process. In a comparative transcriptome screen of pregnant and non-pregnant individuals, hundreds of genes were identified and annotated which are differentially expressed during male pregnancy. None of the different annotation classes however, indicate significant differences in the representation of genes from pregnant and non-pregnant brood pouch tissues. Our study also quantified the effects of cDNA normalization on gene discovery, and shows clearly that normalization is essential in studies that aim for a full representation of the transcriptome. The assembly of the seahorse transcriptome will be used in the construction of a microarray for the comparative analysis of gene expression during pregnancy in other syngnathids and represents a critical first key step towards understanding the evolution of this complex trait.

ZUSAMMENFASSUNG

Alle Seepferdchen und Seenadeln besitzen verschiedene Formen männlicher Schwangerschaft. Männliche Schwangerschaft ist ein komplexer morphologischer und physiologischer Prozess ähnlich der Schwangerschaft bei Säugetieren. Die genetische Kodierung dieses komplexen Merkmals aber ist praktisch unbekannt, was detaillierte Studien zur Evolution dieses Merkmales beträchtlich behindert. Um künftig solche Studien zu ermöglichen, wurde bereits bekanntes Wissen über die beteiligten Prozesse in Form eines Reviews zusammengetragen. Ausserdem wurden die an der Schwangerschaft beteiligten Gene mittels differentieller cDNA-AFLP-Analysen und neuer Sequenziermethoden ermittelt. Anfängliche Versuche, Unterschiede in der Genexpression während der männlichen Schwangerschaft mittels eines neuen cDNA-AFLP-Ansatzes zu identifizieren, schlugen fehl. Eine umfassende computerbasierte Optimierung wurde unternommen, um cDNA-AFLPs für sämtliche Eukaryoten zu optimieren, für die genomische Daten nicht verfügbar sind. Neue Sequenziermethoden wurden schliesslich eingesetzt, um die an der männlichen Schwangerschaft beteiligten Gene zu identifizieren. Mehr als 38.000 cDNA- Fragmente konnten sequenziert werden und wurden soweit möglich auch annotiert. Hunderte von während der Schwangerschaft herauf- oder herabregulierten Genen wurden identifiziert. Mit Hilfe der vorliegenden Arbeit entstand ein umfassenderes Bild sowohl von den Prozessen der männlichen Schwangerschaft als auch den an der Schwangerschaft der Seepferdchen beteiligten Gene.

Die vorliegende Arbeit ist in vier Kapitel unterteilt. Kapitel I und III wurden bereits in der internationalen, kritisch begutachteten Fachpresse publiziert. Die Kapitel II und IV sind in Vorbereitung zur Publikation.

Kapitel I

Als Grundlage für weitergehende Studien zur Evolution der männlichen Schwangerschaft wurden die Vorgänge bei männlicher Schwangerschaft der Seepferdchen und Seenadeln (syngnathide Fische) mit denen der Schwangerschaft der Säugetiere zusammengetragen und verglichen. Bei den syngnathiden Fischen trägt das Männchen die sich entwickelnden Jungtiere in

spezialisierten Brutstrukturen aus, in denen die Jungtiere geschützt, osmoreguliert und mit Sauerstoff versorgt werden. Es ist wahrscheinlich, dass das Männchen die Jungtiere während ihrer Entwicklung auch mit Nährstoffen versorgt. Direkte Vergleiche von männlicher Schwangerschaft bei syngnathiden Fischen mit anderen Formen der Lebendgeburt zeigen Parallelen in der Physiologie, der Morphologie und auch in den Veränderungen in exprimierten Genen. Unsere Zusammenfassung jüngster Forschungsergebnisse zeigt darüber hinaus Ähnlichkeiten wie auch Unterschiede zwischen syngnathider und Säugetier-Schwangerschaft auf. Dieser Vergleich dient als Grundlage für weitergehende Studien zur Evolution eines komplexen Merkmals, der männlichen Schwangerschaft.

Kapitel II

Polymorphismen in amplifizierten Fragmentlängen (AFLP) werden häufig als universelles DNA-fingerprinting-Werkzeug gebraucht und lassen sich in hocheffektive automatisierte Abläufe einbinden, wenn fluoreszenzmarkierte Oligonukleotide eingesetzt werden. Damit können dann sehr grosse Mengen an Fragmenten auf automatisierten Sequenziermaschinen getestet werden. AFLPs sind relativ günstig, wenn die Kosten auf die Anzahl getesteter Marker umgerechnet werden. Die zentrale Komponente von AFLPs, die fluoreszenzmarkierten Oligos, bleibt teuer. Indem man diesen Anteil der experimentellen Kosten durch die Verwendung der sogenannten Endlabelling-Methode reduziert, sollten AFLPs als Werkzeug auch für Laboratorien mit geringem Budget erschwinglich werden. Die vorgestellte Alternative entspricht hinsichtlich statistischer Vergleiche der traditionellen AFLP-Methode und erzeugt vergleichbare Ergebnisse. Unterschiede in der Grösse und Anzahl von erzeugten Fragmenten lassen jedoch nicht zu, dass partielle Datensätze, die mittels beider Methoden erzeugt wurden, miteinander verbunden werden können. Durch die deutlich reduzierten Gestehungskosten und vergleichbare Qualität bietet sich jedoch die neue AFLP-Methode als echte Alternative zu traditionellen fluoreszenz-markierten AFLP-Experimenten an.

Kapitel III

Differentiell exprimierte Gene können mittels der cDNA-AFLP-Methodologie detektiert werden, indem man Merkmale des Organismus mit cDNA-Expressionsprofilen korreliert. Dieser Ansatz ist jedoch nicht trivial, da AFLPs methodologisch komplex sind und durch die taxonomische Divergenz der zu analysierenden Arten sich das AFLP-Design von Art zu Art deutlich ändern kann. Wir haben mit Hilfe von Modellierung cDNA-AFLPs optimiert und Schlüsselfaktoren identifiziert, die die Qualität von cDNA-AFLP-Experimenten massiv beeinflussen. In- silico-Simulationen an 92 eukaryotischen Arten fast aller grossen taxonomischen Gruppen zeigen, dass die Wahl der verwendeten Restriktionsenzyme die Qualität eines Screens deutlich beeinflusst. Die von uns analysierten Daten zeigen einen gewissen Einfluss der Stammesgeschichte, wobei sich erweist, dass dieser Einfluss vor allem in den Veränderungen des GC-Gehaltes begründet liegt. Dieser ist ein zweiter Schlüsselfaktor, der die Qualität eines Screens beeinflusst. Während wir cDNA-AFLPs für eine grosse Menge von Organismen optimierten, zeigte sich auch ein strikt linearer Zusammenhang zwischen der Anzahl der pro Reaktion erhaltenen Fragmente und der Grösse des analysierten cDNA-Pools. Dieser Zusammenhang erlaubt es nun, die Anzahl der Gene in einem Gewebe zu schätzen, eine Anwendung, die um so wichtiger wird, je mehr neue Sequenziermethoden eingesetzt werden, um differentiell exprimierte Gene zu identifizieren

Kapitel IV

Untersuchungen zum Verständnis der Evolution von komplexen Formen der Reproduktion wurden bisher durch das Fehlen von Zwischenformen erschwert. Syngnathide Fische sind ein ideales Modellsystem für solche Untersuchungen, da rezente Formen eine grosse Diversität an rudimentären und komplexeren Formen der männlichen Schwangerschaft aufweisen. Unglücklicherweise ist über die genetische Regulation der männlichen Schwangerschaft dagegen nur wenig bekannt. Kenntnis der bei syngnathiden Fischen an der männlichen Schwangerschaft beteiligten Gene ist essentiell für vergleichende evolutionäre Studien, die den Ursprung dieser Art der Fortpflanzung zu klären suchen. Wir haben hier das erste Referenz-Transkriptom des Seepferdchens zusammengestellt, welches aus 38.419 Contigs besteht und mehr als 30.000

unterschiedliche cDNAs darstellt. Funktionelle Annotationen für ca. 27% dieser Contigs erlauben einen ersten, umfassenden Blick auf Genfunktionen, biologische Prozesse und die zelluläre Lokalisation der Contigs während der Schwangerschaft. Mittels einer vergleichenden Analyse von schwangeren und nicht-schwangeren Individuen wurden Hunderte von Genen identifiziert und auch annotiert, die während der männlichen Schwangerschaft differentiell exprimiert sind. Keine der verschiedenen Klassen der Annotation zeigt jedoch signifikante Unterschiede in der Anzahl von Genen aus schwangeren und nicht-schwangeren Geweben auf. Im Rahmen unserer Studie wurden auch die Auswirkungen der Normalisierung auf die Entdeckung noch unbekannter Gene quantifiziert, es wurde ebenso klar aufgezeigt, dass die Normalisierung bedeutend ist für Studien, deren Ziel es ist, ein möglichst komplettes Transkriptom zu erhalten. Dieses Transkriptom eines Seepferdchens wird auch zur Herstellung eines Microarrays verwendet und für die vergleichende Analyse von Genexpression während der männlichen Schwangerschaft in anderen Syngnathiden eingesetzt. Es ist damit ein erster, essentieller Schritt zum Verständnis der Evolution dieses komplexen Merkmals.

GENERAL INTRODUCTION

Modes of reproduction in fishes

Fishes exhibit a tremendous diversity of forms of reproduction (Breder and Rosen 1966). These modes range from the broadcast spawning of millions of small eggs to elaborate forms of male, female and bi-parental care, and several groups of fish have developed internal fertilization and/or forms of viviparity (live-bearing; Breder and Rosen 1966). Outstanding among viviparous groups are male-pregnant seahorses and pipefish (order Syngnathiformes), in which males heavily invest into reproduction (Kuiter 2000) and the traditional sex-roles are frequently reversed (Berglund and Rosenqvist 2003, Wilson et al. 2003, Jones et al 2005).

Male pregnancy in syngnathid fishes

Male pregnancy is an extreme form of paternal care unique to syngnathid fishes (Breder and Rosen 1966; Kuiter 2000) analogous to female pregnancy in mammals. Eggs transferred from females competing for access to males (sex role reversal), are fertilized and incubated in a pouch or pouch-like structure on the male abdomen or tail. The eggs are osmoregulated and aerated during their development (Leiner, 1934, Linton and Soloff, 1964) and genes expressed during incubation have been shown to have an *in vitro* antibacterial effect (Melamed et al. 2005). Though a marked maternal contribution still exists as a consequence of egg production, the male may also provide nutrients to the embryos (Ahnesjö 1992; Ripley and Foran 2006). Juveniles are released at birth through the partial (seahorses) or complete (pipefishes) opening of the pouch, or through hatching from individual egg compartments (Carcupino et al. 2002; Teske et al. 2003; Ripley and Foran 2006). At the same time, placenta-like structures are also expelled in only some of all species which have been studied (Ripley and Foran 2006).

Five morphologically distinct types of male brood pouch on either the abdomen (Gastrophori) or the tail (Urophori) can be identified across the Syngnathidae (Breder and Rosen 1966). The discrimination of morphotypes is based upon increasing morphological complexity (Duncker 1915; Wilson et al.

2003). In the simplest type of this form of reproduction (i), eggs are externally attached to the ventral surface of the pregnant male, while more elaborate forms include (ii) the containment of individual eggs in membranous compartments, (iii) the protection of eggs with plates of body armour or with skin folds, (iv) bilateral pouch folds growing together to form a closed pouch and ultimately (v) the derived, complex and enclosed pouch of seahorse. Representatives of each pouch form can be observed in both Gastrophori and Urophori syngnathid lineages, (Figure 1; Wilson et al. 2001, Wilson et al. 2003).

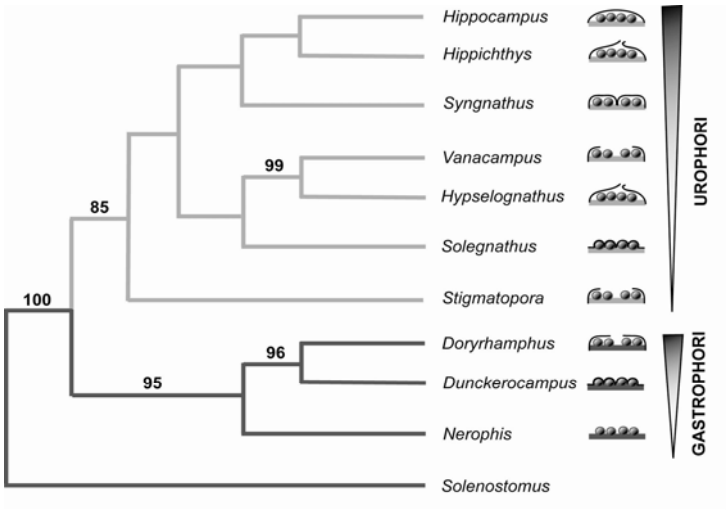

Figure 1: Simplified phylogenetic relationships of syngnathid fishes. Figure modified from Wilson et al. (2001, 2003). Consensus bootstrap values are indicated for all branches with bootstrap support>80%. Gastrophori = abdominal brooder, Urophori=tail brooder.

As the male prepares to receive a new clutch of eggs, a series of processes leads the formation of brooding structures, such as ventral gluing areas or pouches. Upon the completion of the development of the broody organ, males become able to carry a clutch of fertilized embryos during pregnancy. Males can only receive embryos after they reach reproductive maturity, which is accompanied by a lengthy period that leads to alterations in expression levels of paternal immune genes (Melamed et al. 2005), and involves changes in the osmotic regulation of the eggs in their brooding structures. In addition, oxygen is supplied to the eggs, and antibacterial activity in the pouch can be observed (Carcupino et al. 2002; Melamed et al. 2005). Nutrient transfer to the embryos occurs during this period, either directly through paternal transfer possibly via the degradation of unfertilized eggs (Ahnesjö 1992; Ripley and Foran 2006). Male pregnancy ends in a period of labor and birth of juveniles, at times accompanied by expulsion of placenta-like structures. The pregnancy cycle can be repeated multiple times during the breeding season. Pouch structures remain present in a reduced form in sexually inactive males.

Evolution of Male Pregnancy

Male pregnancy is one of the key innovations of the Syngnathidae family and evolved from fish without paternal care outside of the group (Nelson 1994) more than 50 million years ago (MYA), as suggested by fossil record (Patterson 1993; Teske et al. 2003). Phylogenetic relationships within the Gastrophori are well resolved (Fig. 1) (Wilson et al. 2001, Wilson et al. 2003). The basal lineage of Gastrophori (*Nerophis* spp.) has a simple brooding structure, an open gluing area for eggs at the abdomen (Duncker 1915; Kuiter 2000). From this, complex structures with skin or pouch-like folds covering attached eggs appear to have evolved (Duncker 1915; Kuiter 2000). It remains unclear what time spans were involved, as no fossil data exist for this lineage. In parallel to the Gastrophori, a set of morphologically more complex pouch types evolved in a rapid diversification among the Urophori between 20 and 52 MYA (Patterson 1993; Teske et al. 2003). The exact sequence of the evolution of male pregnancy in this group is unclear as the phylogeny of Urophori remains largely unresolved (Figure 1).

Close similarities in the form of male pregnancy of the two syngnathid lineages, suggest that similar genetic mechanisms may be responsible for generating these structures. As limited genetic data exist for syngnathid fishes, the investigation of this hypothesis requires the initial characterization of genome-level data for the group. A good candidate species for such characterization should also share features of established model species: relatively short generation time, established culture in the lab, and sufficiently high reproductive rates to allow statistical testing. A good candidate species would also be large enough to provide sufficient amounts of tissues and would be of interest to a wider audience. The seahorse *Hippocampus abdominalis* (Figure 2) is a good candidate species which combines many of the listed features. This species is accommodated to subtropical marine waters and can be kept and bred under laboratory conditions (Woods 2000). Reaching up to 35cm in length, this is the largest seahorse species and produces hundreds of offspring per clutch (Kuiter 2000).

Evolution of complex traits

Key innovations such as male pregnancy are often complex traits and are of particular interest in the evolution of species diversity (*e.g.* pharyngeal jaws in cichlid fishes; Skúlason and Smith 1995). Complex traits can evolve from simpler

components through the recruitment of unrelated parts of independent functional units (Steeg et al. 1988), or may result from the *de novo* subfunctionalization of genes generated during large-scale duplication (Force et al. 1999). This complementation of gene functions occurs when the two resulting gene copies carry different mutations, such that both copies together produce the same amount of mRNA as that produced before the duplication event. The presence of excess gene copies after the duplication may be detrimental to the organism, and this excess needs to be down-regulated to avoid abnormalities in growth and development (Force et al. 1999). While a good part of the literature on the evolution of complexity addresses questions such as the rise of multicellular organisms and accompanying increasing genomic complexity (Lynch and Conery 2003) or the origin of brain complexity in humans (Bradbury 2005), nothing is known about the *de novo* evolution of the complex male pregnancy trait and its genetic control.

Figure 2. Two male potbelly seahorses *Hippocampus abdominalis*, presenting their inflated brood pouches. Picture taken from http://de.wikipedia.org/wiki/Seepferdchen.

The genetic basis of complex traits: differential displays

Fundamental to studies on the evolution of complex traits such as male pregnancy is a detailed knowledge on both genetic and morphological makeup of the trait. Comparative genomic studies offers a power means to identify the genetic basis of functional innovation via the comparison of correlations between genetic and morphological changes. Unfortunately, the closest sequenced relative of syngnathid fishes, the stickleback *Gasterosteus aculeatus*, is a species which does not exhibit male pregnancy and diverged at least 50 million years ago from the syngnathids (Stölting and Wilson 2007). Both the evolutionary divergence time as well as the novelty of the character under study means that comparative genomic studies using sequences from existing model organisms are unlikely to provide any insights into the evolution of this trait in the syngnathids.

Dissecting the genetics of male pregnancy hence requires *de novo* sequencing methods. cDNA sequencing approaches such as EST projects can provide snapshot-information of many expressed genes in a tissue of interest, but

this type of data alone can provide only little information on the underlying genetics. Differential display approaches offer a mean to identify differences in patterns of gene expression in target tissues, and recent years have seen an increase in available methods for the identification of such genes whose expression patterns are significantly correlated with traits of interest (Liang and Pardee 1992). The identification of differentially expressed genes is particularly challenging in non-model organisms for which extensive genomic resources are unavailable, as methods have to be used which function independently of the unknown cDNA sequences. In such cases, the differential analysis of expressed genes can be achieved by means of cDNA-AFLPs, which allow the detection of presence/absence differences in gene expression (Breyne et al. 2003, Stölting et al. 2009). The cDNA-AFLP technique involves the digestion of cDNA preparations with two restriction enzymes. To analyze the produced fragments, adaptors are ligated to each restriction fragment, which then serve as oligonucleotide-binding sites for two subsequent rounds of PCR. By adding a few selective base pairs to these primer sequences, the amplified fragment pool is reduced in complexity such that a suitable number of fragments can be visualized (Vos et al. 1995, Meudt and Clarke 2007). By comparing the presence or absence of individual fragments in individual cDNA libraries after size separation, one can identify genes correlated to the trait of interest.

Detect candidate genes associated with the traits offers a particular powerful method to next generation sequencing techniques (Braverman et al. 2005, Morozova and Marra 2008). Massive parallel sequencing approaches can provide several hundred million base pairs of sequence information per run, providing the means to identify a large number of expressed genes per transcriptome. This method is also unbiased, though modifications to standard protocols are necessary to minimize the representation of highly expressed transcripts in next generation sequencing. As this method allows the identification of differences in gene expression and provides the raw data necessary for the identification of the genes themselves, next generation sequencing has revolutionized the study of gene expression data in non-model systems. Entire transcriptomes can now be sequenced completely, but analysis methods struggle to cope with the available wealth of sequence information and the need to assemble and annotate produced contigs.

Objectives

The present study aims to describe the morphological and physiological processes of male pregnancy in the seahorse *Hippocampus abdominalis*, and applies cDNA-AFLPs differential displays and next-generation sequencing to identify and describe the genetic basis involved in male pregnancy.

In **Chapter I**, physiological and morphological processes during male pregnancy in syngnathids are summarized and compared to other forms of viviparity. Many of the changes which occur during viviparity are superficially similar even in distant related organisms, suggesting that common suite of gene functions might be required. A circumspect foundation for further studies on male pregnancy is provided, which reviews the male pregnancy literature with a focus on the evolution of a complex trait.

Differential displays approaches can be used to identify genes required for a particular trait. **Chapter II** optimizes one such approach, cDNA-AFLP, by fluorescently end-labelling AFLP fragments. In replacing individual fluorescently-labelled oligonucleotides with a single universal labelled primer, setup costs of the AFLP experiments can be significantly reduced. Several alternative universal primers are compared.

Initial efforts to screen the seahorse transcriptome using cDNA-AFLP were unsuccessful (data not shown). **Chapter III** investigated the assay design of cDNA-AFLP experiments using an extensive eukaryote-wide *in silico* simulation experiment. Key factors to successful assay design were identified here, novel versatility were added to the cDNA-AFLP technique, and consistent eukaryote-wide patterning of cDNA-AFLP selective PCRs was identified.

Next-generation sequencing technology is used in **Chapter IV** to provide reference transcriptomes of the seahorse *Hippocampus abdominalis*, and to identify genes correlated to the male pregnancy. Five transcriptome-wide cDNA libraries have been sequenced, annotated and compared, and several thousand potential male pregnancy candidates are identified.

References

Ahnesjö I. 1992. Consequences of male brood care: weight and number of newborn in a sex-role reversed pipefish. *Functional Ecology* 6:274-281.

Berglund A, Rosenqvist G. 2003. Sex role reversal in pipefish. *Advances in the Study of Behavior, 32*, 32:131-167.

Bradbury J. 2005. Molecular insights into human brain evolution. PLoS Biology 3:e50.

Breder CM., Rosen DE. 1966. Modes of reproduction in fishes. Natural History Press, New York.

Breyne P, Dreesen R, Cannoot B, Rombaut D, Vandepoele K, Rombauts S, Vanderhaeghen R, Inze D, Zabeau M. 2003. Quantitative cDNA-AFLP analysis for genome-wide expression studies. *Molecular Genetics and Genomics* 269:173-179.

Carcupino M, Baldacci A, Mazzini M, Franzoi P. 2002. Functional significance of the male brood pouch in the reproductive strategies of pipefishes and seahorses: a morphological and ultrastructural comparative study on three anatomically different pouches. *Journal of Fish Biology* 61:1465-1480.

Duncker G. 1915. Revision der Syngnathidae. *Jahrbuch der Hamburgischen Wissenschaftlichen Anstalten* 32:9-120.

Force A, Lynch M, Pickett FB, Amores A, Yan Y-I, Postlethwait J. 1999. Preservation of duplicate genes by complementary, degenerative mutations. *Genetics* 151:1531-1545.

Götz S, Garcia-Gomez JM, Terol J, Williams TD, Neda MJ, Robles M, Talon M, Dopazo J, Conesa A: High-throughput functional annotation and data mining with the Blast2GO suite. *Nucleic Acids Research* 2008, 36:3420-3435

Jones AG, Rosenqvist G, Berglund A, Avise JC. 2005. The measurement of sexual selection using Bateman's principles: An experimental test in the sex-role-reversed pipefish Syngnathus typhle. *Integrative and Comparative Biology* 45:874-884

Kuiter RH. 2000. Seahorses, pipefish and their relatives: Syngnathiformes. Zoonetics, Seaford, Australia.

Leiner VM. 1934. Der osmotische Druck in den Bruttaschen der Syngnathiden. *Zoologischer Anzeiger* 108: 273-289

Liang P, Pardee AB: Differential display of eukaryotic messenger-RNA by means of the polymerase chain-reaction. *Science* 1992, 257:967-971.

Linton JR, Soloff BL. 1964. The physiology of the brood pouch of the male sea horse *Hippocampus erectus*. *Bulletin of Marine Science of the Gulf and Carribbean* 14(1): 45-61

Lynch M, Conery JS. 2003. The origins of genome complexity. *Science* 302:1401-1404.

Margulies M, Egholm M, Altman WE, Attiya S, Bader JS, Bemben LA, Berka J, Braverman MS, Chen YJ, Chen Z, Dewell SB, Du L, Fierro JM, Gomes XV, Godwin BC, He W, Helgesen S, Ho CH, Irzyk GP, Jando SC, Alenquer ML, Jarvie TP, Jirage KB, Kim JB, Knight JR, Lanza JR, Leamon JH, Lefkowitz SM, Lei M, Li J et al. 2005. Genome sequencing in microfabricated high-density picolitre reactors. *Nature* 437:376-380

Melamed P, Xue Y, Poon JFD, Wu Y, Xie H, Yeo J, Foo TWJ, Chua HK. 2005. The male seahorse synthesizes and secretes a novel C-type lectin into the brood pouch during early pregnancy. *FEBS Letters* 272:1221-1235.

Meudt HM, Clarke AC: Almost forgotten or latest practice? AFLP applications, analyses and advances. Trends in Plant Science 2007, 12:106-117.

Morozova O, Marra MA: Applications of next-generation sequencing technologies in functional genomics. *Genomics* 2008, 92:255-264

Nelson JS. 1994. Fishes of the world. John Wiley & Sons, Inc., New York.

Patterson C. 1993. Chapter 36. Osteichthyes: Teleostei. Pp. 1–145 *in* M. J. Brenton, ed. The Fossil Record. Chapman & Hall, London, England.

Ripley JL, Foran CM. 2006. Differential parental nutrient allocation in two congeneric pipefish species (Syngnathidae: *Syngnathus* spp.). *The Journal of Experimental Biology* 209:1112-1121.

Skúlason S, Smith TB. 1995. Resource polymorphisms in vertebrates. *Trends in Ecology and Evolution* 10:366-370.

Steeg PS., Bevilacqua G, Kopper L, Thorgeirsson UP, Talmadge JE, Liotta LA, Sobel ME. 1988. Evidence for a novel gene associated with low tumor metastatic potential. *Journal of the National Cancer Institute* 80:200-204.

Stölting KN, Gort G, Wüst C, Wilson AB. 2009. Eukaryotic transcriptomics *in silico*: Optimizing cDNA-AFLP efficiency. *BMC Genomics* 10, 565.

Stölting KN, Wilson AB. 2007. Male pregnancy in seahorses and pipefish: beyond the mammalian model. *Bioessays* 29:884-896.

Teske PR, Cherry MI, Matthee CA. 2003. The evolutionary history of seahorses (Syngnathidae: *Hippocampus*): molecular data suggest a West Pacific origin and two invasions of the Atlantic Ocean. *Molecular Phylogenetics and Evolution* 30:273-286.

Vos P, Hogers R, Bleeker M, Reijans M, Vandelee T, Hornes M, Frijters A, Pot J, Peleman J, Kuiper M, Zabeau M. 1995. AFLP - A new technique for DNA-fingerprinting. *Nucleic Acids Research* 23:4407-4414.

Wilson AB, Ahnesjö I, Vincent A, Meyer A. 2003. The dynamics of male brooding, mating patterns, and sex roles in pipefishes and seahorses (family Syngnathidae). *Evolution* 57:1374-1386.

Wilson AB, Vincent A, Ahnesjö I, Meyer A. 2001. Male pregnancy in seahorses and pipefishes (family Syngnathidae): rapid diversification of paternal brood pouch morphology inferred from a molecular phylogeny. *The Journal of Heredity* 92:159-166.

Woods CMC: Preliminary observations on breeding and rearing the seahorse *Hippocampus abdominalis* (Teleostei: Syngnathidae) in captivity. *NZ J Mar Freshwater Res* 2000, 34:475-485

CHAPTER I: Male Pregnancy in Seahorses and Pipefish: Beyond the Mammalian Model

Kai N. Stölting and Anthony B. Wilson

Published in: *BioEssays* 2007, 29:884-896

Summary

Pregnancy has been traditionally defined as the period during which developing embryos are incubated in the body after egg-sperm union. Despite strong similarities between viviparity in mammals and other vertebrate groups, researchers have historically been reluctant to use the term pregnancy for non-mammals in recognition of the highly developed form of viviparity in eutherians. Syngnathid fishes (seahorses and pipefishes) have a unique reproductive system, where the male incubates developing embryos in a specialized brooding structure in which they are aerated, osmoregulated, protected and likely provisioned during their development. Recent insights into physiological, morphological and genetic changes associated with syngnathid reproduction provide compelling evidence that male incubation in these species is a highly specialized form of reproduction akin to other forms of viviparity. Here, we review these recent advances, highlighting similarities and differences between seahorse and mammalian pregnancy. Understanding the changes associated with the parallel evolution of male pregnancy in the two major syngnathid lineages will help to identify key innovations that facilitated the development of this unique form of reproduction and, through comparison with other forms of live bearing, may allow the identification of a common set of characteristics shared by all viviparous organisms.

Introduction

Pregnancy is defined as the gestational period lasting from the implantation of a fertilized zygote to the release of developed embryos at parturition (Knobil and Neill 1998). While viviparity has also been traditionally used to describe the condition of giving birth to active free-living young (Wake 1992, Froese and Pauli 2006), some researchers have used more-stringent definitions of the term, incorporating internal fertilization and development within the maternal reproductive system (Wourms and Lombardi 1992). The use of the term in this way by definition excludes the possibility of male viviparity. Male internal incubation can however be highly developed and may include complex physiological and morphological adaptations for the protection and provisioning of embryos during their development. Given parallels in the reproductive changes associated with internal incubation of embryos in males and females, we use the more inclusive definition of viviparity. For detailed definitions of the terms used here, please refer to Table 1.

Although viviparity is found in all vertebrate groups except birds (Rothchild 2003), male viviparity is extremely rare. One of the few instances of male viviparity is found in the amphibian genus *Rhinoderma*, where males incubate eggs in modified vocal sacs after a period of extra-corporal development, providing nutrients and respiratory care for larvae until metamorphosis is completed (Goicoechea et al. 1986). In this group, fertilization is external and embryos develop for more than 20 days outside the body until muscular activity by the embryo triggers internalization by the male (Goicoechea et al. 1986).

An even more remarkable case of male viviparity can be found in syngnathid fishes (seahorses and pipefish), a group of organisms in which males incubate developing embryos in a specialized brooding patch or pouch on their body surface (Kuiter 2000, Rothchild 2003). While syngnathid viviparity is clearly an independently derived system, gestation in male seahorses and pipefish requires a complex series of morphological and physiological modifications of paternal tissues analogous to those found in viviparous females. In order to better understand the key characteristics of pregnancy and the applicability of this term to viviparous males, we first turn to the mammals, the group for which viviparity has been most thoroughly studied.

Pregnancy in mammals: evolution and diversity

Despite the ubiquitous use of the term pregnancy in mammals, mammalian reproduction is diverse and maternal investments of both time and energy vary widely among species. Although the mammalian lineage is thought to date back only about 210 million years (Pough et al. 1999), a diversity of reproductive modes have been realized in this group. While basal lineages were most likely oviparous, early Eutheria (higher placental mammals) and Metatheria (marsupials) both possessed forms of viviparity (Pough et al. 1999). The extant therian group is at least 145 million years old and contains more than 4400 species in 125 families (Pough et al. 1999).

During the evolution of higher mammals, egg-yolk-producing vitellogenin genes were lost and compensatory trophic structures evolved in maternal tissues (Rothchild 2003). The placenta is the primary trophic structure of mammalian pregnancy, a highly specialized organ that is derived from both maternal and fetal tissues (Gude et al. 2004). Despite the relative recency of its evolution in therian mammals, placental structure is more diverse than that of any other mammalian organ (Stulc 1997). In the epitheliochorial placenta of artiodactyls, the trophoblast is separated from the maternal blood supply by several layers of thelial cells while, in the endotheliochorial placenta of carnivores, the trophoblast is only restricted from the maternal blood supply by a single layer of maternal endothelium (Stulc 1997). One of the most-common types of placenta is the hemochorial placenta of primates and rodents, in which maternal blood is in direct contact with the embryonic chorion (Beck1976, Stulc 1997).

All therian mammals possess a placenta, but there are several major differences between eutherian and metatherian reproduction, which may reflect the independent evolution of viviparity in these two groups (Zeller 1999). Eutherian gestation time is positively correlated with body size, and the lactation period is usually shorter than the gestation time (Pough et al. 1999). In marsupials, however, gestation is short, while lactation can be extended, and there is no correlation between gestational duration and body size (Hayssen et al. 1985). While a vestigial remnant of an oviparous ancestor remains in marsupials (egg-shell membranes), these features have been lost in placental mammals (Pough et al. 1999). Marsupial reproduction has been suggested to be an adaptation to unstable arid environments, but there appears to be little evidence that

environments of ancestral eutherians and metatherians were categorically different (Hayssen et al. 1985). Instead, recent work suggests that the short gestation/long lactation of metatherians and the long gestation/short lactation of eutherians may simply be alternate means of achieving the same reproductive outcome (Pough et al. 1999).

Major differences in the form, complexity and duration of gestation in mammals make it difficult to identify a set of defining characteristics for pregnancy of use in other vertebrate groups (Rothchild 2003). Nonetheless, while the particulars of mammalian pregnancy vary substantially among species, several processes are common to all eutherians. Early stages of blastocyst growth during eutherian pregnancy occur without a direct embryonic-maternal connection (Cross et al. 1994). The implantation of the zygote occurs after trophoblast formation and involves intensified cell proliferation around the blastocyst (Cross et al. 1994). Following the formation of the primary placenta, placental growth continues during pregnancy to meet the increasing requirements of the developing embryo (Schneider 1996). The establishment of a fully functional placenta enables efficient exchange of nutrients and waste products between fetal and maternal blood supplies (Gude et al. 2004). The placenta also produces estrogen, progesterone and growth hormone, endocrine compounds that promote physiological and morphological changes in both the mother and the embryo (Gude et al. 2004). At parturition, the connection between placenta and fetus is severed and placental structures are expelled along with the fetus (Cross et al. 1994). Pregnancy in all mammals is followed by an extended period of postparturition care to allow the completion of juvenile development (Clutton-Brock 1994). Table 2 details characteristics of the pregnancy process in the domestic mouse (Mus musculus), a particularly valuable model species for the study of the hemochorial placenta and human pregnancy. The reader is directed to several excellent reviews of mammalian pregnancy for further details on the processes briefly outlined here (Cross et al. 1994, Rothchild 2003, Gude et al. 2004).

While mammalian viviparity is highly complex, recent studies clearly demonstrate that viviparity in non-eutherians can be equally elaborate (Rothchild 2003, Blackburn 2005). As mammalian viviparity is highly derived, comparative studies in other vertebrate groups may provide insights into the morphological and physiological changes associated with the evolution of viviparity. Although the

sequence of events leading to the evolution of viviparity is clearly different between mammals, reptiles and fishes (Blackburn 2005), comparative approaches across groups may allow the identification of common features of pregnancy shared by all viviparous organisms (Blackburn 2005).

The evolution of viviparity: different pathways yield similar outcomes

The ancestor of all vertebrates was most likely oviparous (egg laying; Pough et al. 1999) and viviparity is believed to have originated as many as 140 times in the vertebrate lineage (Crespi and Semeniuk 2004). Oviparity remains the prominent mode of reproduction in all vertebrates with the exception of mammals, and occurs in >85% of reptiles, >90% of amphibians, and 100% of birds (Dulvy and Reynolds 1997, Pough et al. 1999). While viviparity has repeatedly evolved in vertebrates, there are very few instances of subsequent reversals from viviparity to oviparity (Reynolds et al. 2002). This may be due to the accelerated development of viviparity after the evolution of egg retention and internal fertilization, which is thought to be caused by intensified parent-offspring conflict for resources (Crespi and Semeniuk 2004). Alternatively, the paucity of transitions from viviparity to oviparity may simply reflect the relative recency of viviparity in comparison to the ancestral mode of oviparous reproduction (Reynolds et al. 2002).

Viviparity has significant energetic costs for the mother and increases predation reproductive risks, which may considerably reduce her total lifetime output (Goodwin et al. 2002). Although viviparous organisms often have reduced clutch size, fitness benefits associated with viviparity may be achieved via increased offspring survival. Juvenile survival benefits are largely due to increased size of viviparous offspring, which can be achieved via developmental independence from environmental fluctuations in temperature and/or oxygen supply, as well as reduced predation pressures for the embryo during its internal development (Goodwin et al. 2002). In order to accommodate internally developing offspring, viviparous organisms have evolved increased body size to meet space and energy constraints (Goodwin et al. 2002).

Viviparity and oviparity are often presented as dichotomous modes of reproduction, but it should not be forgotten that viviparity itself is a continuum from incubation of yolk-rich eggs in the female (lecithotrophic viviparity) via yolk supplementation to placental or placental-analogous structures (Reynolds et al.

2002). Although these three phases have characterized the evolution of viviparity in all vertebrates, pregnancy has evolved along very different pathways in different taxonomic groups. Phylogenetic reconstructions suggest that mammalian pregnancy is derived from a group of oviparous ancestors who actively supplemented eggs with nutrients during their development (a form of matrotrophic oviparity), while egg retention and placentation simultaneously evolved during the development of squamate viviparity (Blackburn 2006). Despite variation in the processes involved in the evolution of viviparity in different groups, considerable morphological and functional similarities can be found in highly derived forms. The evolution of viviparity in fishes most closely fits the traditional model and viviparous fishes appear to have evolved from oviparous ancestors via successive steps of egg retention, eggshell reduction and placentation (Blackburn 2006).

Modes of reproduction in fishes

Fishes are a large and diverse group of vertebrates, including species of the ray-finned (Actinopterygii), lobe-finned (Sarcopterygii) and cartilaginous (Chondrichthyes) fishes (Froese and Pauli 2006). With a total of approximately 30,000 described species (Froese and Pauli 2006), fish exhibit a wide variety of reproductive modes ranging from simple broadcast spawning (a form of oviparity) to advanced forms of viviparity (Breder and Rosen 1966).

Viviparity has been realized in as many as 54 fish families, and is thought to have independently evolved from egg laying at least thirty times (Crespi and Semeniuk 2004, Blackburn 2005). Thirteen of these origins have been identified in actinopterygian fishes, including the independent origin of male viviparity in the Syngnathidae (Crespi and Semeniuk 2004, Blackburn 2005). In sarcopterygians, a single origin of viviparity has been inferred for the two coelacanth species, while the six recognized lungfish species are egg laying (Froese and Pauly 2006). The remaining 16 origins of viviparity in fishes occurred during the evolution of sharks, rays and skates (chondrichthyans).

Oviparity is thought to be the ancestral reproductive mode of ray-finned fishes and is found in about 97-98% of most species (Dulvy and Reynolds 1997). As all actinopterygians lack a uterus, gestation in viviparous species occurs in either the follicle or ovarian cavity (Schindler and Hamlett 1993). The highest frequency of independent origins of viviparity among ray-finned fishes is found in

the Atherinomorpha, a large clade of 1500 fish species including the Beloniformes, Cyprinodontiformes and Atheriniformes (Mank and Avise 2006). Four origins of viviparity have been identified in atherinomorph fishes and have led to such specialized reproductive strategies as sperm storage and superfetation, the simultaneous development of multiple broods (Turner 1937, Wourms 1981). The repeated origins of viviparity in the atherinomorphs has been attributed to the high frequency of internal fertilization in this group (Mank and Avise 2006). As the reproductive biology of many species of ray-finned fishes is still poorly studied, further independent origins of viviparity may ultimately be inferred in this group (Blackburn 2005).

Chondrichthyans are also considered ancestrally oviparous species, but viviparity has evolved in between 40-55% of all extant forms (Wourms 1981, Dulvy and Reynolds 1997). All chondrichthyan species have internal fertilization (Blackburn 2005), and both aplacental and placental styles of embryo supplementation have evolved in this group (Hamlett and Hysell 1998). Among aplacental forms, embryos are supplied via the yolk sac or trophonemata, alternatively feeding on siblings or nurse eggs. In higher placental forms, additional nutrients are supplied to developing offspring upon depletion of yolk stores. Viviparity in elasmobranchs involves osmoregulation, increased uterine surface areas for respiratory and metabolic exchange, and intensified vascularization of the uterine wall (Hamlett and Hysell 1998).

A set of reproductive modifications accompanies viviparity in fish: (a) a decrease in egg number, (b) internal fertilization, (c) absorption of maternally secreted nutrients through the yolk sac, and (d) a period of intracorporal gestation varying in length until a large proportion of embryonic development is completed (Wourms 1981). Gestation in fish includes changes in the fetal-maternal relationships in developmental, morphological, trophic, osmoregulatory, respiratory, endocrinological and immunological systems (Wourms 1981, Wourms and Lombardi 1992, Wourms 1994). Embryos are incubated in the ovarian cavity, in the follicle, in specialized compartments such as the pouch of male seahorses, or other internal structures (Schindler and Hamlett 1993, Dulvy and Reynolds 1997).

Various forms of embryonic nutrition have been identified in viviparous fish, including strict lecithotrophy (yolk feeding), adelphophagy (sibling feeding),

oophagy (egg feeding) as well as maternal provisioning (Schindler and Hamlett 1993). The latter includes nourishment via a variety of placental analogs such as trophonemata, epithelia (gill, epidermis, fin), trophotaeniae (hypertrophied intestinal projections), branchial or yolk sac placenta and follicular pseudoplacentas derived from maternal tissues (Wourms 1981). Due to major differences in the level of maternal provisioning, fetal weight change during development can vary substantially among species (Wourms 1981).

Although substantial variation in viviparous reproduction can be found in fishes, male viviparity has evolved only once during the evolution of this group, in seahorses and pipefishes (family Syngnathidae) (Crespi and Semeniuk 2004). Despite the unique morphological and physiological challenges associated with the evolution of male viviparity, recent studies of syngnathid fishes have highlighted a diversity of different forms of live bearing in this group and identified a range of complex specializations associated with the evolution of male pregnancy (Herald 1959, Carcupino et al. 2002).

Male pregnancy in seahorses and pipefishes: new insights reveal a complex phenomenon

Syngnathid fishes are a group of 232 species (Nelson 2006), that exhibit a wide diversity of brooding types and structures varying in their complexity and location on the male body (Wilson et al. 2001, Kuiter 2000). Two syngnathid subfamilies are identified based on the relative position of the brood pouch: abdominal brooders (Hippocampus) (Gastrophori) and tail brooders including the seahorse (Urophori) (Fig. 1). Male brood pouches have independently increased in complexity during the evolution of both lineages (Wilson et al. 2005). Seahorses (with 33 recognized species; Foster and Vincent 2004) have the most-complex pouch structure and also undergo the most significant physiological changes during embryo incubation. Despite the general trend towards more complex brooding structures in the evolution of syngnathids, considerable variability may also exist among congeneric members of the same general pouch type (Ripley and Foran 2006).

Although the fossil record for this group is incomplete, the oldest syngnathid fossils date to approximately 50 million years (Benton 1993). Despite considerable diversification in this group, there remain extant representatives of almost all major

pouch types, offering the possibility to use comparative methods to study pouch evolution and diversification (Wilson et al. 2001, Wilson et al. 2003). In mammals, while many different forms of incubation exist, it has been difficult to reconstruct the process of evolution of pregnancy due to the relative paucity of transitory forms (Rothchild 2003). Male pregnancy in syngnathid fishes evolved from a group with a diversity of reproductive modes, ranging from free spawners (*Pegasus* spp.) to species with female incubation (*Solenostomus* spp.) (Wilson and Orr, unpublished data). While *Solenostomus* is closely related to syngnathid fishes, it is unlikely that pelvic fin bearing in *Solenostomus* is homologous with syngnathid male parental care due to fundamental differences in pouch morphology and function (Wetzel and Wourms 1995).

In all species of syngnathid fishes, the female transfers her yolk-rich eggs (Foster and Vincent 2004) to the male's pouch, a brooding structure located below the male's gonopore, such that intra-pouch fertilization is achieved during egg transfer (Watanabe et al. 2000, Van Look et al. 2007). Sperm cells are shed above the pouch and enter the pouch lumen (Watanabe et al. 2000), so that sperm-egg union in syngnathids occurs without the necessity of extended sperm movement and/or lengthy zygotic migrations to the site of implantation. Polyspermia, a potential problem for the oocyte during fertilization, is avoided in syngnathid fishes by a massive reduction in sperm (as few as 150 sperm per testis in seahorses; Van Look et al. 2007), the lowest sperm production of any fish species (Stockley et al. 1997). While more basal syngnathids have been suggested to have a form of external fertilization, testes of these species are also reduced (Kvarnemo and Simmons 2004) and experimental work on one of these species (*Nerophis ophidion*) has demonstrated that sperm activation requires the presence of ovarian fluid (Ah-King et al. 2006), indicating that sperm must be released during egg transfer. The evolution of reduced sperm number in syngnathid fishes has likely occurred as consequence of reduced sperm competition in these species (Stockley et al. 1997; see below).

Upon fertilization, syngnathid zygotes implant quickly (Boisseau 1969) and cell differentiation occurs in brooding tissues as epithelial structures enclose the embryos (Fig. 2b). Vascularization of the inner connective layers of the seahorse male's pouch increases considerably after implantation and even more so after the eggs hatch (Laksanawimol et al. 2006) (Figs. 2d and 3). Changes in pouch

morphology during incubation (Figs. 2 and 3) clearly indicate that the role of the seahorse pouch is far more than simple protection, and there is evidence for osmoregulatory, aerative, nutritive and possible immunoprotective roles of the male brood pouch (Leiner 1934, Linton and Soloff 1964, Carcupino et al. 2002, Melamed et al. 2005, Dzyuba et al. 2006, Laksanawimol et al. 2006).

In marine seahorses and pipefish, the osmolality of pouch fluid changes substantially during incubation, increasing from that of paternal blood at fertilization to that of the surrounding marine environment later in development (Leiner 1934, Linton and Soloff 1934). In estuarine species, osmolality of pouch fluid remains similar to paternal blood, buffering developing embryos against potentially major fluctuations in environmental salinity (Quast and Howe 1980, Watanabe et al. 1999). Recent work has identified mitochondrial-rich cells (MRCs) lining the brood pouch of several pipefish species (Watanabe et al. 1999, Carcupino et al. 2002). MRCs are typically found in gill tissue of teleost fishes and play an important role in adult osmoregulation, suggesting that they may play a similar role in regulating osmolality of the pouch environment during incubation (Watanabe et al. 1999, Carcupino et al. 2002). Although brood pouch osmolality is also actively regulated during seahorse incubation (Leiner 1934, Linton and Soloff 1964), MRCs have not been identified in the seahorse brood pouch (Carcupino et al. 2002), indicating that other mechanisms of ion transport must be responsible for osmoregulation in these species.

While the pouch epithelium of pipefish species with rudimentary brooding structures (ex: *Nerophis* spp., Fig. 1) is similar to normal skin tissue, fundamental changes occur prior to and during incubation in species with more complex pouches (Carcupino et al. 2002). In species with complex brooding structures, brood pouch tissue is heavily vascularized throughout incubation (Fig. 2), a morphological change which is believed to be important for gas exchange between the developing embryo and the paternal blood supply (Carcupino et al. 2002). Microridges lining the brood pouch surface of both seahorses and pipefishes (Fig. 3) increase the surface area across which diffusion of inorganic and organic compounds can take place (Carcupino et al. 2002). While the eggs of most syngnathid species are spherical, the oocytes of seahorses are pear-shaped, an adaptation that further maximizes embryonic surface area for ionic and gas

exchange in the completely enclosed brood pouches of these species (Boisseau 1967).

The importance of patrotrophy during syngnathid incubation remains unclear and, while the presence of considerable yolk indicates that much of the energy required for embryonic development is maternally derived, various studies have suggested active nutrient supplementation by the father during development in both *Hippocampus* and *Syngnathus* (Boisseau 1967, Haresign and Shumway 1981). Seahorse brood pouch fluid is thought to be derived from paternal blood serum and is extremely protein-rich at the time of fertilization (Boisseau 1967). The seahorse brood pouch is also lined with modified secretory flame-cone cells (Fig. 3; Carcupino et al. 2002), which may play a role in digesting maternally derived proteins into amino acids within the pouch (Boisseau 1967). As the embryonic chorion is semi-permeable (Ripley and Foran 2006), diffusive transport of pouch nutrients to developing embryos is likely possible, but evidence of a significant paternal energetic contribution to seahorse embryos is equivocal. An experimental approach used intraperitoneal injection of a radiolabelled amino acid to demonstrate that pipefish embryos are capable of absorbing paternally derived nutrients (Haresign and Shumway 1981). As active nutrient supplementation by the parent is a defining character of the mostdeveloped forms of viviparity, the clarification of the role of patrotrophy in syngnathid pregnancy is essential.

Recent genetic work indicates that C-type lectins (CTLs), a family of proteins that exhibit antibacterial activity in vitro, are secreted in abundance by brood pouch tissues during seahorse incubation (Melamed et al. 2005). High levels of CTLs are present during early incubation and protein production decreases through subsequent stages of development (Melamed et al. 2005), suggesting that these compounds may play an important protective role prior to the development of the innate immune system of the embryos themselves. Determining whether these compounds are also produced in species with more rudimentary brooding structures will help to clarify the timing of the development of immune function in syngnathid incubation. The gestation time of syngnathid embryos is tightly linked to the temperature of the external environment and incubation times can range between 9 and 69 days depending on ambient temperatures (Woods 2000, Foster and Vincent 2004). Once gestation is completed at parturition, a pseudoplacenta may be expelled along with released

juveniles (Ripley and Foran 2006). The male's pouch undergoes further morphological changes as it reverts to its non-reproductive state (Laksanawimol et al. 2006). After parturition, juvenile syngnathids are free-living and no further parental care is provided.

Hormonal regulation strongly influences gestation in all viviparous species. One of the key endocrine hormones involved in seahorse pregnancy is prolactin (PRL). Over 300 separate functions of PRL have been identified in vertebrates, more than that of all other pituitary hormones combined (Bole-Feysot et al. 1998). In addition to its importance in osmoregulation, growth and immunoregulation, PRL plays a critical role in parental behavior and increased expression of PRL is associated with paternal care behavior in birds, mammals and fishes (Schradin and Anzenberger 1999). In seahorses, interruption of PRL synthesis by hypophysectomy leads to the disruption of brooding tissues and spontaneous abortions during pregnancy (Boisseau 1967, Boisseau 1969). Natural growth and development of embryos and maintenance of male brood pouch activity is recovered in hypophysectomized seahorses by treatment with exogenous PRL (Boisseau 1967). Interestingly, while the knockout of prolactin receptor (PRLR) in female mice causes major reproductive defects, reproductive function of males is only modestly affected by its disruption (Bachelot and Binart 2007). While the normal function of the male's brood pouch in hypophysectomized seahorses is not rescued by estradiol (O) treatment, treatment with testosterone (T) at an early stage of pregnancy recovers pouch function (Boisseau 1967), indicating that brood pouch production is at least partially under testicular control. Similarly, progesterone (PR) treatment of hypophysectomised seahorses fully rescues the normal function of the brood pouch (Boisseau 1967). This result indicates that PRL production is essential for the secretion of T and PR in seahorses. Exogenous PR treatment also recovers natural embryonic development and implantation in PRLR-deficient female mice (Binart et al. 2000). Investigations of other vertebrate groups indicate that, while the major components of the hypothalamic- pituitary-gonadal axis are present in both oviparous and viviparous species, major shifts in the timing, duration and levels of hormone production are associated with the evolution of viviparity (Callard et al. 1992). The highest levels of PR production in oviparous species occur prior to ovulation, while PR production in viviparous species occurs after ovulation is complete (Callard et al. 1992), a shift that is

thought to be critical for the development of egg retention and yolk loss in viviparous species. Although efforts have been made to measure the levels of circulating hormones during syngnathid incubation, the noninvasive determination of hormone levels is difficult in these species due to the restricted amounts of blood obtainable from each individual (Mayer et al. 1993). In spite of this limitation, pooled plasma analyses of brooding and non-brooding pipefish species (genus Syngnathus) indicate that levels of circulating androgens change during male incubation, approaching those detected in female pipefish (Mayer et al. 1993). While efforts were also made to measure circulating PR in this study, levels of this hormone were below the detection limit of the radioactive immunoassay method used. As a temporal shift in PR production is associated with the evolution of viviparity in both elasmobranchs and reptiles, the quantification of fluctuations in circulating PR during syngnathid pregnancy will be invaluable to determine whether the evolution of viviparity in syngnathid males shows a similar pattern of hormone production during pregnancy.

While the genetic study of syngnathid pregnancy is still in its infancy, three recent studies have identified candidate genes that are differentially expressed in the male seahorse or pipefish brood pouch during pregnancy (Zhang et al. 2003, Melamed et al. 2005, Harlin-Cognato et al. 2006). Putative functions of candidate genes involved in pregnancy include haematopoiesis, innate and acquired immune system responses and osmoregulation as well as modifications in cytoskeletal organization (cell proliferation, cell growth) and extracellular matrices (Zhang et al. 2003, Melamed et al. 2005). As many of these functions are also pivotal during mammalian pregnancy (e.g. endometrical remodeling, lectin production and hormonal fluctuations), it is tempting to speculate that at least some of these structures and/or portions of the underlying genetic regulatory networks are homologous (Abouheif 1999) in syngnathids and mammals. Such comparisons, although compelling, await functional characterization of gene function during syngnathid pregnancy.

Table 2 summarizes the major characteristics of male pregnancy in syngnathid fishes. As morphological and physiological traits outlined here are often derived from studies of single species, considerable variation of most traits likely exists within the family, and it is premature to derive general conclusions for this group. If we hope to gain a comprehensive understanding of the development

and diversification of male pregnancy in this group, future research must develop particular model species that vary in their brooding structures, supplementing detailed studies of target species with comparative work on other specialized species in the family.

Outlook and suggestions for future research

There remains much to do in uncovering the genetic and phenotypic changes that occur during seahorse reproduction, work that will undoubtedly lead to new insights into the process of male pregnancy. At the same time, a greater understanding of syngnathid reproduction will open the system for the study of critical research questions in a diversity of disciplines (see below). Seahorses are some of the few marine fish species that can be readily cultured under laboratory conditions. With a short generation time (3-12 months), high fecundity for viviparous species (50-2000 offspring per brood; Foster and Vincent 2004), and a small haploid genome size (500-1000 Mb; Hardie and Hebert 2004), syngnathid fishes offer a tractable model for the study of morphological, reproductive and behavioral variation under controlled laboratory conditions.

Seahorses and pipefish as models for sexual selection

Syngnathid fishes are already important model organisms in the study of the role of relative parental investment on the direction and intensity of sexual selection (Berglund and Rosenqvist 2003, Wilson et al. 2003, Jones et al. 2005). The bulk of traditional sexual selection theory has been derived from, and tested on, species where females invest highly in reproduction and males contribute little more than their gametes (Darwin 1871, Bateman 1948). Seahorses and pipefish have offered an opportunity to test this theory in a system where males make a substantial contribution to reproduction. True to the expectations of the parental investment theory of sexual selection (Trivers 1972), the majority of syngnathid fishes are sex-role reversed (i.e. females compete most intensely for access to mates) (Vincent et al. 1992, Wilson et al. 2003). There are, however, several exceptions to this rule, and research in this area seeks to determine the potential explanations for these exceptions (Wilson and Martin-Smith, 2007), with an aim to further refining a general theory of sexual selection.

Although research into pre-mating sexual selection is well established in syngnathid fishes, the unique mode of reproduction in seahorses and pipefishes raises the intriguing possibility that post-copulatory sexual selection also plays an important role in this group. The study of sperm competition and cryptic female choice in polyandrous animals is an active area of research. Many species mate repeatedly and relatively indiscriminately (Arnqvist and Rowe 2005). As a single copulation is often more than adequate for the fertilization of all eggs carried by a female, researchers have long been puzzled as to why animals mate multiply, when mating increases the risk of predation and reduces foraging time. Parker (1970) was the first to recognize that sperm must compete with one another after copulation to successfully fertilize each egg. Further research has found that this phenomenon is relatively widespread and that cryptic female choice may play an important role in selecting particular sperm for fertilization (Ward 2000, Arnqvist and Rowe 2005).

As fertilization takes place internally in syngnathid fishes, seahorse and pipefish males have complete confidence in paternity (Jones and Avise 2001, Wilson and Martin-Smith 2007) and sperm competition among males is not possible, a phenomenon that may explain the reduced testes size and sperm:egg ratio (2.5:1) in these species (Kvarnemo and Simmons 2004, Van Look et al. 2007). Egg competition is, however, possible and mechanisms of selective fertilization of eggs in polygynous syngnathids may offer males the ability to cryptically choose which eggs to fertilize. As outlined in Table 2, up to 50%of eggs transferred to a male's pouch fail to develop to term (Ahnesjö 1996). While this may simply be due to sperm-egg incompatibilities, it may also be the result of selective fertilization. Pipefish embryos have a semi-permeable chorion (Ripley and Foran 2006) and, as yolk-rich eggs are a rich energy source, unfertilized eggs may be reabsorbed, either by the male himself, or by neighboring embryos, acting as nuptial gifts and/or nurse eggs to maximize growth and thus survival of fertilized embryos (Ahnesjö 1996).

Intrapouch position and its potential effect on embryo development

Intrauterine position (IUP) has long been recognized to play an important role in the development of mammalian embryos (Ryan and Vandenbergh 2002). Depending on the location of embryos in the uterus and their relative position to

one another, the availability of food, oxygen and essential minerals can vary substantially (Ryan and Vandenbergh 2002). At the same time, embryos can influence the development of their neighbors via amniotic transfer of hormones and IUP has been shown to have a significant effect on morphology, physiology and behavior of offspring of most litter-bearing mammals (Ryan and Vandenbergh 2002). Brood sizes of syngnathid fishes can reach up to 2000 embryos, creating ample opportunity for hormonal communication and potentially antagonistic interactions among developing embryos for optimal implantation sites. As indicated above, pipefish embryos lack a rigid chorion (Ripley and Foran 2006), and if this phenomenon is widespread in syngnathid fishes, hormonal communication via the pouch fluid may play a critical role in the development of morphology and physiology of seahorse and pipefish offspring. Despite considerable efforts, research has yet to determine the mechanisms of sex determination in syngnathid fishes. If sex is largely environmentally determined, intrapouch hormone fluctuations and/or gradients may play a critical role in determining offspring sex ratios.)

Conclusions

Mammalian pregnancy and seahorse reproduction exhibit compelling morphological and functional similarities (Table 2), which are being further illuminated by recent investigations of the genetic regulation of syngnathid reproduction. Considering these parallels and the historic use of the term, it seems logical to term syngnathid reproduction an evolving form of male pregnancy. All syngnathid species exhibit lecithotrophic viviparity and the presence of specialized trophic cells in the seahorse brood pouch (Carcupino et al. 2002) suggests an even-more-significant paternal contribution to embryonic development in these species.

Although we have a relatively comprehensive understanding of mammalian pregnancy, our knowledge of syngnathid reproduction is still very basic by comparison. As more researchers discover the syngnathid system and recognize particularities relevant for their own research, experience gained in the study of mammalian pregnancy is likely to inform research in this area and to suggest unexpected and fruitful research directions. While the underlying physiological processes of pregnancy in syngnathids and mammals are likely very different, the

fundamental questions and problems are similar and should be approached in similar ways. With a greater understanding of the genetic, morphological and physiological changes associated with male pregnancy in syngnathid fishes, this system promises a unique comparative model for researchers working on other forms of viviparity. Syngnathid pregnancy has evolved in males, an exceptional development that provides the opportunity to explore how the diversification of this system has been influenced and constrained by a male background. Two morphologically distinct lineages of male pregnancy have evolved in parallel in the Gastrophori and Urophori (Fig. 1). Are the genetic networks involved in syngnathid pregnancy identical in these two lineages and similar to those operating in other vertebrates? How does hormonal control of male pregnancy in syngnathids compare to mammalian reproduction, and how 'female' does a male have to be to become pregnant? Given large structural differences in brooding structures between closely related syngnathid species, how do modes of incubation differ and how have higherlevel structures evolved? With a clearer understanding of the functional similarities and differences in pregnancy in viviparous organisms, the answers to these questions will likely influence the way that we study pregnancy and its evolution in the coming decades.

Acknowledgments

Many thanks to H. Greven (University of Düsseldorf) and J. Wetzel (Presbyterian College) for constructive feedbackon the manuscript. Thanks to P. Damrongphol (Mahidol University) for providing pouch section photographs and to P. Brauchli for assistance in figure preparation.

References

Abouheif E. 1999. Establishing homology criteria for regulatory gene networks: prospects and challenges. *Novartis Found Symp* 222:207- 221.

Ah-King M, Elofsson H, Kvarnemo C, Rosenqvist G, Berglund A. 2006. Why is there no sperm competition in a pipefish with externally brooding males? Insights from sperm activation and morphology. *J Fish Biol* 68:958-962.

Ahnesjö I. 1996. Apparent resource competition among embryos in the brood pouch of a male pipefish. *Behav Ecol Sociobiol* 38:167-172.

Arnqvist G, Rowe L. 2005. Sexual conflict. Princeton, NJ: Princeton University Press.

Azzarello MY. 1991. Some questions concerning the Syngnathidae brood pouch. *Bull Mar Sci* 49:741-747.

Bachelot A, Binart N. 2007. Reproductive role of prolactin. *Reproduction* 133:361-369.

Bateman AJ. 1948. Intra-sexual selection in Drosophila. *Heredity* 2:349- 368.

Beck F. 1976. Comparative placental morphology and function. Env Health Persp 18:5-12.

Benton MJ. 1993. The fossil record 2. London: Chapman & Hall.

Berglund A, Rosenqvist G, Svensson I. 1986. Reversed sex-roles and parental energy investment in zygotes of two pipefish (Syngnathidae) species. *Mar Ecol Prog Ser* 29:209-215.

Berglund A, Rosenqvist G. 2003. Sex role reversal in pipefish. *Adv Stud Behav* 32:131-167.

Binart N, Helloco C, Ormandy CJ, Barra J, Clement-Lacroix P, et al. 2000. Rescue of preimplantatory egg development and embryo implantation in prolactin receptor-deficient mice after progesterone administration. *Endocrinology* 141:2691-2697.

Blackburn DG. 2005. Amniote perspectives on the evolutionary origins of viviparity and placentation. In: Uribe MC, Grier HJ, editors. Viviparous Fishes. Homestead: New Life Publications. p 319- 340.

Blackburn DG. 2005. Evolutionary origins of viviparity in fishes. In: Uribe MC, Grier HJ, editors. Viviparous Fishes. Homestead: New Life Publications. p 303-317.

Blackburn DG. 2006. Squamate reptiles as model organisms for the evolution of viviparity. *Herpetol Monogr* 131-146.

Boisseau JP. 1967. Les re´gulations hormonales de l'incubation chez un vertebré mâle: Recherches sur la reproduction de l'hippocampe. Universite de Bordeaux, 379 p.

Boisseau JP. 1969. Prolactin et l'incubation chez l'hippocampe. Compt Rend Acad Sci Paris, Colloq Int 177:205-215.

Bole-Feysot C, Goffin V, Edery M, Binart N, Kelly PA. 1998. Prolactin (PRL) and its receptor: Actions, signal transduction pathways and phenotypes observed in PRL receptor knockout mice. *Endocr Rev* 19:225-268.

Breder CM, Rosen DE. 1966. Modes of reproduction in fishes. New York: Natural History Press.

Callard IP, Fileti LA, Perez LE, Sorbera LA, Giannoukos G, et al. 1992. Role of the corpus-luteum and progesterone in the evolution of vertebrate viviparity. *Am Zool* 32:264-275.

Carcupino M, Baldacci A, Mazzini M, Franzoi P. 2002. Functional significance of the male brood pouch in the reproductive strategies of pipefishes and seahorses: a morphological and ultrastructural comparative study on three anatomically different pouches. *J Fish Biol* 61:1465-1480.

Chan RS, Gargett CE. 2006. Identification of label-retaining cells in mouse epithelium. *Stem Cells* 24:1529-1538.

Clutton-Brock TH. 1991. The evolution of parental care. Princeton, New Jersey: Princeton University Press.

Crespi B, Semeniuk C. 2004. Parent-offspring conflict in the evolution of vertebrate reproductive mode. *Am Nat* 163:635-653.

Cross JC, Werb Z, Fisher SJ. 1994. Implantation and the placenta: Key pieces of the development puzzle. *Science* 266:1508-1518.

Darmani H, Al Hiyasat AS. 2005. The resin monomer triethylene glycol dimethacrylate exhibits reproductive toxicity in male mice. *Reprod Fertil Dev* 17:401-406.

Darwin C. 1871. The descent of man, and selection in relation to sex. London, England: J. Murray.

Dulvy NK, Reynolds JD. 1997. Evolutionary transitions among egg- Laying, live-bearing and maternal inputs in sharks and rays. *Proc R Soc B* 264:1309-1315.

Dzyuba B, Van Look KJW, Cliffe A, Koldewey HJ, Holt WV. 2006. Effect of parental age and associated size on fecundity, growth and survival in the yellow seahorse *Hippocampus kuda*. *J Exp Biol* 209:3055- 3061.

Foster SJ, Vincent A. 2004. Life history and ecology of seahorses: implications for conservation and management. *J Fish Biol* 65:1- 61.

Froese R, Pauly D. 2006. FishBase. World Wide Web electronic publication www.fishbase.org.

Goicoechea O, Garrido O, Jorquera B. 1986. Evidence for a trophic paternal-larval relationship in the frog *Rhinoderma darwinii*. *J Herpetology* 20:168-178.

Goodwin NB, Dulvy NK, Reynolds JD. 2002. Life history correlates of the evolution of live bearing in fishes. *Phil Trans R Soc B* 357:259- 267.

Gude NM, Roberts CT, Kalionis B, King RG. 2004. Growth and function of the normal human placenta. *Throm Res* 114:397-407.

Haas O, Simpson GG. 1946. Analysis of some phylogenetic terms, with attempts at redefinition. *Proc Am Philosophical Soc* 90:319-349.

Hamlett WC, Hysell MK. 1998. Uterine specializations in elasmobranchs. *J Exp Zool* 282:438-459.

Hardie DC, Hebert PDN. 2004. Genome-size evolution in fishes. *Can J Fish Aquat Sci* 61:1636-1646.

Haresign TW, Shumway SE. 1981. Permeability of the marsupium of the pipefish *Syngnathus fuscus* to 14C-alpha amino isobutyric acid. *Comp Biochem Physiol* 69a:603-604.

Harlin-Cognatio A, Hoffman EA, Jones AG. 2006. Gene cooption without duplication during the evolution of a male-pregnancy gene in pipefish. *Proc Natl Acad Sci* USA 103:19407-19412.

Hayssen V, Lacy RC, Parker PJ. 1985. Metatherian reproduction- Transitional or transcending. *Am Nat* 126:617-632.

Herald ES. 1959. From pipefish to seahorse-a study of phylogenetic relationships. *Proc Cal Acad Sci* 29:465-473.

Jones AG, Avise JC. 2001. Mating systems and sexual selection in male-pregnant pipefishes and seahorses: Insights from microsatellite-based studies of maternity. *J Hered* 92:150-158.

Jones AG, Rosenqvist G, Berglund A, Avise JC. 2005. The measurement of sexual selection using Bateman's principles: An experimental test in the sex-role-reversed pipefish *Syngnathus typhle*. *Integr Comp Biol* 45:874-884.

Knobil E, Neill JD, editors. 1998. Encyclopedia of reproduction. San Diego: Academic Press.

Kornienko ES. 2001. Reproduction and development in some genera of pipefish and seahorses of the Family Syngnathidae. *Russ J Mar Biol* 27: S15-S26.

Kuiter RH. 2000. Seahorses, pipefish and their relatives: Syngnathiformes. Seaford, Australia: Zoonetics. 242 p.

Kvarnemo C, Simmons LW. 2004. Testes investment and spawning mode in pipefishes and seahorses (Syngnathidae). *Biol J Linn Soc* 83: 369-376.

Laksanawimol P, Damrongphol P, Kruatrachue M. 2006. Alteration of the brood pouch morphology during gestation of male seahorses, *Hippocampus kuda. Mar Freshw Res* 57:497-502.

Leiner VM. 1934. Der osmotische Druck in den Bruttaschen der Syngnathiden. *Zool Anz* 108:273-289.

Linton JR, Soloff BL. 1964. The physiology of the brood pouch of the male sea horse *Hippocampus erectus*. *Bull Mar Sci Gulf Carib* 14:45- 61.

Linzer DIH, Fisher SJ. 1999. The placenta and the prolactin family of hormones: Regulation of the physiology of pregnancy. *Mol Endocrinol* 13:837-840.

Mank JE, Avise JC. 2006. Supertree analyses of the roles of viviparity and habitat in the evolution of atherinomorph fishes. *J Evol Biol* 19:734- 740.

Mayer I, Rosenqvist G, Borg B, Ahnesjö I, Berglund A, et al. 1993. Plasma levels of sex steroids in three species of pipefish (Syngnathidae). *Can J Zool* 71:1903-1907.

Mclaren A, Michie D. 1956. Studies on the transfer of fertilized mouse eggs to uterine foster-mothers. 1. Factors affecting the implantation and survival of native and transferred eggs. *J Exp Biol* 33:394-416.

Melamed P, Xue Y, Poon JFD, Wu Q, Xie H, et al. 2005. The male seahorse synthesizes and secretes a novel C-type lectin into the brood pouch during early pregnancy. *FEBS Letters* 272:1221- 1235.

Nelson JS. 2006. Fishes of the World. Hoboken, New Jersey: John Wiley & Sons.

Norwitz ER, Schust DJ, Fisher SJ. 2001. Mechanisms of disease - Implantation and the survival of early pregnancy. *N Engl J Med* 345: 1400-1408.

Parker GA. 1970. Sperm competition and its evolutionary consequences in insects. *Biol Rev Camb Philos Soc* 45:525.

Peters H. 1970. Migration of gonocytes into mammalian gonad and their differentiation. *Phil Trans R Soc B* 259:91-101.

Plusa B, Hadjantonakis A-K, Gray D, Piotrowska-Nitsche K, Jedrusik A, et al. 2005. The first cleavage of the mouse zygote predicts the blastocyst axis. *Nature* 434:391-395.

Poortenaar CW, Woods CMC, James PJ, Giambartolomei FM, Lokman PM. 2004. Reproductive biology of female big-bellied seahorses. *J Fish Biol* 64:717-725.

Pough FH, Janis CM, Heiser JB. 1999. Vertebrate Life. Upper Saddle River, New Jersey: Simon & Schuster.

Quast WD, Howe NR. 1980. The osmotic role of the brood pouch in the pipefish *Syngnathus scovelli*. *Comp Biochem Physiol A* 67:675- 678.

Reynolds JD, Goodwin NB, Freckleton RP. 2002. Evolutionary transitions in parental care and live bearing in vertebrates. *Phil Trans R Soc B* 357:269-281.

Rinkenberger J, Werb Z. 2000. The labyrinthine placenta. *Nat Gen* 25: 248-250.

Ripley JL, Foran CM. 2006. Differential parental nutrient allocation in two congeneric pipefish species (Syngnathidae: *Syngnathus* spp.). *J Exp Biol* 209:1112-1121.

Rothchild I. 2003. The yolkless egg and the evolution of eutherian viviparity. *Biol Reprod* 68:337-357.

Ryan BC, Vandenbergh JG. 2002. Intrauterine position effects. *Neurosci Biobehav Rev* 26:665-678.

Schindler JF, Hamlett WC. 1993. Maternal-embryonic relations in viviparous teleosts. *J Exp Zool* 168:378-393.

Schneider H. 1996. Ontogenic changes in the nutritive function of the placenta. *Placenta* 17:15-26.

Schradin C, Anzenberger G. 1999. Prolactin, the hormone of paternity. *News Physiol Sci* 14:223-231.

Soares MJ, Alam SMK, Konno T, Ho-Chen JK, Ain R. 2006. The prolactin family and pregnancy-dependent adaptations. *Anim Sci J* 77: 1-9.

Stockley P, Gage MJG, Parker GA, Moller AP. 1997. Sperm competition in fishes: The evolution of testis size and ejaculate characteristics. *Am Nat* 149:933-954.

Stulc J. 1997. Placental transfer of inorganic ions and water. *Physiol Rev* 77:805-836.

Tang M, Xu Y, Julian J, Carson D, Tabibzadeh S. 2005. Lefty is expressed in mouse endometrium in estrous cycle and peri-implantation period. *Hum Reprod* 20:872-880.

Travis J. 1993. Immunology-Tracing the immune systems evolutionary history. *Science* 261:164-165.

Trivers RL. 1972. Parental investment and sexual selection. In: Campbell B, editor. Sexual selection and the descent of man. London, England: Heinemann. p 136-179.

Turner CL. 1937. Reproductive cycles and superfetation in poeciliid fishes. *Biol Bull* 72:145-164.

Van Look KJW, Dzyuba B, Cliffe A, Koldewey HJ, Holt WV. 2007. Dimorphic sperm and the unlikely route to fertilisation in the yellow seahorse. J Exp Biol 210:432-437.

Vincent A, Ahnesjö I, Berglund A, Rosenqvist G. 1992. Pipefishes and seahorses: Are they all sex role reversed? *Trends Ecol Evol* 7:237-241.

Wake MH. 1992. Evolutionary scenarios, homology and convergence of structural specializations for vertebrate viviparity. *Am Zool* 32:256-263.

Walker VR, Korach KS. 2004. Estrogen receptor knockout mice as a model for endocrine research. *ILAR Journal* 45:455-461.

Wang MW, Heap RB, Taussig MJ. 1989. Blocking of pregnancy in mice by immunization with anti-idiotype directed against monoclonal anti-progesterone antibody. *Proc Natl Acad Sci* USA 86:7098- 7102.

Ward PI. 2000. Cryptic female choice in the yellow dung fly *Scathophaga stercoraria* (L.). *Evolution* 54:1680-1686.

Warner CM, Exley GE, McElhinny AS, Tang CY. 1998. Genetic regulation of preimplantation mouse embryo survival. *J Exp Zool* 282:272-279.

Wassarman PM, Jovine L, Litscher ES. 2001. A profile of fertilization in mammals. *Nat Cell Biol* 3:E59-E64.

Watanabe S, Hara M, Watanabe K. 2000. Male internal fertilization and introsperm-like sperm of the seaweed pipefish (*Syngnathus schlegeli*). *Zool Sci* (Tokyo) 17:759-767.

Watanabe S, Kaneko T, Watanabe K. 1999. Immunocytochemical detection of mitochondria-rich cells in the brood pouch epithelium of the pipefish, Syngnathus schlegeli: structural comparison with mitochondria- rich cells in the gills and larval epidermis. *Cell Tissue Res* 295:141- 149.

Wetzel J, Wourms JP. 1995. Adaptations for reproduction and development in the skin-brooding ghost pipefishes, *Solenostomus*. *Env Biol Fish* 44:363-384.

Wilson AB, Ahnesjö I, Vincent A, Meyer A. 2003. The dynamics of male brooding, mating patterns, and sex roles in pipefishes and seahorses (Family Syngnathidae). *Evolution* 57:1374-1386.

Wilson AB, Martin-Smith KM. 2007. Genetic monogamy despite social promiscuity in the pot-bellied seahorse (*Hippocampus abdominalis*). *Mol Ecol* 16:2345-2352.

Wilson AB, Vincent A, Ahnesjö I, Meyer A. 2001. Male pregnancy in seahorses and pipefishes (Family Syngnathidae): Rapid diversification of paternal brood pouch morphology inferred from a molecular phylogeny. *J Heredity* 92:159-166.

Woods CMC. 2000. Preliminary observations on breeding and rearing the seahorse *Hippocampus abdominalis* (Teleostei: Syngnathidae) in captivity. NZ *J Mar Freshwater Res* 34:475-485.

Wourms JP, Lombardi J. 1992. Reflections on the evolution of piscine viviparity. *Am Zool* 32:276-293.

Wourms JP. 1981. Viviparity: The maternal-fetal relationship in fishes. *Am Zool* 21:473-515.

Wourms JP. 1994. The challenges of piscine viviparity. *Isr J Zool* 40:551- 568.

Zeller U. 1999. Mammalian reproduction: Origin and evolutionary transformations. *Zool Anz* 238:117-130.

Zhang N, Xu B, Mou C, Yang W, Wei J, et al. 2003. Molecular profile of the unique species of traditional Chinese medicine, Chinese seahorse (*Hippocampus kuda* Bleeker). *FEBS Letters* 550:124-134.

Table 1 Glossary

Term	Definition
Adelphophagy	Embryonic cannibalism of siblings (Schindler and Hamlett 1993)
Analogy	Identity of structure or function in different lineages due to convergent evolution (Haas and Simpson 1946)
Blastocyst	Early bi-layered developmental stage during embryogenesis in which the embryo consists of an some ectodermal component and an inner cell mass enveloping a liquid filled cavity
Histotrophe	Uterine milk - Usually fluid supplemental nutritive substances supplied to the embryosof matrotrophic fishes
Homology	Identity of structure or function resulting from common ancestry (Haas and Simpson 1946)
Hypophysectomy	Ablation of the pituitary gland
Lecithotrophy	Provisioning of the developing embryo by yolk-derived nutrients during development
Matrophagy	Provision of maternal nutrients other than yolk (Schindler and Hamlett 1993)
Matrotrophy	Direct embryonic provisioning by the mother
Oophagy	In utero feeding of embryos on eggs
Oviparity	A reproductive mode in which females lay unfertilized or undeveloped eggs
Patrotrophy	Direct embryonic provisioning by the father
Placenta	Ephemeral organ during gestation expelled at birth, responsible for filtration, nutrient transfer and metabolic and endocrine processes and consisting of a fetal and a parental component
Pseudoplacenta	Ephemeral organs of unknown tissue origin and/or function expelled at parturition
Trophoblast	External cell layer of developing embryo responsible for implantation and the formation of the placenta; functions include pregnancy hormone production, fetal immune protection, increased maternal vascular blood flow and delivery
Trophonemata	Extensions from the uterine mucosa for nutrient delivery and respiration
Trophotaeniae	Perianal embryonic appendages for nutrient uptake and gas exchange
Viviparity	Live bearing - Extended embryonic development inside the parent
Standard definitions taken from Encyclopedia of Reproduction (Knobil and Neill 1998) unless otherwise indicated.	

Table 2 Comparison between characteristics of mammalian and syngnathid pregnancy. The domestic mouse (*Mus domesticus*) is used here as the mammalian model.

Stage of Pregnancy	Mouse (Mammalian) Characteristic	Similar/ Different/ Unknown (=/≠/?)	Syngnathid Characteristic
Egg production	Atresia of standing oocytes (Peters 1970, Rothchild 2003)	≠	Continuous egg production (Kornienko 2001, Poortenaar et al. 2004)
Fertilization	Sperm transfer from the male to the female (Wassarman et al. 2001)	≠	Egg transfer from female to male (Herald 1959)
	Internal fertilization in the oviduct (Wassarman et al. 2001)	=	
	<20 eggs fertilized per mating (Mclaren and Michie 1956)	≠	Intrapouch fertilization (Watanabe et al. 2000, Van Look et al. 2007)
	$6x10^6$ sperm / testis (Darmani and Al Hiyasat 2005)	≠	Up to 2000 fertilized eggs per mating (Foster and Vincent 2004)
	6 mg testes/g body weight (Darmani and Al Hiyasat 2005)	≠	Highly reduced sperm number (as few as 150 sperm / testis;Watanabe et al. 2000, Van Look et al. 2007) 1 mg testes/g body weight (Kvarnemo and Simmons 2004)
Implantation	6-10 days post-fertilization (Nowritz et al. 2001)	≠	Immediate implantation in pouch epithelium after fertilization (Boisseau 1969)
Morphological adaptation	Extensive endometrical remodeling during gestation (Tang et al. 2005)	=	Extensive alteration of the brood pouch inner tissue layers (Laksanawimol et al. 2006)
Aeration	Embryonic-placental interface highly vascularized (Rinkenberger and Werb 2000)	=	Internal surface of brood pouch highly vascularized (Carcupino et al. 2002)
Ion Exchange	Passive exchange of Na^+ and Cl^- / Active transport of K^+, Mg^{2+}, Ca^{2+} and P_i (Stulc 1997)	=	Paternal osmoregulation of pouch salinity (Leiner 1934, Linton and Soloff 1964) Mitochondrial-rich cells which line the brood pouch in pipefish likely serve an osmoregulatory role (Carcupino et al. 2002)
Embryonic nutrient supply	Small eggs with little or no yolk (80µm) (Rothchild 2003, Plusa et al. 2005)	≠	Large yolk-rich eggs (900-2000µm; Kornienko 2001, Foster and Vincent 2004)
		≠	
	Matrotrophy: Energy supply via the placenta (Rothchild 2003)	=	*Lecithotrophy*: Embryos are almost exclusively dependent on yolk for nutrients (Berglund et al. 1986, Azzarello 1991)
		?	Semi-permeable chorion (Ripley and Foran 2006)
		?	Minor paternal nutrient contributions likely (Boisseau 1967, Haresign and Shumway 1981, Azzarello 1991, Laksanawimol et al. 2006)
Immune responses		=	Putative trophic role of specialized secretory cells in seahorses (Carcupino et al. 2002)
	Changes in innate and adaptive immune system (Travis 1993)		Lectin production associated with antibacterial activity *in vitro* (Melamed et al. 2005)

Table 2 continued

Birth	Via parturition, including explusion of placenta (Cross et al. 1994) followed by remodeling of epithelia (Chan and Gargett 2006)	=	Expulsion of pseudoplacenta in pipefish with release of free-living juveniles (Watanabe et al. 1999) and/or embryo release and renewal of inner pouch epithelia (Laksanawimol et al. 2006)
Post-natal care	Highly developed parental care (Clutton-Brock 1991)	≠	No parental care (Foster and Vincent 2004)
Duration of pregnancy	20-21 days (Cross et al. 1994)	≠	Temperature-dependent (9-69 days; Woods 2000, Foster and Vincent 2004)
Embryo survival	15-50% mortality prior to implantation (Warner et al. 1998)	=	20-50% embryos inviable (Ahnesjö 1996)
Hormonal regulation	Increased circulating prolactin (PRL) during early pregnancy (Linzer and Fisher 1999, Soares et al. 2006)	=	PRL critical for pouch maintenance and embryo development (Boisseau 1967)
	Progesterone (PR; Wang et al. 1989)	=	Exogenous PR treatment rescues brood pouch function in hypophysectomised seahorses (Boisseau 1967)
	Estrogen (ER; Walker and Korach, 2004)	≠	No fluctuation in circulating ER during incubation (Mayer et al. 1993)

Figure 1 Phylogenetic relationships of syngnathid fishes

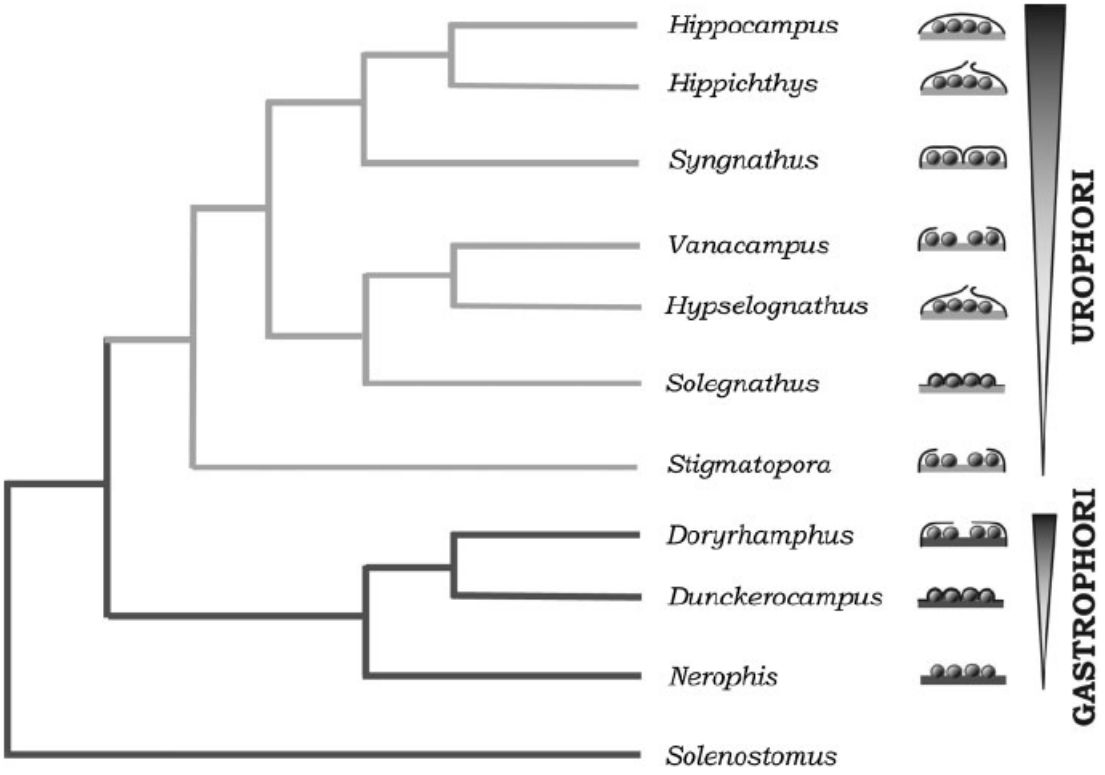

Phylogenetic relationships of syngnathid fishes (Wilson et al. 2001, Wilson et al. 2003). Pouch morphology is depicted by schematic pouch cross sections; coloured triangles indicate increasing complexity. Phylogenetic analyses suggests that independent increases in pouch complexity have occurred in both major pouch lineages (Wilson et al. 2003). Morphological and molecular phylogenetic analyses indicate that *Solenostomus* spp. are the closest living relatives of syngnathid fishes (Wilson and Orr, unpublished data). Note: Only one genus per pouch type is shown here. Gastrophori=Abdominal brooder; Urophori=tail brooder.

Figure 2 Morphological and histological changes during seahorse pregnancy

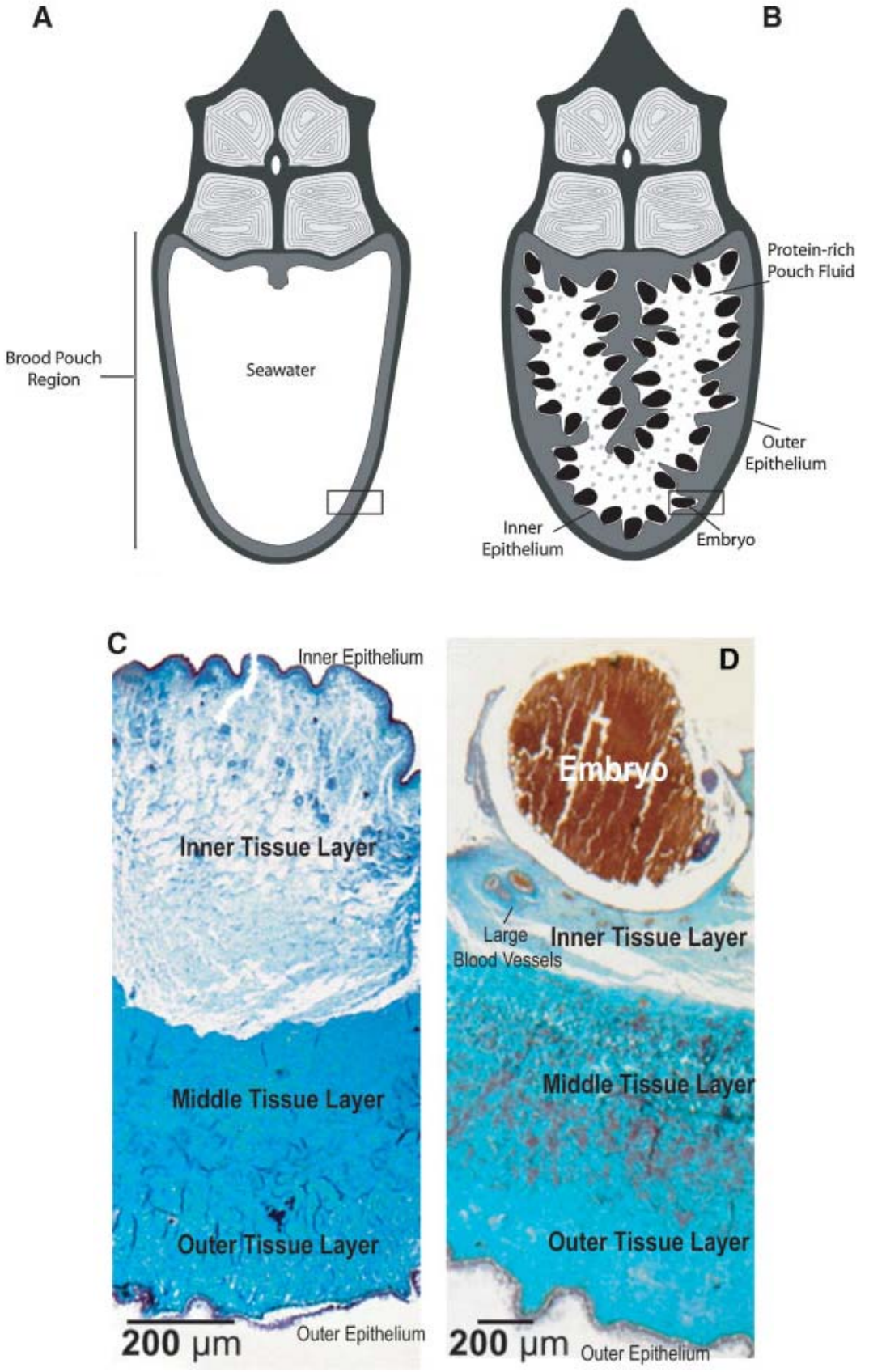

Major morphological and histological changes occur during seahorse pregnancy: A: Cross-section of a seahorse brood pouch prior to incubation; B: Cross-section of an incubating seahorse brood pouch; C: Haematoxylin/eosin (HE)-stained section of a nonincubating male brood pouch; D: HE-stained section of incubating male pouch. A folded inner epithelial layer and smooth outer epithelial layer cover the brood-pouch tissues. Inner tissue layer, middle tissue layer with smooth muscle fibres and outer tissue layer indicated; muscle fibres are likely involved in the process of parturition (Laksanawimol et al. 2006). Note increased density of large blood vessels around the embedded embryo during incubation. Images C & D: Reproduced with permission from Marine and Freshwater Research 57:497-502, Figure 1 (P Laksanawimol, P Damrongphol & M Kruatrachue).

Figure 3 Brood pouch cellular specialization and differentiation during male pregnancy

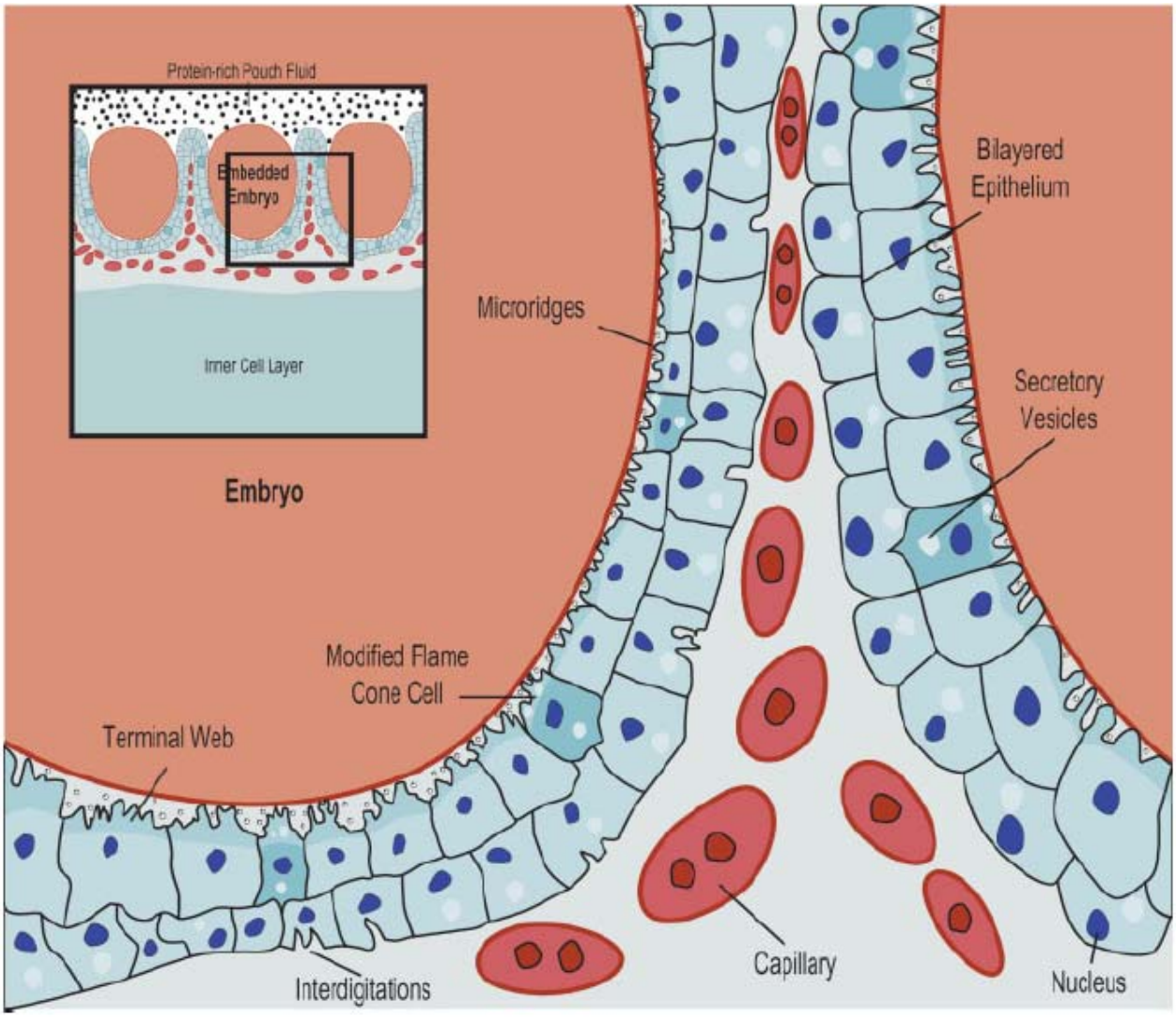

Brood pouch cellular specialization and differentiation occurs during male pregnancy of seahorses (Boisseau 1967, Carcupino et al. 2002, Laksanawimol et al. 2006). Note stratification of the pseudo-columnar inner epithelium into a bi-layered epithelium during incubation, accompanied with changes in inner layer thickness and increased vascularisation of pouch tissue surrounding the embryo.

CHAPTER II: Cost-Effective Fluorescent Amplified Fragment Length Polymorphism Analyses

Kai N. Stölting, Wolf U. Blankenhorn, and Anthony B. Wilson

For publication in: *Molecular Ecology Resources*

Abstract

Amplified fragment length polymorphisms (AFLP) are a widely used multi-purpose DNA fingerprinting tool. The ability to size-separate fluorescently-labelled AFLP fragments on an automated DNA sequencer has provided a means for high-throughput genome screening, an approach particularly useful in non-model organisms. While the 'per-band-generated' costs for each AFLP marker are low, fluorescently-labelled oligonucleotides remain costly. We present a cost-effective method for fluorescently endlabelling AFLPs that should make this tool more readily accessible for laboratories with reduced budgets. Standard fluorescent AFLPs and its endlabelled alternatives are repeatable and produce similar numbers of fragments, though, given the differences in the AFLP profiles generated with the two methods, it is not recommended to combine data generated using both approaches. For researchers commencing a new AFLP project, the AFLP-endlabelling method outlined here is easy to implement, as it does not require major changes to PCR protocols and should significantly reduce the costs of AFLP experiments.

Background

Amplified fragment length polymorphism (AFLP) analyses are some of the most widely used DNA fingerprinting techniques (Vos et al. 1995, Meudt et al. 2007). The AFLP method can be used on all types of double-stranded nucleic acids, and has been used to rapidly fingerprint both genomic DNA (henceforth: DNA) and complementary DNA produced from messenger-RNA (henceforth: cDNA). The AFLP method involves the double-digestion of (c)DNA with two restriction enzymes (typically: *EcoRI* and *MseI*). Digests are followed by two rounds of preselective and selective PCR-amplification. Selective amplifications use up to three selective base pairs to reduce the absolute number of fragments screened per PCR. PCR products are then separated by size on a traditional agarose or acrylamide gel apparatus. The length of size-separated fragments is recorded, and the presence or absence of a fragment of a given size is compared across samples. The use of high-throughput fluorescent sequencing machines permits the rapid screening of large numbers of fragments in many samples, and has now become standard for AFLPs.

AFLP analyses (Vos et al. 1995) are commonly used in population genetic and parentage studies and have been used for phylogenetic inference and genetic mapping in both model and non-model organisms (Meudt et al. 2007). AFLPs are also a powerful tool for the identification of both candidate genes (Bachem et al. 1996, Stölting et al. 2009) and genomic markers (Terauchi et al. 1999). The nearly 3000 (as of December 2009, ISI Web of Knowledge search, using “AFLP” or “amplified fragment length polymorphism” as topic) AFLP studies published since the initial description of the method in 1995 highlight the impact this method has had on population genomics. Given that AFLPs do not require previous knowledge of the underlying DNA sequence, this method is particularly attractive for genome-level studies of non-model organisms.

While the per-marker-generated costs of AFLP are relatively low, start-up costs can be high, and a significant portion of the costs associated with high-throughput AFLP approaches is due to the need for individually fluorescently-labelled oligonucleotides. These labelled oligonucleotides are required for the automated detection of fragments generated by each combination of selective primers, and a single probe can cost upwards of US$100 (Applied Biosystems). For high throughput screens, the price of fluorescently-labelled selective

oligonucleotides (oligos) can constitute a large fraction of experimental costs. Often, labelled oligonucleotides will be purchased for a single study and, as fluorescently-labelled oligos are light-sensitive and deteriorate over time, a substantial fraction of this financial investment is ultimately wasted. These costs can be prohibitive in studies where the number of selective PCRs undertaken is critical for the screening success. This is especially the case with cDNA-AFLP screens, which require the execution of many selective PCRs per sample (Stölting et al. 2009).

Despite these costs, high throughput AFLP analyses may still be cost-effective when expenses are considered on a "per-marker" basis. One obvious approach to minimize the costs of an AFLP experiment is to maximize the number of fragments screened per PCR reaction. If this were feasible, the total number of amplifications required could be greatly reduced. Considerably fewer fluorescently-labelled AFLPs would be needed, and the overall costs of the screen could be minimized. Gort and colleagues (2006) illustrated the potential problems associated with this approach, demonstrating that high-throughput screening may increase the risk of obtaining size-homoplasious DNA fragments with similar electrophoretic motility. A decrease in the number of fragments screened per reaction can significantly increase the quality of the screen (Gort et al. 2006). There is thus a trade-off between data quantity and quality, negating the potential benefits of screening large numbers of fragments in a single AFLP reaction.

Here, we provide a cost-effective alternative for large scale high-throughput AFLP screening, adapting the microsatellite-endlabelling method of Schuelke (2000) for fluorescently-labelled AFLPs. In brief, Schuelke's M13-endlabelling method uses a single fluorescently-labelled oligonucleotide containing a standard M13 (-21) sequence. By including this M13 sequence at the 5'-end of one of the two unlabelled selective PCR primers, standard PCR can incorporate the fluorescent label. The use of a high annealing temperature during the first cycles of a PCR reaction generates large numbers of unlabelled products with the selective primers. After several cycles of product-specific PCR, the annealing temperature is reduced, allowing the incorporation of the fluorescently-labelled M13 probe into the complementary PCR product. Labelled PCR products can thus be generated which are extended by the length of the fluorescent adaptor but are otherwise homologous to those produced in a standard fluorescent PCR. In spite

of the frequent use of the M13 adaptor in microsatellite endlabelling, *in silico* PCR software suggests that this adaptor sequence may not be ideally suited as PCR primer (Kalendar et al. 2009). We designed two additional endlabelling alternatives with improved base composition (Table 1). We term these additional endlabelled alternatives ELA1 and ELA2 and test their function together with the M13 label *in vitro*.

Our aims are here to apply the endlabelling technique to fluorescent AFLPs and to provide a concise, easy-to-implement protocol for this method. We compare endlabelled AFLP products to those generated by standard fluorescent methods and test methods for improving the performance of endlabelled AFLP alternatives. We also test whether data produced with standard and endlabelled AFLPs can be directly combined. As one of the major advantages of fluorescently-labelled AFLPs is the opportunity for automated scoring, we compare the relative performance of endlabelled and standard AFLPs both with automated scoring and the more traditional (and more time consuming) manual detection.

Results

Endlabelled and standard fluorescent AFLPs produce similar numbers of fragments per reaction (205-219 fragments per reaction, Table 1). While the internal repeatability of manually-scored standard AFLPs is high (>92%, Table 1), the repeatability of manually-scored endlabelled AFLPs (ELA1 data shown here) averages ~80% (Table 1). A direct comparison of the repeatability of standard and endlabelled methods should be based on common fragments produced by both methods. 148 homologous fragments could be identified for the AFLP reaction carried out here, and the repeatability estimates for this reduced dataset are similar to those reported for the full datasets (Table 1), indicating that the reduced internal repeatability of endlabelled AFLPs is not due to spurious products generated with this method. The internal repeatabilities of both endlabelled and standard AFLPs are much lower when fragments are scored using the automated fragment calling routines implemented in GENEMAPPER (Table 1). Standard labelled AFLPs are ~76% repeatable when using automated scoring, while only ~70% of endlabelled AFLPs fragments can be reliably recovered.

We tested alternative endlabelling primers to evaluate which method recovers the greatest number of fragments generated with standard AFLP (Table 2). 62 – 72% of the reference standard fragments can be recovered using manually-scored endlabelling methods, values that reduce by ~6% when using automated scoring (Table 2). Among the three fluorescently-endlabelled alternatives, the ELA1 adaptor is best at recovering the reference standard (148/205 bands recovered=72.2% recovery, Table 2). Considering that up to 45% of the fragments generated in the reference standard are not recovered using endlabelled primers, it is not advisable to combine data generated using standard and endlabelled AFLP.

Purging of unreliable fragments can increase fragment recovery rates (Table 2, compare lines A and B), especially when using automated scoring (up to 10% improvement over unpurged data, compare A and B, Table 2). In case of manual scoring these unreliable fragments seem to have little effect on the overall recovery of reference standard fragments and such a quality control does not appear to be warranted when data are manually screened (Table 2). It is noteworthy that manual scoring of standard AFLP data produces 178 fragments which are 100% repeatable out of 205 fragments scored in total, substantially

more than the 79 out of 212 fragments which are repeatable when automatic scoring routines are used. When all unreliable fragments are removed from analyses, the recovery rate of automatic scoring is similar to that of the manual scoring method (compare purged data B, Table 2, average recovery across endlabelling methods = 68%, manual=67%).

Discussion and Conclusions

We have implemented Schuelke's (2000) method of fluorescent endlabelling for AFLP data. Endlabelled AFLPs offer a cost-effective means for fluorescently scoring AFLPs, and only minor changes are required to existing AFLP protocols. While the endlabelling method is less repeatable than standard AFLP when data are manually scored, the repeatabilities of endlabelled and traditional fluorescent AFLPs are comparable when using automated scoring (Table 1).

We have tested several alternative adaptor sequences for endlabelled AFLPs which vary in their predicted quality. In contrast to our expectations, primer quality does not explain differences in the performance of these endlabelled methods. Major differences in the repeatabilities of manually-scored endlabelled and standard AFLP fragments remain observable, as well as differences in the lengths and numbers of fragments produced, differences that argue against the combination of endlabelling and traditional fluorescent AFLP data in the same study.

While time-consuming, the manual scoring of fluorescently-labelled AFLP products far outperforms the automated scoring methods implemented in standard software. The performance of automated scoring can be improved by excluding unreliable products, but the determination of product reliability is only possible after extensive screening of replicated PCR reactions. As this screening largely negates the time benefits obtained by automated screening, it is recommended to manually screen AFLP products whenever the reliability of individual products is critical, and particularly in small scale projects. This is particularly important in genetic mapping projects and for experiments in which cDNA-AFLP screening is used to detect differences in the expression of individual genes. In such cases, individual errors can compromise a wider analysis and the time required for manual scoring is justified by its higher repeatability. When conducting large scale screens requiring the AFLP-profiling of many individuals, an initial repeatability screen for each AFLP primer combination can help to increase the quality of the data by providing a means to remove poorly performing AFLP markers from subsequent analyses, a step that can also be used to develop more stringent parameters for automated AFLP scoring, which can improve the reliability of this method (Holland et al. 2008).

Methods

Sampling

We compared the performance of endlabelled and standard fluorescent AFLPs using genomic DNA of eight individual seahorses (*Hippocampus abdominalis*). We used the same eight individuals throughout our analyses to allow for direct comparisons, and each sample was replicated six times to allow for a robust test of repeatability. We generated AFLP fragments with a single selective primer combination – *EcoRI*-ACA and *MseI*-CAA – and compared both manual and automated fragment scoring with standard fluorescent AFLPs and its endlabelled AFLP alternatives.

Laboratory protocols

Only minor modifications to the standard fluorescent AFLP protocols are necessary when using our endlabelling approach. Both methods generate fragments from as little as 100ng double-stranded DNA digested with 10 units of restriction enzymes *EcoRI* (G^AATTC) and *MseI* (T^TAA; New England Biolabs [NEB], Ipswich, MA, USA) each at 37°C for 2 hours. The double-digest is performed in 1x of the *EcoRI*-buffer and 1x BSA and is followed by 15 minute enzyme-inactivation at 65°C.

Ligation reactions in 20µL final reaction volume combine 50 pMol *MseI*- and 5 pMol *EcoRI*-adaptors (final concentrations of 2.5µMol and 0.25µMol, respectively, Table 3) with sticky DNA ends at 37°C for 3 hours using one unit of T4 DNA ligase (NEB) in 1x ligation buffer (NEB). The difference in the relative concentration of adaptors is motivated by the super-abundance of *MseI*–restriction sites compared to those produced by *EcoRI*. The ligation of adaptors is followed by preselective amplifications performed in 20µL reaction volumes. These preselective amplifications contain 1M betaine (Sigma, St. Louis, MO, USA), 0.25mM dNTPs (Roche Diagnostics, Mannheim, Germany), 0.5µM of each *EcoRI* and *MseI* preselective primers (Table 3) and 1 U of Taq polymerase (NEB) in 1x Taq-reaction buffer (NEB). The mixture is cycled in a Tetrad DNA Engine 2 thermal cycler (BioRad, Hercules, CA, USA) limited to a maximum ramping speed

of 1°C per second. The protocol consists of 20 PCR cycles at 94°C for 30sec, 56°C for 60 seconds and 72°C for 60 seconds.

Selective amplification reactions in 5µL total reaction volume provide sufficient amounts of AFLP products for fluorescent sequencing and contain 0.25mM dNTPs, 4.625mM $MgCl_2$ (Sigma, St. Louis, MO, USA), 1x Taq reaction buffer (NEB) and 1 U Taq (NEB). While final concentrations of 0.5µM of both fluorescently-labelled *EcoRI*- and unlabelled *MseI*-selective primers are used in standard AFLP reactions, the endlabelled alternatives contain only 0.125µM of the 5'-tailed unlabelled selective *EcoRI* primer. The DNA sequence of these unlabelled selective *EcoRI* primers consists of the standard *EcoRI*-primer sequence and a 5'-tailing sequence (Table 3). For the endlabelled reactions the selective PCR also contains 0.5µM of the universal labelled oligonucleotide. Here, we test three alternative oligos which differ slightly in their nucleotide composition and in their overall primer quality scores (M13 = 85, ELA1 = 88, ELA2 = 93, predicted by FASTPCR; Kalendar et al. 2009). OneµL of 1:10 diluted preselective PCR product is used in the selective amplification reactions. Selective amplification temperature profiles are identical for both standard and endlabelled AFLPs. An initial denaturing step separates DNA strands for 2 min at 94°C and is followed by 10 touchdown PCR cycles run at 94°C for 30 seconds, 65°C for 30 seconds (decreasing by 1°C per cycle) and 72°C for 60 seconds. This touchdown is followed by 30 additional PCR cycles which are run at a constant 56°C annealing temperature. All other parameters for these 30 PCR cycles are identical to the touchdown steps stated above. Fragment completion is achieved via a 30 minute final elongation step at 72°C.

After amplification, 1µL of the undiluted selective PCR product is mixed with 0.125µL Genescan-500 LIZ Size Standard (Applied Biosystems, Warrington, UK) in a mixture of 10µL formamide (Sigma, St. Louis, MO, USA) and 10µL MilliQ-water for size detection on a 48-capillary automated ABi 3730 sequencer (Applied Biosystems, Warrington, UK).

Fragment Analyses

Automated fragment analysis used the manufacturer's default settings for AFLP projects as implemented in GENEMAPPER 4.0 (Applied Biosystems), while manual scoring was performed on hardcopies of electropherograms generated by

GENEMAPPER. While automated fragment scoring in GENEMAPPER is fast, this method can be susceptible to peak-detection errors (Holland et al. 2008). These errors occur during the fragment calling step, in which the shape of each peak in the electropherogram as well as the absolute strength of its signal are considered by the calling algorithm. We compared the repeatability of the endlabelling AFLP alternative and the standard fluorescent AFLP genotyping using a measure of repeatability calculated from between and within group variances provided by ARLEQUIN 3.11 (Schneider et al. 2000) for each dataset according to the recommendations of Becker (1992). In addition, the average number of pair-wise fragment differences between samples was recorded.

Manual and automated scoring procedures are not necessarily calling identical fragments, and the two datasets may differ substantially in the number and length of fragments scored. To facilitate the direct comparison of these two analysis methods, we analyzed internal repeatabilities independently for each method, and also generated a dataset of homologous fragments present in both methods, which was used to calculate repeatabilities across methods for this subset of the data.

The ligation of the fluorescent endlabel elongates AFLP fragments by the sequence length of the adaptor (Table 3), and this length difference must be taken into account when homologizing fragments by size. Throughout all analyses reported here we analyzed fragments in the range of 100-450bp length (standard AFLPs) and their size-homologous counterparts in the endlabelled AFLP variants. Endlabelled AFLP fragments are 18-20bp longer than standard AFLP fragments (Table 3), and for the endlabelled alternatives this elongation results in an analyzed size range of 118-468bp length (ELA1) and 120-470bp length (ELA2).

In comparing fragment sets generated with the traditional fluorescent AFLP method to those generated with its endlabelling alternatives, all fragments are treated as being equally informative and of comparable quality. However, in standard AFLPs some fragments are less repeatable than are others and these unreliable fragments might be expected to contribute disproportionately to the observed differences between endlabelled and traditional AFLP methods. In order to avoid a negative bias in our comparisons, the reference standard dataset was checked for these potentially ambiguous bands. We compared the overall, un-purged dataset (see A in Table 2), with a dataset from which all bands with less

than 100% internal repeatability were removed (B). If all these highly repeatable AFLP products were recovered with both standard and end-labelled AFLP screens, it would be possible to combine data from these two methods. To evaluate which of the endlabelling oligos tested here performs better under the conditions used for the amplification of standard AFLPs, we compared the rates with which reference standard fragments are recovered in endlabelled AFLPs.

Acknowledgements

Constructive comments from Luc F. Bussière improved the MS. Financial support from the Forschungskredit der Universität Zürich to KNS is and from the University of Zurich to ABW and WUB is gratefully acknowledged.

References:

Bachem CWB, van der Hoeven RS, de Bruijn SM, Vreugdenhil D, Zabeau M, Visser RGF. 1996. Visualization of differential gene expression using a novel method of RNA fingerprinting based on AFLP: Analysis of gene expression during potato tuber development. *Plant Journal* 9:745-753.

Becker WA. 1992. Manual of quantitative genetics. Pullman, WA. Students Book Corporation.

Gort G, Koopman WJM, Stein A. 2006. Fragment length distributions and collision probabilities for AFLP markers. *Biometrics* 62:1107-1115.

Holland BR, Clarke AC, Meudt HM 2008: Optimizing automated AFLP scoring parameters to improve phylogenetic resolution. *Systematic Biology* 57:347-366.

Kalendar R, Lee D, Schulman AH. 2009. FastPCR Software for PCR Primer and Probe Design and Repeat Search. *Genes, Genomes and Genomics*. 3.

Meudt HM, Clarke AC. 2007. Almost forgotten or latest practice? AFLP applications, analyses and advances. *Trends in Plant Science* 12:106-117.

Schneider S, Roessli D, Excoffier L. Arlequin 2000. A software for population genetics data analysis. Ver 2.000. Genetics and Biometry Lab, Dept. of Anthropology, University of Geneva.

Schuelke M 2000. An economic method for the fluorescent labeling of PCR fragments. *Nature Biotechnology* 18:233-234.

Stölting KN, Gort G, Wüst C, Wilson AB 2009. Eukaryotic transcriptomics *in silico*: Optimizing cDNA-AFLP efficiency. *BMC Genomics* 10:565.

Terauchi R, Kahl G 1999. Mapping of the *Dioscorea tokoro* genome: AFLP markers linked to sex. *Genome* 42:752-762.

Vos P, Hogers R, Bleeker M, Reijans M, Vandelee T, Hornes M, Frijters A, Pot J, Peleman J, Kuiper M, Zabeau M 1995. AFLP - A new technique for DNA-fingerprinting. *Nucleic Acids Research* 23:4407-4414.

Table 1 Comparison of the repeatability of manual and automated scoring

Comparison of the repeatability of manual (**man**) and automated (**auto**) scoring of AFLP fragments derived from a single selective primer combination (*EcoRI*-ACA and *MseI*-CAA) using two methods of fluorescent labelling (**standard AFLP**, **ELA1**). Repeatability estimates have been derived from six replicate runs of 8 *Hippocampus abdominalis* individuals and reflect intra-individual repeatability of AFLP fragments. Results are presented for the total dataset (**complete**) as well as the subset of fragments that were recovered with standard and endlabelled AFLP (matching). The total number of scorable fragments (**N (Frag.)**), the number of variable fragments (**Variable frag.**), the number of fragments which are repeatable in all individuals (**100% rep. frag.)** and the average number of pair-wise fragment differences (**Avg diff**) is reported for each method. An asterisks indicates datasets which are used as reference in the estimation of recovery success of endlabelled AFLP methods (Table 2). Repeatability estimates are indicated together with approximate standard errors (**SE**) *sensu* Becker (1992).

Method	Dataset	Scoring Method	N (Frag.)	Variable frag.	100% rep. frag.	Avg diff	Repeatability ± 1SE
Standard AFLP	Complete	Man	**205***	27	**178***	1.758	94.57% (91.53%-97.61%)
Standard AFLP	Matching manually-scored ELA1	Man	148	21	127	1.483	92.15% (87.85%-96.45%)
Standard AFLP	Complete	Auto	**212***	133	**79***	13.175	75.89% (64.61%-87.17%)
Standard AFLP	Matching automatically-scored ELA1	Auto	144	87	57	8.725	76.28% (65.14%-87.42%)
ELA1	Complete	Man	219	57	162	4.992	80.04% (70.29%-89.79%)
ELA1	Matching manually-scored standard AFLP	Man	148	30	118	2.433	81.70% (72.62%-90.78%)
ELA1	Complete	Auto	213	151	62	16.842	69.72% (56.46%-82.98%)
ELA1	Matching automatically-scored standard AFLP	Auto	144	90	54	10.55	69.90% (56.7%-83.1%)

Table 2 Recovery success of standard AFLP fragments

The absolute number and fraction of fragments generated by traditional AFLPs that are also recovered using endlabelled fluorescent AFLP alternatives. Endlabelled AFLP alternatives have been compared to reference standard fragments generated with traditional fluorescent AFLP using *EcoRI*-ACA and *MseI*-CAA (**Std.**). Recovery success is reported for three endlabelled AFLP alternatives (**M13, ELA2, ELA1**) tested on eight *Hippocampus abdominalis* individuals. Here, **A)** reports the comparison for the complete dataset of fragments generated by standard AFLPs, while the dataset reported in **B)** includes only those fragments which are 100% repeatable in all six replicates of 8 individuals using the standard methods. For each comparison, the absolute number of fragments recovered and the recovery rate of reference standard fragments (**Std.**) are indicated. The best-performing method for each comparison is highlighted in bold.

Dataset	Manual scoring				Automated scoring			
	Std.	M13	ELA1	ELA2	Std.	M13	ELA1	ELA2
A	205	141 68.78%	**148** **72.20%**	127 61.95%	212	133 62.74%	**144** **67.92%**	118 55.66%
B	178	122 68.54%	**127** **71.35%**	111 62.36%	79	**57** **72.15%**	**57** **72.15%**	48 60.76%

Table 3 Required oligonucleotides for standard and endlabelled AFLPs

PCR primers (**Primer**) used for standard (**Std**) and endlabelled (**End**) AFLP applications. Base pair sequences (**Sequence**) are indicated in the 5' to 3' orientation, as are the lengths of oligonucleotides in base pairs (**length**) and the estimated annealing temperatures ($\mathbf{T_M}$). The typically used per-reaction concentrations each oligonucleotide are indicated (**Conc.**). Note that *EcoRI* and *MseI* adaptors I and II must be combined before use (see protocol). **N**s indicated in primer sequences should be replaced by selective base pairs.

Primer	Sequence (5' -3')	Length	T_M	Application	Conc.
***EcoRI*-Adaptor I**	CTCGTAGACTGCGTACC	17	51.4°C	Std, End	0.25 µMol
***EcoRI*-Adaptor II**	AATTGGTACGCAGTCTAC	18	49.0°C	Std, End	
***MseI*-Adaptor I**	GACGATGAGTCCTGAG	16	48.1°C	Std, End	2.5 µMol
***MseI*-Adaptor II**	TACTCAGGACTCAT	14	39.8°C	Std, End	
***EcoRI*-PS**	GACTGCGTACCAATTC**A**	17	49.2°C	Std, End	0.5 µMol
***MseI*-PC**	GATGAGTCCTGAGTAA**C**	17	47.1°C	Std, End	0.5 µMol
***EcoRI*-Sel**	GACTGCGTACCAATTC**ANN**	19	51.8°C	Std	0.5 µMol
***MseI*-Sel**	GATGAGTCCTGAGTAA**CNN**	19	49.8°C	Std, End	0.5 µMol
M13	TGTAAAACGACGGCCAGT	18	53.9°C	End	0.5 µMol
ELA1	GACCAAGTCCAGAAGACC	18	52.2°C	End	0.5 µMol
ELA2	GACGTTGTAAAACGACGGCC	20	56.8°C	End	0.5 µMol
***EcoRI*-M13 Sel**	TGTAAAACGACGGCCAGTG-ACTGCGTACCAATTC**ANN**	37	66.5°C	End	0.125 µMol
***EcoRI*-ELA1 Sel**	GACCAAGTCCAGAAGACCG-ACTGCGTACCAATTC**ANN**	37	66.5°C	End	0.125 µMol
***EcoRI*-ELA2 Sel**	GACGTTGTAAAACGACGGC-CGACTGCGTACCAATTC**ANN**	39	67.8°C	End	0.125 µMol

Figure 1 Comparison of traditional and endlabelled fluorescent AFLP

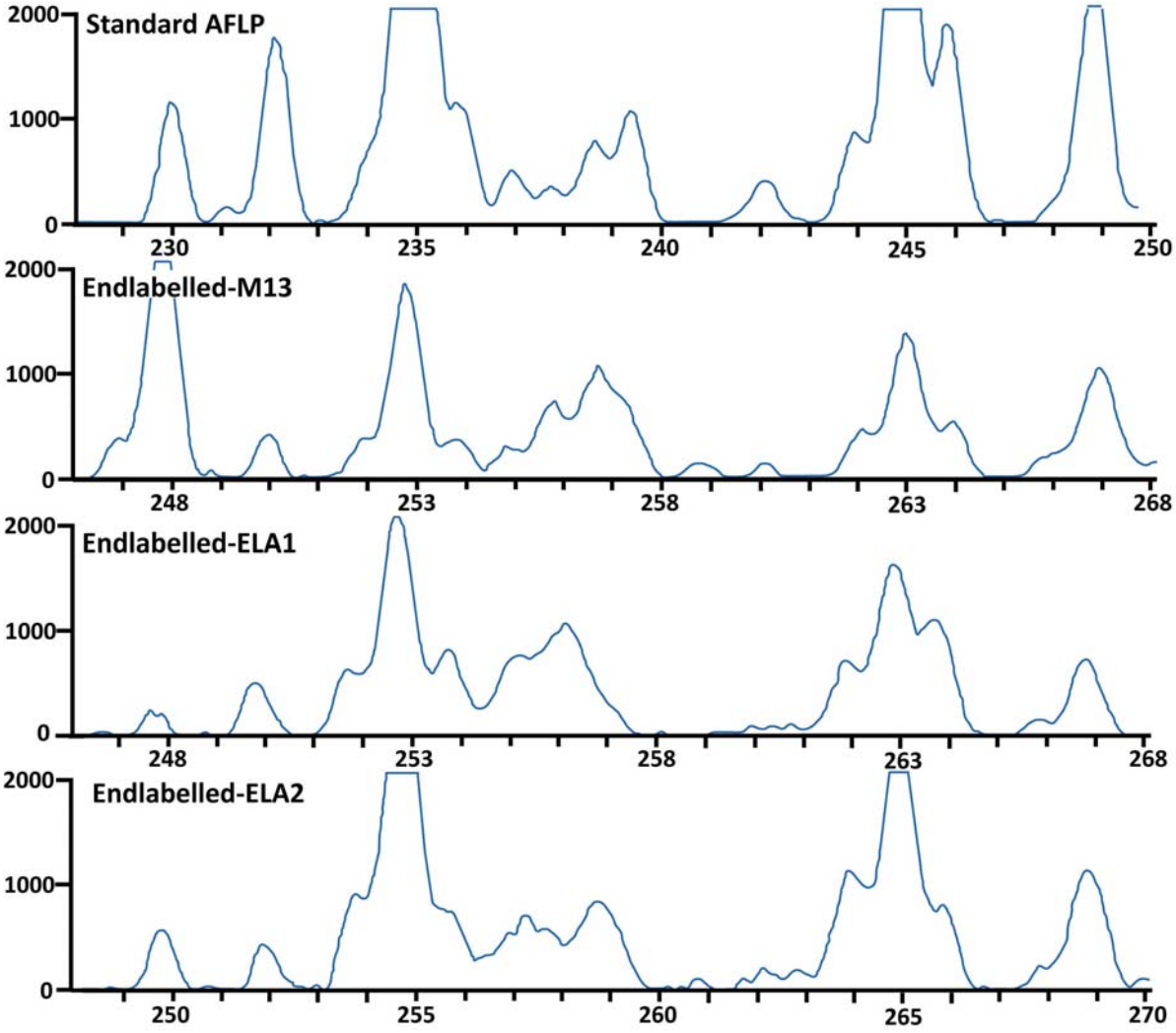

Electropherograms of traditional fluorescently-labelled AFLP (**Standard AFLP, top**) and the endlabelled AFLP alternatives M13, ELA1 and ELA2. This figure depicts partial, 22 base pair long electropherograms from the same *Hippocampus abdominalis* individual. Note: Electropherograms have been offset to incorporate increases in the size of endlabelled AFLP products (M13:18bp, ELA1: 18bp, ELA2:20bp).

CHAPTER III: Eukaryotic Transcriptomics *in silico*: Optimizing cDNA-AFLP Efficiency

Kai N Stölting, Gerrit Gort, Christian Wüst and Anthony B Wilson

Published in: *BMC Genomics* 2009, 10, 565

Abstract

Background: Complementary-DNA based amplified fragment length polymorphism (cDNA-AFLP) is a commonly used tool for assessing the genetic regulation of traits through the correlation of trait expression with cDNA expression profiles. In spite of the frequent application of this method, studies on the optimization of the cDNA-AFLP assay design are rare and have typically been taxonomically restricted. Here, we model cDNA-AFLPs on all 92 eukaryotic species for which cDNA pools are currently available, using all combinations of eight restriction enzymes standard in cDNA-AFLP screens.

Results: *In silco* simulations reveal that cDNA pool coverage is largely determined by the choice of individual restriction enzymes and that, through the choice of optimal enzyme combinations, coverage can be increased from <40% to 75% without changing the underlying experimental design. We find evidence of phylogenetic signal in the coverage data, which is largely mediated by organismal GC content. There is nonetheless a high degree of consistency in cDNA pool coverage for particular enzyme combinations, indicating that our recommendations should be applicable to most eukaryotic systems. We also explore the relationship between the average observed fragment number per selective AFLP-PCR reaction and the size of the underlying cDNA pool, and show how AFLP experiments can be used to estimate the number of genes expressed in a target tissue.

Conclusion: The insights gained from *in silico* screening of cDNA-AFLPs from a broad sampling of eukaryotes provide a set of guidelines that should help to substantially increase the efficiency of future cDNA-AFLP experiments in eukaryotes. *In silico* simulations also suggest a novel use of cDNA-AFLP screens to determine the number of transcripts expressed in a target tissue, an application that should be invaluable as next-generation sequencing technologies are adapted for differential display.

Background

Researchers interested in studying the genetic regulation of particular processes or traits must first identify the genes contributing to the phenotype, a step which can be particularly challenging in organisms for which genomic data are not yet available. Differential display methods have been commonly used to compare levels of gene expression in target tissues at various stages, allowing the identification of sets of genes whose expression patterns are significantly correlated with traits of interest (Liang and Pardee 1992).

Among the available differential display methods, one increasingly popular tool is cDNA-amplified fragment length polymorphism (cDNA-AFLP; Breyne et al. 2003). This method allows the identification of differences in the expression of genes that are correlated to a trait of interest and has proven particularly useful in non-model organisms, as it does not require previous sequence knowledge. The cDNA-AFLP technique involves the digestion of cDNA preparations produced from RNA extractions with two restriction enzymes. To analyze the produced fragments, adaptors are ligated to each restriction fragment, which then serve as oligonucleotide-binding sites for two subsequent rounds of PCR. By adding a few (typically <4), selective base pairs (bp) to these primer sequences, the amplified fragment pool is reduced in complexity such that a suitable number of fragments can be visualized (Vos et al. 1995, Meudt and Clarke 2007). By comparing the presence or absence of individual fragments in individual cDNA libraries after size separation, one can identify genes correlated to the trait of interest. While the use of traditional gels (agarose, acrylamide, spreadex, etc.) is required for the recovery of fragments for further characterization, separation on fluorescent sequencers allows for high throughput and has become standard (Meudt and Clarke 2007).

A well-designed differential display experiment should aim to sample all transcripts present in a target tissue in order to avoid biasing downstream analyses. Optimizing coverage (here defined as the fraction of sequences that appear at least once as fragments of resolvable size (50-500 bp) in an exhaustive cDNA-AFLP screen) is at the heart of designing a successful experiment. Insufficient coverage of the cDNA pool can prevent the detection of genes correlated to the trait of interest, even if gene expression differences underlie trait production. Although complete pool coverage may often not be possible in any

differential display screen, the recent literature indicates that dozens to hundreds of transcript-derived fragments (TDF) correlated to traits of interest can be obtained from the successful application of cDNA-AFLP screens (Table 1). A variety of modified cDNA-AFLP protocols have been proposed to optimize pool screening (Koopman and Gort 2004, Kivioja et al. 2005, Weiberg et al. 2008).

The absolute number of TDFs that are screened per selective amplification is determined by several factors. An increase in the number of selective base pairs will reduce the number of fragments screened per PCR, and the choice of appropriate restriction enzymes can also systematically and substantially affect the quality of a screen, due to functional or evolutionary constraints on the triplets of amino-acid coding cDNA. The total number of fragments obtained is also directly linked to the total cDNA pool size, because the presence of more (different) cDNAs provides more restriction sites, and thus a larger pool is expected to produce more fragments per PCR. It is intuitively appealing to simply maximize the number of fragments screened per PCR to minimize the workload, and in fact the first AFLP studies (Vos et al. 1995) suggested that up to 100 AFLP fragments could be reliably separated. However, subsequent studies have shown that when the number of fragments visualized exceeds ~20 per PCR, there is a significant risk of co-migrating fragments that can confound the reliability of an AFLP screen (Gort et al. 2006). The risk of co-migration is further complicated by the fact that sequences of different lengths may migrate together for a variety of reasons, including physical damage to the DNA molecule, differences in base pair composition and/or methylation (Gunnarsson et al. 2004). For all of these reasons, studies in which the accuracy of AFLP-scoring is critical need to be particularly sensitive to the risks of high-throughput analysis.

Complementary DNA-AFLP optimization problems can be addressed by computational (*in silico*) analysis. These *in silico* approaches are becoming increasingly feasible as genetic databases increase in taxonomic breadth, analytical tools are developed, and computational resources increase in power. As AFLP searches are essentially searches for particular sequence motifs, the implementation of cDNA-AFLP *in silico* is computationally straightforward. Each of these screened sequence motifs is composed of the recognition site of the restriction enzyme and three or fewer selective base pairs, such that analyses are

restricted to searches for up to 43 × 43 = 4096 sequence motifs for a three-selective base pair experiment involving two enzymes.

The first quantitative cDNA-AFLP *in silico* studies approached this optimization problem in individual taxa, identifying several factors that can improve experimental design. Kivioja et al. (2005; Kivioja, unpublished data) suggested that the use of restriction enzymes with 6-bp restriction sites is likely to be disadvantageous in cDNA-AFLP studies due to the fact that such enzymes significantly reduce pool coverage. Again, simply maximizing the number of fragments screened per selective PCR by using restriction enzymes that cut frequently is not necessarily optimal, as this increases the risk of obtaining size-homoplasious fragments (henceforth: collisions) within each selective amplification (Gort et al. 2006). There is thus a tradeoff between data quantity and quality in cDNA-AFLP experiments. Methods have been proposed which would minimize the number of amplifications required per enzyme combination (Kivioja et al. 2005) when the cDNA pool has been previously characterized, but it is unclear whether these approaches have more widespread applicability.

These first *in silico* approaches to the study of cDNA-AFLPs suffer from two significant limitations. First, these studies used cDNA data from a small number of (often closely related) taxa (Koopman and Gort 2004, Kivioja et al. 2005, Gort et al. 2006, Weiberg et al. 2008), an approach that could restrict the wider applicability of their conclusions, as codon usage is known to vary widely across taxonomic groups (Subramanian 2008). As one of the major benefits of AFLPs is their ready applicability to new taxa, this may be a particularly important issue. A second potential limitation of these earlier studies stems from the fact that previous *in silico* analyses of cDNA-AFLPs used RefSeq sequences from curated resources, which are typically biased towards larger and more complete sequences. As this quality of data is rarely available in real-world datasets, insights gained from simulations based on these data may not be relevant for typical research projects. The effects of the raw data themselves on the outcome of the *in silico* optimizations have not yet been unexplored.

To overcome the limitations of previous *in silico* studies, we use a taxonomically diverse eukaryotic dataset to investigate traditional cDNA-AFLP experiments sensu Bachem (1996). Briefly, cDNA is digested with two restriction enzymes, from which subsets of fragments are amplified and then separated by

electrophoresis. Depending on the frequency of restriction enzyme cleavage, multiple fragments may be generated for each cDNA. We maximize cDNA pool coverage and optimize the number of TDFs produced per selective PCR using simulated cDNA-AFLPs on a wide taxonomic sampling of 92 eukaryotic species representing most major groups (See additional file 1: "General information for each species" and additional file 2 "Species composition of included taxonomic groups"). Making use of data from two different repositories, we also investigate whether systematic differences exist between datasets obtained from different databases. After quantifying these effects, we test all 28 combinations of eight commonly used restriction enzymes on all 92 species and assess the relative performance of individual enzymes on cDNA-AFLP screens. By including information on the taxonomic grouping of each species, we are able to investigate whether there is significant phylogenetic signal in the data, a finding which could indicate that different cDNA-AFLP protocols might be necessary for particular taxonomic groups. This quantitative dataset is then used to compare and identify optimal enzyme combinations, both at the species-level and across all eukaryotes.

The cDNA pool-coverages obtained in these global analyses are based on the execution of all possible selective PCRs, but such extensive screens are often infeasible in the laboratory. To investigate potential differences in TDF recovery during selective PCR, we simulate all possible combinations of selective PCRs for each enzyme combination and species and extract information on the number of fragments produced per selective PCR. Because the maximum number of selective amplifications is frequently limited and the selective base pairs used in amplifications are not necessarily independent of each other, we use graphical representations to identify general patterns in the performance of selective amplifications. As a comparison, we perform *in silico* AFLP on simulated DNA and cDNA datasets to address whether cDNA-AFLP patterning in real data differs from neutral expectations.

Our comprehensive *in silico* approach provides a realistic quantitative framework for the design of future cDNAAFLP experiments. In addition to removing the guesswork from the design of such screens for non-model organisms, our *in silico* approach offers a powerful means for identifying general patterns in the transcriptomes of both model- and non-model species.

Results

Consistent results from curated datasets

NCBI and ENSEMBL databases provided a total of 113 pools of cDNA for this study. Twenty-one species were present in both databases, providing an opportunity to investigate the potential effects of database origin on pool coverage. While the data from NCBI and ENSEMBL differed significantly in many characteristics (See additional file 3: "Duplicate species from ENSEMBL and NCBI databases"), the source of the data did not explain a significant proportion of the variation in cDNA pool coverage after controlling for total pool size, average sequence length, GC content and the proportion of ambiguous nucleotides (See additional file 3 and additional file 4: "Influence of database origin on pool coverage"). Duplicated species from the NCBI database were therefore removed to avoid pseudo-replication in subsequent analyses (see Methods).

Sources of variability in cDNA pool coverage

Considerable variability exists in the observed cDNA pool coverage both within and across species (Table 2; see also additional files 1 and 3). Two major sources of variability in coverage can be identified. Sequence characteristics such as average cDNA length and the total pool size explain a significant proportion of the variation in the pool coverage. Of these technical effects, average sequence length explains 38% of the variation in cDNA pool coverage. Less important is the effect of total pool size (14.3% of the variation in coverage explained), while the effect of ambiguous bases on pool coverage is non-significant (Table 2).

A larger portion of the variation in coverage can be explained by biological factors (Table 2), of which the combination of restriction enzymes is most important, explaining 68.9% of the observed variation in coverage. The GC content of the target species explains 28.7% of cDNA pool coverage, and a significant two-way interaction exists between enzyme combination and the GC content of the pool, explaining 55.6% of the variation in coverage. This significant interaction term indicates that optimal enzyme combinations differ among species (see also additional file 1) and suggests that GC content should be considered when choosing optimal restriction enzymes for a cDNA-AFLP screen. Taken

together, our mixed model explains 78% of variation in cDNA pool coverage (Table 2).

The choice of the most appropriate restriction enzymes substantially increases the coverage of a given cDNA pool from less than 40% to more than 75% (Table 3). The effects of restriction enzymes are essentially additive (compare Table 3 and Table 4), indicating that the performance of individual restriction enzymes is not strongly influenced by the second enzyme used in the double digest.

Effects of evolutionary history on cDNA-pool coverage

Analyzing sequence data from a group of organisms with an evolutionary history as old and diverse as that of eukaryotes allows the quantification of the effects of taxonomic substructure on cDNA pool coverage. 68 of the 92 study species could be assigned to eight major taxonomic groups (see also additional file 2) with at least three members per group. This additional predictor (taxonomic group) improves the fit of our model by 16.1% (Table 5). Taxonomic grouping itself explains 62.2% of the variation in pool coverage. Once again, the choice of enzyme combination explains the highest proportion of coverage in this model (79.6%), and the influence of technical effects is less significant. Of these sequence characteristics, the average sequence length has again the strongest influence and explains 54.0% of the variation in cDNA pool coverage, while the total pool size accounts for only 8.2% and the proportion of ambiguous nucleotides does not significantly affect coverage. There is a strong interaction between taxonomic group and enzyme combination ($p < 0.001$) indicating that the optimal enzyme combination varies across groups (see also additional file 2). This difference is mediated in large part by differences in GC content among the taxa included here (70.7% variation explained; Table 5).

A positive relationship between cDNA-AFLP fragment number and pool size

We were interested to see whether a relationship exists between the average number of fragments produced per selective PCR and any of the additional information we collected for each cDNA pool. We found a strong positive correlation between the average fragment number per selective PCR and the size of the cDNA pool in base pairs (Figure 1, Table 3). With an r^2 of 0.63 -

0.98, the average fragment counts generated per PCR provide a reasonable estimate of the size of the underlying cDNA pool.

cDNA length averaged 1113 ± 489 bp across the pools included in the present study (see additional file 1), similar to the recently published estimate of 1346 bp derived from gene predictions in the eukaryotic genome (Xu et al. 2006). Using these estimates, it is possible to convert the estimated total pool sizes in base pairs into absolute numbers of cDNAs. The linear relationship between total cDNA pool size and average fragment number per selective PCR can help minimize the possibility of collisions when optimizing cDNA-AFLP experimental design. In case of a selective PCR regime which employs a two-by-three selective base pair design, the threshold of 20 fragments per PCR reaction to minimize the chance of collisions will rarely be reached in tissues with fewer than 15000 sequences, assuming an average cDNA length of 1346 bp. However, the frequently used two-by-two selective base pair design will yield more than 20 fragments per selective PCR in a pool of only 7500 cDNAs and nearly 100 fragments in a pool of 15000 cDNAs (Figure 1), suggesting that a two-by-two selective base pair design is likely to introduce a significant source of error via collisions in a typical cDNA screen (Gort et al. 2006).

Non-random patterning in cDNA-AFLP arrays

Selective PCRs generally use up to three selective base pairs, and hence a maximum of 43 × 43 = 4096 different selective amplifications are theoretically possible when using two restriction enzymes. According to neutral expectations, each of these selective primer combinations would be expected to produce on average a similar number of fragments. We used array plotting to visualize the relative fragment numbers produced by each potential selective PCR in the typical three-by-three selective base pair design and found considerable structure in empirical data that is not found in simulated cDNA and genomic DNA pools (Figure 2). Such structure is observable for all enzyme combinations (e.g. *Homo sapiens*; Figure 3). As is apparent from Figure 3, restriction-enzyme specific patterning for individual enzymes is highly conserved even when enzymes are used in different combinations, suggesting that the difference between the fragment numbers per selective PCR is largely the result of the individual restriction enzymes (see above). Particular selective PCRs fail to generate any

products and are thus entirely uninformative in cDNA-AFLP screens. In these cases, one or both restriction enzymes cut closely together, producing AFLP products too small to be visualized in the screen (see Discussion). This restriction-enzyme patterning is consist- ent even in distantly related taxa (Figure 4), indicating the strong signal of evolutionary history in the underlying datasets.

Discussion

Complementary DNA-AFLPs are an increasingly popular tool to study differential gene expression, particularly in non-model organisms for which genome data are unavailable (Table 1). The main benefits of the cDNA-AFLP approach are the relative ease of its implementation and its low per-marker costs (Vuylsteke et al. 2006). In addition to the traditional use of cDNA-AFLPs to identify dominant (i.e. presence-absence) markers correlating to traits of interest, recent methods have shown that cDNA-AFLPs can also provide quantitative data (Reijans et al. 2003). Regardless of the goals of a cDNA-AFLP experiment, a successful screen requires high coverage of the underlying cDNA pool. While significant advances have been made in technical aspects of the AFLP methodology, theoretical studies investigating methods for optimizing the cDNA-AFLP screens remain relatively rare, and large scale empirical data - as provided here for eukaryotes - have not yet been used for this purpose (Kivioja et al. 2005, Gort et al. 2006, Weiberg et al. 2008).

Recent years have seen an explosion in cDNA datasets. ENSEMBL and NCBI are two of the most important repositories for cDNA data, and the taxonomic coverage and quality of data in these archives will continue to grow with the development of next-generation sequencing technologies. Given the vast amount of available data - in the present study a total of more than 1.7 million sequences and 2.2 Gbp of cDNA were screened - *in silico* studies offer the potential to address novel research questions and to optimize experimental protocols before undertaking large experimental studies. The cDNA pools included in the present study cover most major extant eukaryotic groups, providing an opportunity to identify broadly applicable conclusions on the most important factors affecting the quality of cDNA-AFLP screens. These cDNA pools range from a few hundred to more than 57,000 sequences (see additional file 1), covering the range of experiments likely to be undertaken in both model- and non-model organisms.

Using previously published and pre-filtered data has the potential to introduce technical artifacts into *in silico* analyses. The database origin of cDNA pools does not affect our coverage optimization after controlling for differences in sequence length, total pool size, GC content and the proportion of ambiguous nucleotides (see additional file 4: "Influence of database origin on pool coverage").

When comparing data derived from different databases, non- ACGT content was found to explain a significant component of pool coverage (see additional file 4). This result is due to an abnormally high proportion of ambiguous nucleotides in the *Gasterosteus aculeatus* cDNA pool obtained from the NCBI repository (1.26%, versus 6 × 10- 6% in the ENSEMBL dataset; see also additional file 3). This effect of non-ACGT nucleotides on coverage disappears when this species is removed from the analysis (data not shown).

cDNA pool coverage in the complete dataset of 92 species (see additional file 1) is significantly affected by both total pool size and average sequence length, which explain 14% and 38% percent of coverage, respectively (Table 2). Because the cDNA-AFLP method requires the presence of at least two restriction sites in proximity to screen each transcript, cDNA sequence length can have a large effect, and a significant reduction in coverage is expected when using short cDNA sequences. While the quality of the cDNA preparation can influence cDNA length, differences in cDNA length between species may also reflect biological reality. Species included in our study differ substantially in average cDNA sequence length (see additional file 1). This difference is most pronounced between plants (coniferopsids, liliopsids and streptophytes), which have an average cDNA length of approximately 800 bp, and mammals, which have an average cDNA sequence length of 1600 bp (see additional file 2). This difference, though more modest, is also evident in the results of recent full-length cDNA sequencing projects. An average cDNA length of ~1.5 kb has been reported in plants (e.g. Ogihara et al. 2004, Alexandrov et al. 2006, Umezawa et al. 2008, Sato et al. 2009), whereas mammals have on average longer full length cDNAs of ~1.7 kb (e.g. Okazaki et al. 2002, Gerhard et al. 2004, Ota et al. 2004, Harhay et al. 2005, Sakate et al. 2007). While these studies indicate cDNA length may vary among taxonomic groups, the biological implications and evolutionary consequences of this variation remain unclear.

Technical issues have an important effect on the outcome of cDNA-AFLP experiments, but the restriction enzymes employed explain the majority of the variation in pool coverage (Table 2, Table 5). Here, three factors are relevant. First, the use of restriction enzymes with 6-bp recognition sites is not recommended for cDNA pools (Kivioja et al. 2005; Kivioja, unpublished data), as it greatly reduces the number of fragments generated per PCR reaction. Second,

among the restriction enzymes tested here, some are far better suited for cDNA-AFLPs than are others. Estimates of the effects of individual enzymes on coverage (Table 4) or their combined effect (Table 3) clearly indicate that the efficiency of the pool coverage can be nearly doubled by choosing the optimal enzyme combination. Of the restriction enzymes included here, CviAII, MseI and CviQI outperform the other enzymes and are as such good candidates for cDNA-AFLP screens in eukaryotes (Table 3, Table 4). Finally, several basic rules should be kept in mind when choosing restriction enzymes. A strong interaction between optimal restriction enzymes and organismal GC content is apparent in all analyses (see also additional file 2). Clearly, restriction enzymes with GC-rich recognition sites are likely to cut more frequently in GC rich genomes than in those with reduced GC content. Similarly, the use of restriction enzymes with recognition sites frequently found in cDNAs could likewise aid in obtaining in-depth pool coverage. As most previous studies have used a six-cutter restriction enzyme together with a four-cutter and have focused on a small number of primer combinations (Table 1), the number of genes correlated to traits of interest has likely been frequently underestimated.

Complementary DNA-AFLPs have been applied to a wide range of eukaryotic taxa, and the ease of implementing this method in new systems is one of its particular strengths. While previous studies proposed suitable enzyme combinations for species for which sequence data are already available (Kivioja et al. 2005), the restricted taxonomic focus of these earlier studies limited the applicability of inferences across a wider array of organisms. As can be seen from Table 5, significant effects of taxonomic grouping exist, and a strong interaction between the taxonomic grouping and the GC content is apparent (compare Table 2 with Table 5). While this indicates that the optimal choice of restriction enzymes differs among taxonomic groups, it also indicates that a large portion of this difference in optimal enzyme choice can be explained by organismal GC content (see additional file 2). By considering GC content prior to undertaking a cDNA-AFLP experiment, researchers should be able to optimize the quality of their screens.

Our *in silico* experiment revealed that cDNA-AFLP performance differs markedly from neutral expectations (Figure 2) and that the observed patterning is highly consistent across taxa (Figure 4). Clearly, cDNA pool coverage could be

even further enhanced through a more explicit incorporation of the results presented here. By selecting only the best performing selective base pair combinations for several independent enzyme pairs, one should be able to maximize pool coverage in a reasonably- sized cDNA-AFLP experiment. We refer the reader to additional file 5: "Arrays of all selective PCRs for all species and enzyme combinations", which provides complete cDNA-AFLP arrays for all species investigated here. Figure 3 indicates that most of this patterning results from the effects of the individual restriction enzymes. This is especially apparent for areas of uninformative selective primer combinations in which particular primer-enzyme combinations fail to generate any cDNA-AFLP products at all. This pattern is a result of the AFLP methodology, where restriction enzymes are used to digest double-stranded DNA and adaptors are ligated directly to the digested cDNA ends. During selective amplifications, the selective base pairs of each primer extend directly 3' from the recognition site. As a consequence, an AFLP screen using four-cutter enzymes and three selective base pairs is equivalent to a motif search for DNA stretches of 7-bp length. When restriction enzymes overlap in one or more base pairs, this motif may contain multiple restriction enzyme recognition sites, producing cDNA fragments shorter than the 50 bp required for visualization. These classes of selective PCRs will thus not produce any fragments of mixed type. The selective amplification of HinP1I-generated fragments with the selective base pairs GCN is one such example (Figure 4). When a given DNA sequence contains the motif GCGCGCN, HinP1I will cleave the sequence at two positions (G^CGC^GCN). Due to this double digest, the use of HinP1I will fail to generate any AFLP fragments containing the GCGCGCN motif. Even when this overlap in recognition sites is only partial, the number of fragments generated by a particular pair of selective primers can be reduced, which might explain a portion of the observed patterning. However, the absence of patterning in the simulated data relative to Homo sapiens (Figure 2) suggests that technical aspects of the cDNA-AFLP method are insufficient to explain the higher level of complexity found in real data. As this structure is remarkably consistent across taxa (Figure 4), factors highly conserved across evolution (such as codon usage) must contribute to this pattern.

During AFLP screens, selective PCRs are used to reduce the complexity of produced fragment pools. The average number of fragments produced during

each selective PCR is positively correlated with the size of the cDNA pool (Figure 1, Table 3). For the restriction enzyme combinations investigated here, the average number of fragments obtained from selective PCRs can be converted into an estimate of the - typically unknown - size of the underlying cDNA pool. This novel versatility of the AFLP methodology - estimating cDNA pool size - should be particularly useful for any study in which knowledge of the underlying transcriptome size is critical. This is especially the case when performing large scale sequencing of the transcriptome, where a preliminary cDNA-AFLP screen may offer a cost-effective means to estimate the number of genes expressed in a tissue of interest.

The linear relationship between average fragment number and total cDNA pool size can also provide guidance when deciding on how many selective base pairs to use. From Figure 1 it is apparent that a two-by-two selective base pair design will often result in fragment numbers that far exceed that optimal for reliable fragment separation (<100 fragments per amplification) or to avoid significant homoplasy (<20 fragments per PCR). A three-by-three selective base pair design is, however, too conservative, in that too few fragments will be screened per PCR reaction (less than 10 fragments per PCR will be generated for datasets containing the equivalent of up to 15000 cDNAs - about 20 Mbp of cDNA sequence). Using a two-by-three selective base pair design appears to be the best option for most cDNA screens, producing 10-20 fragments per amplification (Figure 1; Gort et al. 2006) in cDNA pools of up to 15000 sequences or 20 Mbp, pool sizes expected in vitro in typical mammalian tissues (Carter et al. 2005).

Conclusion

Optimizing the quality of cDNA-AFLP screens

Our *in silico* approach to cDNA-AFLP optimization suggests several key improvements to existing methods of cDNA-AFLP experiments and highlights restriction enzymes likely to be particularly well suited for screening eukaryotes (Table 4, see additional file 1). Matching the GC content of the restriction enzymes with that of the target cDNA is a relatively simple step to optimize experimental design. Consideration of the restriction enzyme recognition sites is particularly important, especially when resources limit the number of selective PCRs that can be performed. Following these recommendations will significantly improve the efficiency of future cDNA-AFLP experiments.

A new application of the cDNA-AFLP methodology

In addition to our methodological suggestions, the comparative approach taken here identified a positive linear relationship between the average fragment numbers per selective PCR and the size of the underlying cDNA pool. This provides a novel method to estimate the number of transcripts present in a cDNA pool via a simple series of cDNA-AFLP screens, an application which will be invaluable as next generation sequencing technologies are adapted for differential display.

Methods

Sampling scheme

An *in silico* routine for AFLPs (Koopman and Gort 2004) was modified here to simulate the AFLP procedure on cDNA datasets. We included the 39 eukaryotic species available from the ENSEMBL repository http://www.ensembl.org/info/data/ftp/index.html as well as all 87 NCBI ftp://ftp.ncbi.nih.gov/repository/UniGene/ cDNA datasets available as of January 2008, providing a taxonomic sample covering all available eukaryotic species. We chose these databases because the frequently used RefSeq databases (Kivioja et al. 2005, Weiberg et al. 2008) lack alternative splice variants, incomplete genes and pseudogenes, sources of cDNA variation commonly present in real world data. As such, our *in silico* optimization of the cDNA-AFLP routine is a much more realistic approximation of experimental (in vitro) conditions. As we wish to help the experimenter in designing experiments for their own target species, our data are based on whole organism cDNA equivalents rather than tissue-specific datasets, for which available data are much more restricted. In the course of this paper we refer to "cDNAs" as those transcript- derived sequences obtained from the above indicated repositories.

cDNA-AFLP simulations

We simulated cDNA-AFLPs for all 28 combinations of eight different restriction enzymes for 126 pools of eukaryotic cDNA (105 species). The eight restriction enzymes used here are commonly used in AFLP screens and were used in a previous simulation study (Kivioja et al. 2005), allowing direct comparison with this earlier work. Enzyme details can be found in Table 4. Only restriction enzymes with 4-bp recognition sites were selected, as 6-bp restriction enzymes have been found to be ill-suited for cDNA-AFLP screens (Kivioja et al. 2005; Kivioja, unpublished data). We also collected information on the number of sequences and the sum of base pairs for each cDNA dataset and recorded nucleotide composition to estimate GC content and the proportion of non-ACGT base pairs (an indication of the overall quality of a dataset). The coverage of each cDNA pool was calculated as the percentage of cDNA transcripts which generated at least one fragment in the standard cDNA-AFLP size range (50 to 500 bp as

commonly used on fluorescent sequencers) in an exhaustive PCR screen of all combinations of three selective base pairs. We termed this fraction "dataset coverage" and used it as our response variable.

Initial analyses revealed that a small number of cDNA datasets contained an unusually high proportion of non- ACGT nucleotides (>10%, data not shown). These datasets consisted of cDNA predictions based on early drafts of genome sequences for 13 mammalian species. Owing to the preliminary nature of these genome projects, many of the predicted cDNA sequences contained extended stretches of ambiguous base pairs ("Ns"). As a consequence, these sequences are effectively composed of two much shorter pieces of unambiguous sequence data. Because the probability of the presence of a particular restriction site is related to the length of a sequence, this reduction of the effective average sequence length can strongly influence the predicted cDNA pool coverage. As the peculiar nature of these poor quality datasets had a strong influence on preliminary GLMs, these species were excluded from further analyses. The remaining 113 datasets included here are listed in additional files 1 and 2.

Our simulations returned information for each dataset and enzyme combination in separate results files. This information was collated into summary files using EXCEL macros and a JAVA routine and imported into SAS 9.1.3. The *in silico* cDNA-AFLP routine, EXCEL macros, JAVA tool, and raw data sets are available upon request from the corresponding authors.

Patterning of selective PCRs

Most AFLP studies use two or three selective base pairs in their selective PCRs. We produced the most inclusive arrays of selective *in silico* PCRs by counting fragment numbers produced for all possible combinations of selective PCRs with three selective base pairs for each dataset and restriction enzyme combination. Three selective base pairs for each selective primer allow for a maximum of 64 × 64 different primer combinations for two enzymes, and thus this most inclusive data array contains 4096 cells. Arrays for all species tested here are available in additional file 5. As some AFLP experiments use fewer selective base pairs, two-by-three and two-by-two selective base pair arrays were produced from the three-by-three array by summation. This summation is possible because the fragment numbers produced by amplifications with two selective base pairs are

identical to those produced by all four selective amplifications obtained with three selective base pairs (ex: AAN for N = A, C, G, T), given that the first two selective base pairs are identical to those of the two base pair selective amplification. The two-by-three selective base pair arrays and the two-by-two selective base pair arrays contained 1024 and 256 cells, respectively.

We investigated the relative information content of all 4096 selective PCR reactions using graphical representations for a subset of PCR arrays. We also simulated DNA and cDNA datasets of 10000 sequences of 1290 bp using the SEQUENCE MANIPULATION SUITE (Stothard 2000). Random DNA datasets were generated assuming equal base pair frequencies, while random cDNA datasets were generated using codon triplets based on the standard eukaryotic genetic code, starting with a start codon and ending with a stop codon. We compared these results with *in silico* cDNA-AFLP data derived from Homo sapiens (Figs. 2, 3). The same procedure was applied to the selective PCR arrays for six different species (Figure 4) to investigate systematic differences in cDNA-AFLP patterns across taxonomic groups. Data were visualized with the SAS/Graph bundle and the R library "Fields" (Fields Development Team 2006).

Partitioning variation in cDNA-pool coverage

Mixed model analyses (Proc MIXED) were used to study the relative importance of sequence characteristics and enzyme combinations in explaining cDNA pool coverage (an arcsine-square root transformed value unless otherwise indicated). All covariates were standardized by mean-centering and dividing by two standard deviations to control for the influence of different scaling factors in our predictor variables, and analyses were weighted by total pool size (in bp) to control for potential differences in variance estimates. We calculated partial R-square coefficients (Edwards et al. 2008), which provide an indication of the strength of the influence of individual covariates on the response variable. Due to correlations between explanatory variables, these values do not necessarily sum to 100%. Complementary DNA pool coverage is expected to vary with the sequence characteristics of the underlying dataset, and average sequence length, GC content, the proportion of ambiguous nucleotides (non-ACGT) and total pool size were thus all included as covariates in our models.

Pools of complementary DNA were obtained from NCBI and ENSEMBL, two sequence repositories that use different methods for the organization and curation of their genetic data. As these differences could introduce an additional source of variation in our analyses, we investigated the importance of database origin, using the 21 taxa for which data were available from both repositories (see additional file 3). We modeled variation in cDNA pool coverage according to database origin, enzyme combination and the interactions of database origin and GC content with the enzyme combination (see additional file 4) in addition to the main effects of the covariates listed above. As coverage estimates for all 28 enzyme combinations were based on the same underlying cDNA pool for each species in each database, we controlled for species origin by incorporating a species (database) random effect. Because database origin did not explain a significant proportion of the variation in cDNA pool coverage after controlling for other covariates (see additional file 4), we removed duplicate species from the NCBI repository from further analyses to eliminate potential biases due to pseudo-replication.

Effects of taxonomic grouping

Testing for the effect of taxonomic grouping (Table 5) was also possible, as 68 of the 92 available species could be assigned to eight taxonomic groups with three or more taxa using the NCBI Taxonomy browser (Wheeler et al. 2000). Similar mixed models were used to investigate the effects of enzyme combination (Table 2; see additional file 1) and taxonomic grouping (Table 5; see additional file 2) on the cDNA pool coverage. These factors entered either analysis in addition to the covariates indicated above and the significant two-way interactions between GC content and enzyme combination/taxonomic group were retained in the final model. Here, we accounted for the nested nature of our data by including species as a random factor.

Because our mixed models estimate the combined effects of the two restriction enzymes, we isolated the individual effects of each restriction enzyme by regressing the untransformed cDNA pool coverage against individual restriction enzymes in a separate model (Table 4). Here, each of the eight restriction enzymes entered the model as dummy variables explaining variation in the cDNA pool coverage. In addition to the individual enzymes, we also included enzyme

combination in the model to determine how much additional variation in coverage could be explained by enzyme interactions. As such, we were able to identify the separate effects of individual enzymes and their interactions on pool coverage. Parameter estimates from this linear regression are reported in Table 4, together with information on each restriction enzyme.

Estimating underlying cDNA pool sizes by AFLP fragment number

Finally, we performed simple linear regression of the average fragment numbers per species and enzyme combination obtained during each selective PCR against the total size of the cDNA pool to explore whether the average number of fragments obtained per selective PCR provides information on the size of the underlying cDNA pool. This total pool size estimate can be directly transformed into an estimate of the total number of different cDNAs present in the studied pool by assuming an average sequence length of 1300-1400 bp (Xu et al. 2006). By performing linear regressions of the average fragment numbers per selective PCR and enzyme combination for the 2×2, 2×3 and 3×3 arrays against the total cDNA pool size, we were able to determine the optimal number of selective base pairs for a given total pool size in order to minimize collisions (20 fragments per PCR; Gort et al. 2006), to optimize separation (50- 100 fragments, Vos et al. 1995) or to maximize the total number of fragments produced per selective PCR (up to 450 fragments can be scored over a typical AFLP screen of 50 to 500 bp). Figure 1 summarizes our findings and Table 3 reports regression coefficients and equations.

Acknowledgements

The authors thank Stefanie Bauerfeind, Marco Demont, Tadeusz Kawecki, Wim Koopman, Peter Wandeler, Andreas Wagner and members of the Wilson Laboratory for critical discussion of results. Yves Choffat provided technical assistance during the experiment, and Lukas Keller helped with SAS programming questions. Special thanks are due to Martin A. Schäfer, Erik Postma, Wolf Blanckenhorn and David Berger for statistical advice.

Financial support from the Forschungskredit der Universität Zürich (KNS), the Swiss National Science Foundation (ABW), the University of Zurich (ABW, CW), and Wageningen University (GG) is gratefully acknowledged.

References

Alexandrov NN, Troukhan ME, Brover VV, Tatarinova T, Flavell RB, Feldmann KA. 2006. Features of Arabidopsis genes and genome discovered using full-length cDNAs. *Plant Mol Biol* 60:69-85.

Aquea F, Arce-Johnson P. 2008. Identification of genes expressed during early somatic embryogenesis in Pinus radiata. *Plant Physiol Bioch* 46:559-568.

Bachem CWB, van der Hoeven RS, de Bruijn SM, Vreugdenhil D, Zabeau M, Visser RGF. 1996. Visualization of differential gene expression using a novel method of RNA fingerprinting based on AFLP: Analysis of gene expression during potato tuber development. *Plant J* 9:745-753.

Breyne P, Dreesen R, Cannoot B, Rombaut D, Vandepoele K, Rombauts S, Vanderhaeghen R, Inze D, Zabeau M. 2003. Quantitative cDNA-AFLP analysis for genome-wide expression studies. *Mol Genet Genomics*, 269:173-179.

Carter MG, Sharov AA, VanBuren V, Dudekula DB, Carmack CE, Nelson C, Ko MS. 2005. Transcript copy number estimation using a mouse whole-genome oligonucleotide microarray. *Genome Biol* 6:R61.

Edwards LJ, Muller KE, Wolfinger RD, Qaqish BF, Schabenberger O. 2008. An R^2 statistic for fixed effects in the linear mixed model. *Statistics in Medicine* 27:6137-6157.

Fields Development Team: Fields: Tools for spatial data. 2006 [http://www.image.ucar.edu/GSP/Software/Fields/]. National Center for Atmospheric Research, Boulder, CO

Gerhard DS, Wagner L, Feingold EA, Shenmen CM, Grouse LH, Schuler G, Klein SL, Old S, Rasooly R, Good P, Guyer M, Peck AM, Derge JG, Lipman D, Collins FS. 2004. The status, quality, and expansion of the NIH full-length cDNA project: The Mammalian Gene Collection (MGC). *Genome Res* 14:2121-2127.

Gort G, Koopman WJM, Stein A. 2006. Fragment length distributions and collision probabilities for AFLP markers. *Biometrics* 62:1107-1115.

Gunnarsson GH, Thormar HG, Gudmundsson B, Akesson L, Jonsson JJ. 2004. Two-dimensional conformation-dependent electrophoresis (2D-CDE) to

separate DNA fragments containing unmatched bulge from complex DNA samples. *Nucleic Acids Res* 32:e23.

Harhay GP, Sonstegard TS, Keele JW, Heaton MP, Clawson ML, Snelling WM, Wiedmann RT, Van Tassell CP, Smith TP. 2005. Characterization of 954 bovine full-CDS cDNA sequences. *BMC Genomics* 6:166.

Hsu TW, Tsai WC, Wang DP, Lin S, Hsiao YY, Chen WH, Chen HH. 2008. Differential gene expression analysis by cDNA-AFLP between flower buds of *Phalaenopsis* Hsiang Fei cv. H. F. and its somaclonal variant. *Plant Sci* 175:415-422.

Huang YC, Chang YL, Hsu JJ, Chuang HW. 2008. Transcriptome analysis of auxin-regulated genes of *Arabidopsis thaliana*. *Gene* 420:118-124.

Kivioja T, Arvas M, Saloheimo M, Penttila M, Ukkonen E. 2005. Optimization of cDNA-AFLP experiments using genomic sequence data. *Bioinformatics* 21:2573-2579.

Koopman WJM, Gort G. 2004. Significance tests and weighted values for AFLP similarities, based on *Arabidopsis in silico* AFLP fragment length distributions. *Genetics* 167:1915-1928.

Liang P, Pardee AB. 1992 Differential display of eukaryotic messenger- RNA by means of the polymerase chain-reaction. *Science* 257:967-971.

Meudt HM, Clarke AC. 2007. Almost forgotten or latest practice? AFLP applications, analyses and advances. *Trends Plant Sci* 12:106-117.

Miao L, Shou S, Zhu Z, Jiang F, Zai W, Yang Y. 2008. Isolation of a novel tomato caffeoyl CoA 3-O-methyltransferase gene following infection with the bacterium *Ralstonia solanacearum*. *J Phytopathol* 156:588-596.

Muller LA, Craciun AR, Ruytinx J, Lambaerts M, Verbruggen N, Vangronsveld J, Colpaert JV. 2007. Gene expression profiling of a Zn-tolerant and a Zn-sensitive *Suillus luteus* isolate exposed to increased external zinc concentrations. *Mycorrhiza* 17:571-580.

Neveu C, Charvet C, Fauvin A, Cortet J, Castagnone-Sereno P, Cabaret J. 2007. Identification of levamisole resistance markers in the parasitic nematode *Haemonchus contortus* using a cDNA-AFLP approach. *Parasitology* 134:1105-1110.

Ogihara Y, Mochida K, Kawaura K, Murai K, Seki M, Kamiya A, Shinozaki K, Carninci P, Hayashizaki Y, Shin I, Kohara Y, Yamazaki Y. 2004.

Construction of a full-length cDNA library from young spikelets of hexaploid wheat and its characterization by large-scale sequencing of expressed sequence tags. *Genes Genet Syst* 79:227-232.

Okazaki Y, Furuno M, Kasukawa T, Adachi J, Bono H, Kondo S, Nikaido I, Osato N, Saito R, Suzuki H, Yamanaka I, Kiyosawa H, Yagi K, Tomaru Y, Hasegawa Y, Nogami A, Schonbach C, Gojobori T, Baldarelli R, Hill DP, Bult C, Hume DA, Quackenbush J, Schriml LM, Kanapin A, Matsuda H, Batalov S, Beisel KW, Blake JA, Bradt D, et al. 2002. Analysis of the mouse transcriptome based on functional annotation of 60,770 full-length cDNAs. *Nature* 420:563-573.

Ota T, Suzuki Y, Nishikawa T, Otsuki T, Sugiyama T, Irie R, Wakamatsu A, Hayashi K, Sato H, Nagai K, Kimura K, Makita H, Sekine M, Obayashi M, Nishi T, Shibahara T, Tanaka T, Ishii S, Yamamoto J, Saito K, Kawai Y, Isono Y, Nakamura Y, Nagahari K, Murakami K, Yasuda T, Iwayanagi T, Wagatsuma M, Shiratori A, Sudo H, et al. 2004. Complete sequencing and characterization of 21,243 full-length human cDNAs. *Nature Genet* 36: 40-45.

Pathan AAK, Devi KU, Vogel H, Reineke A. 2007. Analysis of differential gene expression in the generalist entomopathogenic fungus *Beauveria bassiana* (Bals.) Vuillemin grown on different insect cuticular extracts and synthetic medium through cDNA-AFLPs. *Fungal Genet Biol* 44:1231-1241.

Pellny TK, Van Aken O, Dutilleul C, Wolff T, Groten K, Bor M, De Paepe R, Reyss A, Van Breusegem F, Noctor G, Foyer CH. 2008. Mitochondrial respiratory pathways modulate nitrate sensing and nitrogen-dependent regulation of plant architecture in Nicotiana sylvestris. *Plant J* 54:976-992.

Polesani M, Desario F, Ferrarini A, Zamboni A, Pezzotti M, Kortekamp A, Polverari A. 2008. cDNA-AFLP analysis of plant and pathogen genes expressed in grapevine infected with Plasmopara viticola. *BMC Genomics* 9:142.

Reijans M, Lascaris R, Groeneger AO, Wittenberg A, Wesselink E, van Oeveren J, de Wit E, Boorsma A, Voetdijk B, Spek H van der, Grivell LA, Simons G. 2003. Quantitative comparison of cDNA-AFLP, microarrays, and GeneChip expression data in *Saccharomyces cerevisiae*. *Genomics* 82:606-618.

Sakate R, Suto Y, Imanishi T, Tanoue T, Hida M, Hayasaka I, Kusuda J, Gojobori T, Hashimoto K, Hirai M. 2007. Mapping of chimpanzee full-length cDNAs

onto the human genome unveils large potential divergence of the transcriptome. *Gene* 399:1-10.

Sato K, Shin I, Seki M, Shinozaki K, Yoshida T, Takeda K, Conte M, Kohara Y. 2009. Development of 5006 full-length cDNAs in barley: a tool for accessing cereal genomics resources. *DNA Res* 16:81-89.

Stothard P. 2000. The sequence manipulation suite: JavaScript programs for analyzing and formatting protein and DNA sequences. *Biotechniques* 28:1102.

Subramanian S. 2008. Nearly neutrality and the evolution of codon usage bias in eukaryotic genomes. *Genetics* 178:2429-2432.

Umezawa T, Sakurai T, Totoki Y, Toyoda A, Seki M, Ishiwata A, Akiyama K, Kurotani A, Yoshida T, Mochida K, Kasuga M, Todaka D, Maruyama K, Nakashima K, Enju A, Mizukado S, Ahmed S, Yoshiwara K, Harada K, Tsubokura Y, Hayashi M, Sato S, Anai T, Ishimoto M, Funatsuki H, Teraishi M, Osaki M, Shinano T, Akashi R, Sakaki Y, et al. 2008. Sequencing and analysis of approximately 4000 soybean cDNA clones from a full-length-enriched cDNA library. *DNA Res* 15:333-346.

Vos P, Hogers R, Bleeker M, Reijans M, Vandelee T, Hornes M, Frijters A, Pot J, Peleman J, Kuiper M, Zabeau M. 1995. AFLP - A new technique for DNA-fingerprinting. *Nucleic Acids Res* 23:4407-4414.

Vuylsteke M, Daele H Van Den, Vercauteren A, Zabeau M, Kuiper M. 2006. Genetic dissection of transcriptional regulation by cDNA-AFLP. *Plant J* 45:439-446.

Wee CW, Lee SF, Robin C, Heckel DG. 2008. Identification of candidate genes for fenvalerate resistance in *Helicoverpa armigera* using cDNA-AFLP. *Insect Mol Biol* 17:351-360.

Weiberg A, Pöhler D, Morris J, Karlovsky P 2008. Improved coverage of cDNA-AFLP by sequential digestion of immobilized cDNA. *BMC Genomics* 9:480.

Wheeler DL, Chappey C, Lash AE, Leipe DD, Madden TL, Schuler GD, Tatusova TA, Rapp BA. 2000. Database resources of the National Center for Biotechnology Information. *Nucleic Acids Res* 28:10-14.

Xu L, Chen H, Hu XH, Zhang RM, Zhang Z, Luo ZW. 2006. Average gene length is highly conserved in prokaryotes and eukaryotes and diverges only between the two kingdoms. *Mol Biol Evol* 23:1107-1108.

Table 1 Results of cDNA-AFLP screens from ten recent publications

TDFs are the number of transcript-derived fragments produced in each screen, while PC indicates the number of primer combinations tested in each study. Mean TDF indicates the average numbers of fragments generated per primer combination, while Corr TDF identifies the number of transcript-derived fragments that were found to be correlated to the trait under investigation. Restriction enzymes (RE) listed in column RE1 are characterized by recognition sites of 6 bp, while RE2 (here: MseI) is a 4 bp-cutter.

RE1	RE2	PC	TDFs	Mean TDF	Corr. TDF	Reference
BstYI	MseI	60	4000	66.67	63	(Aquea et al. 2008)
BstYI	MseI	64	3793	59.27	213	(Muller et al. 2007)
BstYI	MseI	128	10440	81.56	223	(Pellny et al. 2008)
BstYI	MseI	128	7000	54.69	1196	(Polesani et al. 2008)
BstYI	MseI	256	5900	23.05	378	(Huang et al. 2008)
EcoRI	MseI	64	3220	50.31	34	(Miao et al. 2008)
EcoRI	MseI	128	2269	17.73	25	(Hsu et al. 2008)
EcoRI	MseI	256	12500	48.83	525	(Wee et al. 2008)
HindIII	MseI	32	4320	135.00	26	(Neveu et al. 2007)
PstI	MseI	80	1200	15.00	46	(Pathan et al. 2007)
	Average	119.6	5464.2	55.2	272.9	
	Median	104.0	4160.0	52.5	138.0	

Table 2 The relative contribution of enzyme combinations to cDNA pool coverage

Variance partitioning addressing the contribution of enzyme combination (28 combinations) on pool coverage for 92 eukaryotic species (see additional file 1). Species was included as a random factor in a mixed model analysis which aimed to determine the influence of individual factors or interactions (Source). cDNA pool coverage was weighted by the number of sequences per species to account for variation in available sequence data. The numerator and denominator (Kenward-Roger corrected) degrees of freedom (Num df/Den df) are provided. F statistics (F) and the significance (Sig.) of the overall model, factors and interactions are reported. The proportion of the variation in cDNA pool coverage which is explained by each factor/interaction is indicated as Partial R-square values (Edwards et al. 2008)

Source	Num df	Den df	F	Sig.	Partial R^2
Model	58	2248.56	134.76	<0.001	77.66
Total pool size (bp)	1	85.40	14.25	<0.001	14.30
Average sequence length	1	86.29	52.87	<0.001	37.99
GC content	1	86.60	34.89	<0.001	28.72
Non-ACGT content	1	84.49	0.05	0.823	<0.01
Enzyme combination	27	2428.48	199.26	<0.001	68.90
Enzyme combination*GC content	27	2428.48	112.38	<0.001	55.55

Table 3 Average cDNA pool coverages by enzyme combination across 92 eukaryotes

Descriptive statistics on the average cDNA pool coverage obtained for each enzyme combination across all 92 species (see additional file 1), sorted by decreasing mean coverage. The average coverage by enzyme combination and standard deviation (Coverage ± SD) are indicated, as are the minimum and maximum cDNA pool coverages for individual enzyme combinations (Min-Max Coverage). R-Square indicates the correlation coefficient for the relationship of total cDNA pool size (Nbp) and the average number of fragments produced per selective PCR (AF). The linear regression equation for this relationship is indicated.

Enzyme Combination	Coverage ± SD	Min-Max Coverage	R^2	Regression Equation
MseI & CviAII	76.13 ± 10.51	42.07 - 91.97	0.94	Nbp=1849399*AF+294835
CviAII & CviQI	72.55 ± 10.32	46.44 - 93.68	0.98	Nbp=1924913*AF+1067365
CviAII & TaqI	69.56 ± 13.62	32.19 - 96.94	0.85	Nbp=2152800*AF+933639
MseI & CviQI	66.63 ± 10.32	36.63 - 86.15	0.94	Nbp=2731950*AF-862614
CviAII & MaeII	64.16 ± 13.93	33.34 - 91.88	0.91	Nbp=2309466*AF+1759142
MaeI & CviAII	63.20 ± 11.42	21.81 - 85.13	0.90	Nbp=2306663*AF+3307692
MseI & TaqI	62.69 ± 14.23	28.35 - 90.91	0.72	Nbp=2995858*AF+626737
HpaII & CviAII	62.00 ± 18.32	9.45 - 93.30	0.94	Nbp=1890564*AF+3666024
TaqI & CviQI	61.26 ± 14.41	25.91 - 94.55	0.76	Nbp=2726475*AF+2079328
MseI & MaeI	58.28 ± 12.22	27.61 - 79.49	0.84	Nbp=2852998*AF+2622539
MseI & MaeII	57.15 ± 12.86	29.81 - 84.18	0.85	Nbp=3630319*AF-565133
MaeII & CviQI	55.70 ± 15.43	23.57 - 88.18	0.85	Nbp=3156237*AF+1906975
MaeI & CviQI	54.91 ± 11.08	21.14 - 81.68	0.91	Nbp=3400108*AF+2063017
TaqI & MaeII	54.86 ± 17.23	19.16 - 92.44	0.64	Nbp=2762584*AF+4754785
HpaII & MseI	54.39 ± 14.73	12.13 - 87.81	0.92	Nbp=3607697*AF+484514
HpaII & CviQI	54.14 ± 18.34	9.05 - 91.74	0.88	Nbp=2623528*AF+3657451
HinP1I & CviAII	53.57 ± 19.96	5.08 - 95.05	0.85	Nbp=2260683*AF+4996193
HpaII & TaqI	53.54 ± 19.47	8.04 - 93.28	0.72	Nbp=2433331*AF+5040020
MaeI & TaqI	52.26 ± 13.47	17.71 - 85.30	0.80	Nbp=4183276*AF+518528
HpaII & MaeII	49.93 ± 19.70	5.49 - 89.29	0.79	Nbp=2690086*AF+4940474
HinP1I & CviQI	47.88 ± 19.79	5.27 - 89.77	0.79	Nbp=2909507*AF+5271739
MaeI & MaeII	47.76 ± 12.04	15.32 - 78.81	0.93	Nbp=4923589*AF-278386
HinP1I & TaqI	47.32 ± 20.70	4.26 - 91.43	0.63	Nbp=2600056*AF+7269281
HinP1I & MseI	46.22 ± 15.07	6.86 - 87.60	0.84	Nbp=4211767*AF+2594577
HpaII & MaeI	45.75 ± 15.11	4.16 - 80.64	0.92	Nbp=4048888*AF+3106105
HinP1I & HpaII	45.05 ± 22.78	1.36 - 94.75	0.78	Nbp=2272295*AF+6925901
HinP1I & MaeII	44.15 ± 20.69	4.08 - 89.75	0.71	Nbp=2937393*AF+6703632
HinP1I & MaeI	39.00 ± 15.30	2.53 - 77.47	0.89	Nbp=5159080*AF+3260514

Table 4 Effects of individual restriction enzymes on cDNA-pool coverage

The effects of individual restriction enzymes on cDNA-pool coverage, based on all 92 species (Table 3; see additional file 1). The percentage of total cDNA pool coverage explained by each enzyme has been estimated. The degrees of freedom (df) of each factor included in the model (source) are indicated. Enzymes are sorted by decreasing coverage, and restriction sites of each restriction enzyme are listed. Details on the significance of each factor (Sig.) in this analysis and corresponding F-statistics are given (see Methods).

Source (Restriction Site)	df	SS I	F	Sig.	Coverage Estimate
CviAII (C^ATG)	1	121.08	4806.32	<0.001	43.63
MseI (T^TAA)	1	153.42	6090.19	<0.001	32.49
CviQI (G^TAC)	1	69.09	2742.53	<0.001	31.06
TaqI (T^CGA)	1	52.69	2091.52	<0.001	30.20
MaeI (C^TAG)	1	63.15	2506.75	<0.001	25.79
MaeII (A^CGT)	1	86.56	3436.05	<0.001	24.66
HpaII (C^CGG)	1	136.20	5406.74	<0.001	23.34
HinP1I (G^CGC)	1	137.28	5449.32	<0.001	17.12
Enzyme combination	20	0.78	1.55	0.056	n/a

Table 5 Effects of taxonomic grouping and enzyme combination on pool coverage

Variance partitioning addressing the influence of enzyme combination (28 combinations) and taxonomic grouping on pool coverage for 68 species (see additional file 2). Species was included as a random factor and cDNA pool coverage was weighted by the number of sequences per species to account for variation in available sequence data. Denominator degrees of freedom were Kenward-Roger corrected. Partial R-square indicates the proportion of the variation in cDNA pool coverage which is explained by each factor/interaction (Edwards et al. 2008).

Source	Num df	Den df	F	Sig.	Partial R^2
Model	254	1485.02	87.57	<0.001	93.74
Taxonomic group	7	57.37	13.48	<0.001	62.19
Total pool size (bp)	1	55.88	5.00	0.029	8.22
Average sequence length	1	56.31	66.16	<0.001	54.02
GC content	1	56.56	12.12	0.001	17.65
Non-ACGT content	1	56.59	0.75	0.389	1.31
Enzyme combination	27	1593.69	230.17	<0.001	79.59
Enzyme combination * GC content	27	1593.69	142.71	<0.001	70.74
Enzyme combination * Taxonomic group	189	1593.69	21.05	<0.001	71.40

Figure 1 A positive relationship between cDNA pool size and the number of fragments per PCR.

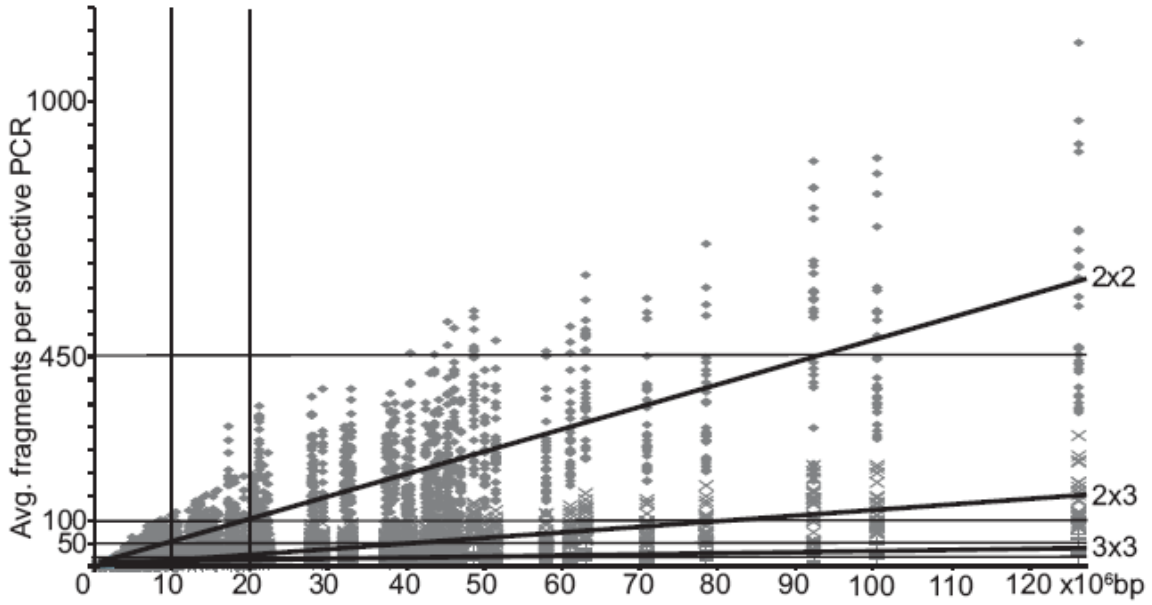

Linear regressions of average fragment numbers produced during *in silico* selective cDNA-AFLP PCRs against the absolute cDNA pool size in bp. Symbols indicate the average fragment numbers produced per enzyme combination and species for selective amplifications using 2 × 2 (diamonds), 2 × 3 (crosses) and 3 × 3 (pluses) selective base pairs, respectively. Duplicate species have been removed from this analysis. The numbers of selective base pairs used for each primer in the selective PCR are indicated, and regression lines have been added for each of the three amplification types. The correlation coefficient for each of the three datasets is 0.74. The production of fewer than 20 fragments per PCR minimizes the possibility of collisions (Gort et al. 2006), while up to 100 fragments per reaction are often desired when performing AFLP on genomic DNA (Vos et al. 1995). A maximum of 450 fragments can be separated in the typical size range of AFLP screens (50-500 bp). Vertical reference lines indicate the total cDNA pool size range expected in a typical tissue expressing between 7500 and 15000 different cDNAs (Carter et al. 2005) assuming an average cDNA length of 1346 bp (Xu et al. 2006).

Figure 2 Empirical cDNA-AFLP data are highly structured.

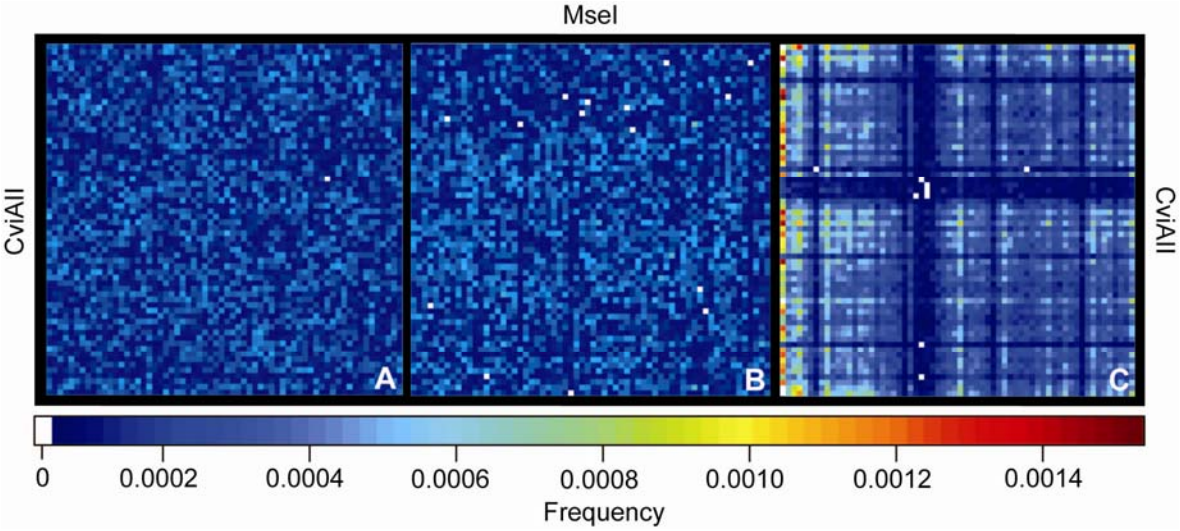

Patterning of cDNA-AFLP data. A and B: Patterning of complete arrays of selective PCR amplifications using CviAII and MseI restriction enzymes for (A) simulated random DNA, (B) simulated cDNA (following the standard eukaryotic codon table; Stothard 2000), and (C) Homo sapiens cDNA. 10000 sequences of 1290 bp were simulated for both the DNA and cDNA datasets. Pixel intensity reflects the relative proportion of products obtained during selective *in silico* PCR. Pixels are ordered by selective base pairs: AAA (left, top) to TTT (bottom, right). White pixels indicate that no fragments were generated for this combination of selective base pairs.

Figure 3 Characteristic cDNA-AFLP patterns are generated by individual restriction enzymes.

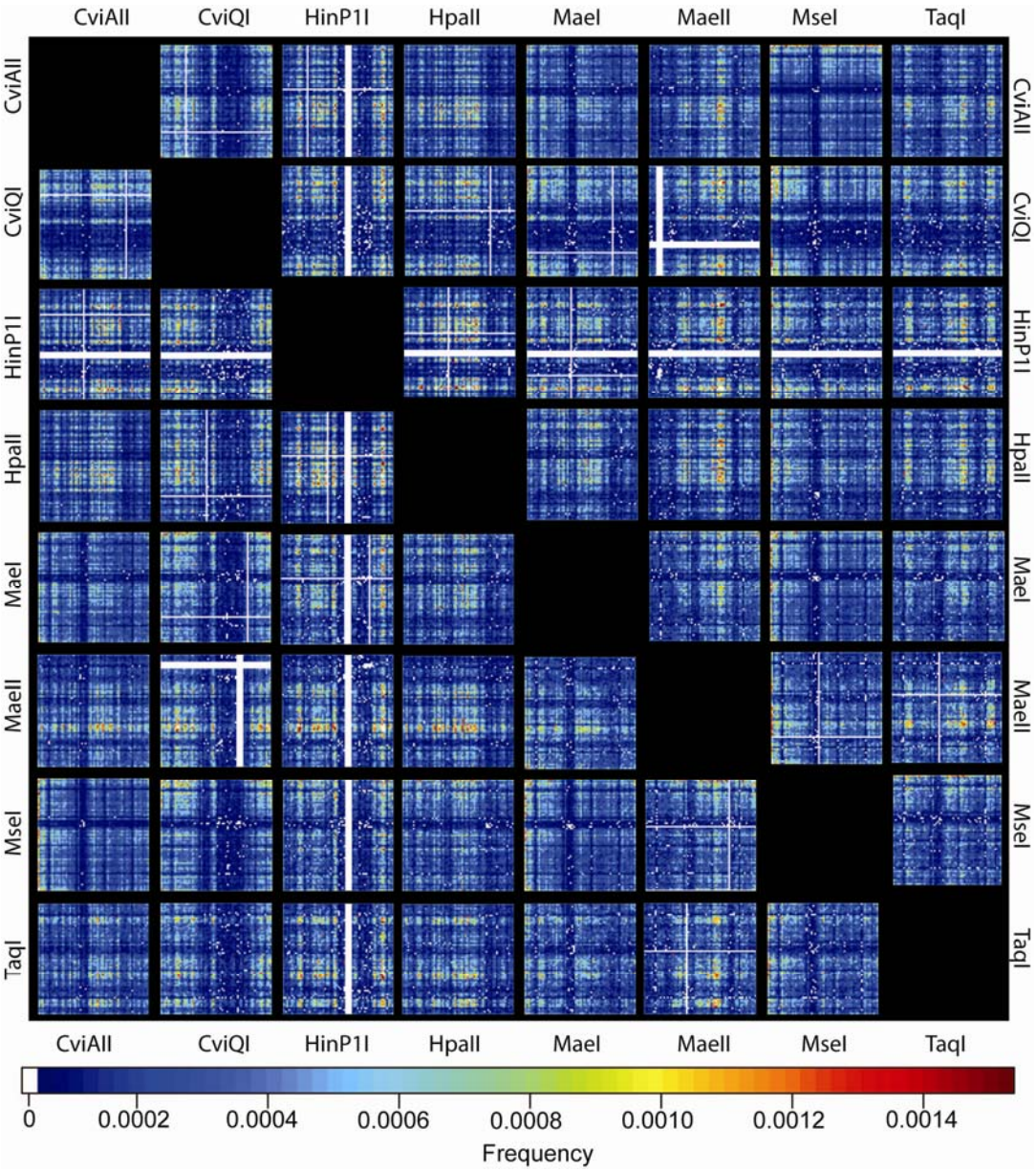

Overview of the *Homo sapiens* selective cDNA-AFLP PCR arrays for all enzyme combinations tested here. The layout of arrays follows Figure 2. Note the consistent patterning of arrays, with characteristic ridges and trenches for enzyme combinations which contain the same enzyme. Arrays above the diagonal are mirror images of those below the diagonal. Selective primer combinations yielding no amplifications are highlighted in white. The pixel intensity indicates the relative proportion of fragments amplified in a given selective PCR combination.

Figure 4 cDNA-AFLP patterning is consistent across all eukaryotes.

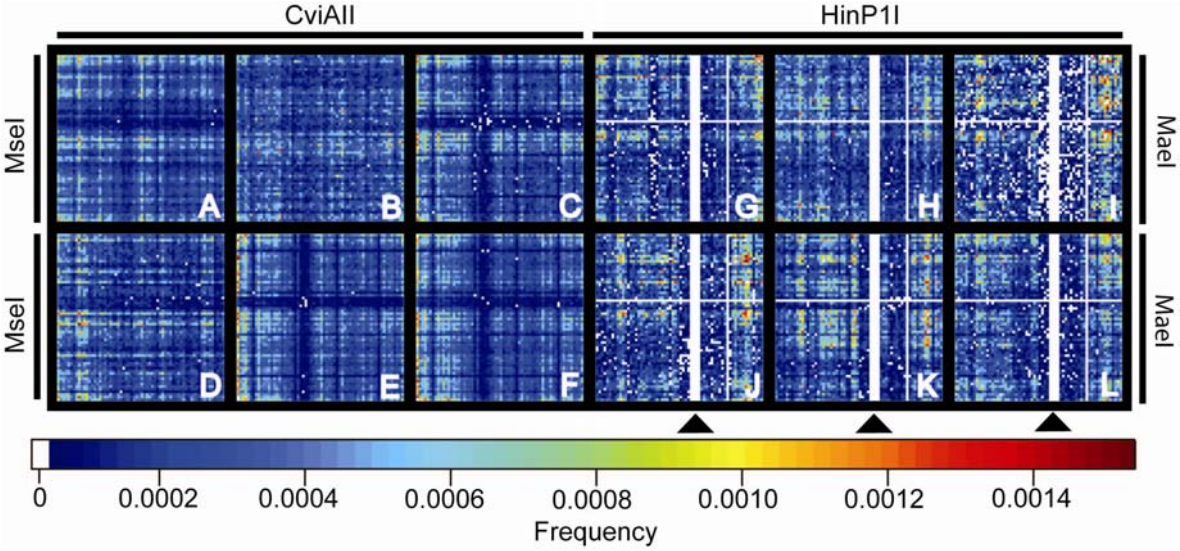

Arrays of all possible cDNA-AFLP selective PCR combinations for the best (A-F) and worst (G-L) restriction enzyme combinations. Six species per enzyme combination are included. A-F restriction enzymes CviAII and MseI, G-L restriction enzymes HinP1I and MaeI. A/G *Arabidopsis thaliana*, B/H *Drosophila melanogaster*, C/I *Gallus gallus*, D/J *Gasterosteus aculeatus*, E/K *Homo sapiens*, F/L *Xenopus laevis*. Arrowheads pointing to white areas in the arrays indicate primer combinations with GCN-selective base pair motifs, which fail to produce any fragments in a cDNA-AFLP screen with these enzymes (see Discussion).

Additional file 1 - General information for each species

General information for each of the 92 eukaryotic species included in the present study. Source identifies the database from which sequence pools were derived. The number of sequences included in each pool (N Seq) and the total pool size in base pairs (bp) are indicated. Avg Seq Lgt reports on the average sequence length, % GC indicates the percentage of GC nucleotides and Non-ACGT states the proportion of ambiguous nucleotides in each pool. Coverage ± SD reports the average percent coverage obtained across all 28 combinations of 8 tested restriction enzymes. The enzyme combination that provided the deepest cDNA pool coverage is indicated for each species.

Species	Source	N Seq	Total pool size (bp)	Avg Seq Lgt	% GC	Non-ACGT	Coverage ± SD	Min-Max coverage	Best Combination
Acrythosiphon pisum	NCBI	6557	4044893	616.88	33.09	0.02	38.73 ± 15.71	16.03 - 70.95	MseI - CviQI
Aedes aegypti	ENSEMBL	18061	27616123	1529.05	47.98	0.02	74.92 ± 7.17	59.49 - 85.72	HpaII - TaqI
Anopheles gambiae	ENSEMBL	13133	20879537	1589.85	55.26	0	78.05 ± 12.71	49.41 - 92.32	TaqI - CviQI
Apis mellifera	NCBI	9791	13386956	1367.27	37.15	0.02	54.04 ± 15.89	28.75 - 79.91	MseI - TaqI
Aquilegia formosa x pubescens	NCBI	8065	7359417	912.51	41	0	51.88 ± 21.58	17.15 - 91.97	MseI - CviAII
Arabidopsis thaliana	NCBI	29974	43315662	1445.11	42.16	0.02	67.76 ± 14.26	41.39 - 88.45	MseI - CviAII
Bombyx mori	NCBI	9939	7662004	770.9	39.02	0.1	56.14 ± 11.90	35.87 - 77.49	MseI - CviQI
Bos taurus	ENSEMBL	28958	49808680	1720.03	52.5	0.01	61.64 ± 7.63	49.56 - 79.20	CviAII - CviQI
Branchiostoma floridae	NCBI	11507	8085133	702.63	41.81	0.25	45.71 ± 17.69	23.53 - 84.70	CviAII - CviQI
Brassica napus	NCBI	26287	20322912	773.12	44.99	0.17	59.90 ± 11.75	38.83 - 80.12	MseI - CviAII
Caenorhabditis elegans	ENSEMBL	28981	40353676	1392.42	42.34	0	63.29 ± 13.18	34.74 - 84.00	CviAII - TaqI
Canis familiaris	ENSEMBL	27301	42169482	1544.61	51.89	0	59.50 ± 8.84	46.10 - 80.16	CviAII - CviQI
Chlamydomonas reinhardtii	NCBI	11276	16939170	1502.23	63.71	0.02	73.22 ± 16.24	40.40 - 95.05	HinP1I - CviAII
Ciona intestinalis	ENSEMBL	19858	29064597	1463.62	41.6	0	64.88 ± 13.73	39.04 - 90.20	MseI - CviAII
Ciona savignyi	ENSEMBL	20359	32691732	1605.76	44.98	0	71.86 ± 10.99	48.09 - 88.73	MseI - CviAII
Citrus clementina	NCBI	6107	6788422	1111.58	44.43	0.06	63.58 ± 11.26	44.20 - 88.83	MseI - CviAII
Citrus sinensis	NCBI	9699	7370218	759.89	41.84	0.06	48.11 ± 14.69	25.29 - 82.75	MseI - CviAII
Coccidioides posadasii	NCBI	3994	3776554	945.56	49.82	0	76.32 ± 8.47	60.49 - 93.54	CviAII - TaqI
Danio rerio	ENSEMBL	31841	51017126	1602.25	48.09	0	67.11 ± 8.90	50.64 - 84.63	MseI - CviAII

Dictyostelium discoideum	NCBI	5960	4195845	704	29.36	0.29	22.42 ± 19.10	1.36 - 65.32	MseI - CviAII
Drosophila melanogaster	ENSEMBL	20909	48315668	2310.76	49.91	0	84.67 ± 6.18	71.79 - 92.33	CviAII - TaqI
Equus caballus	ENSEMBL	27192	46568281	1712.57	50.03	0	56.74 ± 8.04	42.77 - 75.27	CviAII - CviQI
Felis catus	ENSEMBL	15993	20792059	1300.07	53.89	0	54.92 ± 9.45	39.87 - 74.44	HpaII - CviAII
Filobasidiella neoformans	NCBI	3559	7052090	1981.48	50.33	0	86.26 ± 6.26	70.86 - 96.94	CviAII - TaqI
Fundulus heteroclitus	NCBI	4573	3367792	736.45	47.39	0.55	48.34 ± 12.03	25.39 - 72.12	MseI - CviAII
Gadus morhua	NCBI	10792	7919862	733.86	43.2	0.04	52.86 ± 13.68	30.47 - 84.51	MseI - CviAII
Gallus gallus	ENSEMBL	22291	39792561	1785.14	48.61	0	61.38 ± 9.22	43.79 - 81.48	CviAII - CviQI
Gasterosteus aculeatus	ENSEMBL	27629	45847847	1659.41	55.02	0	70.69 ± 15.89	39.48 - 89.39	HpaII - CviAII
Gibberella moniliformis	NCBI	5259	4752592	903.71	51.71	0	68.29 ± 13.27	41.51 - 93.61	CviAII - TaqI
Glycine max	NCBI	24518	17344657	707.43	41.21	0.43	40.93 ± 16.26	17.90 - 80.96	MseI - CviAII
Gossypium hirsutum	NCBI	16404	12887278	785.62	42.98	0.05	51.70 ± 16.22	24.66 - 85.10	MseI - CviAII
Gossypium raimondii	NCBI	3295	2698120	818.85	43.93	0.02	53.46 ± 17.15	23.70 - 87.95	MseI - CviAII
Helianthus annuus	NCBI	7969	5407728	678.6	42.8	0.07	50.47 ± 13.71	27.42 - 79.57	MseI - CviAII
Homo sapiens	ENSEMBL	48803	125500000	2571.64	49.68	0	71.73 ± 6.9	61.95 - 85.59	CviAII - CviQI
Hordeum vulgare	NCBI	22853	20147314	881.6	51.19	0.22	63.14 ± 7.96	49.55 - 79.50	CviAII - TaqI
Hydra magnipapillata	NCBI	10923	7092578	649.33	32.88	0.05	35.29 ± 17.12	9.79 - 75.38	MseI - CviAII
Lactuca sativa	NCBI	7848	6566967	836.77	42.92	0.05	54.32 ± 16.68	27.13 - 86.96	MseI - CviAII
Lotus japonicus	NCBI	13659	7282469	533.16	42.23	0.11	33.12 ± 13.89	14.84 - 71.72	MseI - CviAII
Macaca fascicularis	NCBI	10799	17252467	1597.6	45.93	0.04	64.36 ± 11.38	46.16 - 88.40	MseI - CviAII
Macaca mulatta	ENSEMBL	38146	70430633	1846.34	50.36	0.01	62.24 ± 7.45	52.42 - 78.74	CviAII - CviQI
Malus x domestica	NCBI	16913	10632914	628.68	44.88	0.07	46.35 ± 11.43	27.74 - 70.45	MseI - CviAII
Medicago truncatula	NCBI	17785	12924130	726.69	39.72	0.39	43.07 ± 17.13	17.03 - 83.13	MseI - CviAII
Meleagris gallopavo	NCBI	960	679555	707.87	47.42	0.08	38.07 ± 12.05	17.71 - 69.48	CviAII - CviQI
Molgula tectiformis	NCBI	8534	6725171	788.04	35.42	0.32	47.35 ± 17.86	21.69 - 88.73	MseI - CviAII
Monodelphis domestica	ENSEMBL	33279	57497869	1727.75	48.1	0	58.51 ± 11.68	38.49 - 83.06	CviAII - CviQI
Mus musculus	ENSEMBL	40959	99678366	2433.61	49.98	0	71.96 ± 7.36	60.58 - 87.00	CviAII - CviQI
Neurospora crassa	NCBI	2209	1269530	574.71	51.57	0.13	48.56 ± 11.72	27.61 - 71.48	CviAII - TaqI
Nicotiana tabacum	NCBI	13207	10073670	762.75	41.46	0.28	46.96 ± 15.63	21.71 - 80.91	MseI - CviAII
Oncorhynchus mykiss	NCBI	25264	21635734	856.39	45.1	0.6	50.12 ± 14.27	28.64 - 82.10	MseI - CviAII
Ornithorhynchus anatinus	ENSEMBL	27383	37194655	1358.31	53.33	0.01	59.13 ± 10.3	40.07 - 79.33	HpaII - CviAII
Oryctolagus cuniculus	NCBI	6517	5377786	825.19	49.96	0.02	39.71 ± 8.82	26.21 - 61.49	MseI - CviAII
Oryza sativa	NCBI	40742	62731750	1539.73	50.75	0.09	72.75 ± 6.63	60.58 - 86.03	CviAII - TaqI
Oryzias latipes	ENSEMBL	24662	38325234	1554.02	52.36	0.01	65.66 ± 12.19	44.21 - 82.86	HpaII - CviAII
Ovis aries	NCBI	12195	9682040	793.94	50.36	0.01	46.76 ± 9.72	32.96 - 67.61	CviAII - CviQI
Pan troglodytes	ENSEMBL	34009	78022597	2294.17	49.5	0.01	68.47 ± 7.09	59.02 - 83.68	CviAII - CviQI
Paracentrotus lividus	NCBI	8664	7473899	862.64	43.09	0.31	54.75 ± 15.93	25.67 - 83.55	CviAII - CviQI
Paramecium tetraurelia	NCBI	14325	18863127	1316.8	31.58	0.13	34.66 ± 27.14	1.85 - 84.64	MseI - CviAII

Petromyzon marinus	NCBI	8512	5620756	660.33	47.53	0.01	55.32 ± 11.29	33.13 - 74.02	MseI - CviAII
Phaeodactylum tricornutum	NCBI	6772	6808242	1005.35	50.42	0.08	77.59 ± 12.06	49.79 - 92.76	HpaII - TaqI
Physcomitrella patens	NCBI	17973	14198438	789.99	47.78	0.1	63.70 ± 8.68	50.87 - 85.28	CviAII - TaqI
Phytophtora infestans	NCBI	7270	4996923	687.33	52.75	0.39	70.99 ± 9.98	51.38 - 85.24	CviAII - TaqI
Picea glauca	NCBI	17812	13565571	761.6	40.63	0.64	45.90 ± 16.11	23.70 - 85.03	MseI – CviAII
Picea sitchensis	NCBI	15699	11905367	758.35	42.55	0	48.28 ± 13.53	29.91 - 80.79	MseI - CviAII
Pimephales promelas	NCBI	22442	17900531	797.64	44.3	0.04	51.01 ± 12.26	31.59 - 83.62	MseI - CviAII
Pinus taeda	NCBI	18938	15068523	795.68	43.97	0.14	52.19 ± 12.79	33.39 - 82.41	MseI - CviAII
Pongo pygmaeus	ENSEMBL	24431	43871572	1795.73	50.25	0.01	58.88 ± 7.50	47.64 - 75.85	CviAII - CviQI
Populus balsamifera	NCBI	11310	8229010	727.59	41.07	0	44.05 ± 16.84	19.09 - 83.79	MseI - CviAII
Populus tremula x tremuloides	NCBI	7853	4925686	627.24	42.47	0.04	41.13 ± 15.09	17.80 - 76.91	MseI - CviAII
Populus trichocarpa	NCBI	14059	10473626	744.98	40.93	0	44.54 ± 17.14	18.67 - 84.12	MseI - CviAII
Prunus persica	NCBI	7062	4677442	662.34	42.5	0.12	41.86 ± 13.31	21.81 - 74.45	MseI - CviAII
Rattus norvegicus	ENSEMBL	34704	60508280	1743.55	51.1	0.01	62.60 ± 7.74	51.83 - 81.13	CviAII - CviQI
Saccharomyces cerevisiae	ENSEMBL	6698	9056373	1352.1	39.61	0	64.49 ± 11.14	38.85 - 80.01	MseI - CviAII
Saccharum officinarum	NCBI	15592	12706205	814.92	50.56	0.36	61.23 ± 8.57	44.90 - 77.28	CviAII - TaqI
Salmo salar	NCBI	29722	22077976	742.82	43.34	0.01	44.02 ± 16.83	21.51 - 82.16	MseI - CviAII
Schistosoma japonicum	NCBI	9107	8309606	912.44	35.01	0.09	55.09 ± 21.10	18.79 - 87.44	MseI - CviAII
Schistosoma mansoni	NCBI	9172	5822751	634.84	36.94	0.2	45.46 ± 19.22	14.11 - 75.24	MseI - CviAII
Solanum lycopersicum	NCBI	17849	15412230	863.48	40.55	0.27	47.90 ± 16.61	20.62 - 81.69	MseI - CviAII
Solanum tuberosum	NCBI	19671	15691567	797.7	40.98	0.02	48.51 ± 16.99	21.89 - 83.79	MseI - CviAII
Sorghum bicolor	NCBI	13984	9709132	694.3	51.83	0.02	55.05 ± 9.62	37.25 - 74.96	CviAII - TaqI
Strongylocentrus purpuratus	NCBI	19625	28042628	1428.92	43.49	0.25	62.47 ± 13.54	39.96 - 88.61	MseI - CviAII
Sus scrofa	NCBI	51706	42874695	829.2	47.29	0.09	45.12 ± 10.95	31.94 - 73.95	MseI - CviAII
Taeniopygia guttata	NCBI	11227	8347852	743.55	44.55	0.31	34.33 ± 15.64	17.67 - 77.69	MseI - CviAII
Takifugu rubripes	ENSEMBL	48027	91791931	1911.26	53.96	0	72.10 ± 14.78	43.41 - 88.88	HpaII - CviAII
Tetraodon nigroviridis	ENSEMBL	27991	37821073	1351.19	55.1	0.43	55.53 ± 13.30	30.89 - 73.81	HpaII - CviAII
Toxoplasma gondii	NCBI	6623	4448416	671.66	52.16	0.16	52.63 ± 13.45	27.92 - 74.47	HinP1I - TaqI
Tribolium castaneum	NCBI	9013	12745306	1414.1	44.63	0.62	69.83 ± 7.73	52.41 - 82.41	HpaII - MseI
Trichosurus vulpecula	NCBI	11757	9654352	821.16	40.68	0.73	36.91 ± 22.28	11.89 - 86.68	MseI - CviAII
Triticum aestivum	NCBI	41358	31737158	767.38	50.47	0.86	60.12 ± 7.92	46.51 - 76.64	CviAII - TaqI
Vitis vinifera	NCBI	23129	17999693	778.23	42.64	0.14	45.08 ± 14.72	22.05 - 80.78	MseI - CviAII
Xenopus laevis	NCBI	35518	45020703	1267.55	42.92	0.54	54.19 ± 13.31	34.31 - 86.97	MseI - CviAII
Xenopus tropicalis	ENSEMBL	27711	45111427	1627.92	46.38	0	62.21 ± 9.92	47.74 - 84.39	CviAII - CviQI
Zea mays	NCBI	57495	32228704	560.55	50.58	0.52	38.74 ± 4.90	29.81 - 48.70	CviAII - TaqI

Additional file 2 - Species composition of taxonomic groups

Taxonomic groupings for the 68 eukaryotic species derived from eight taxonomic groups with three or more representatives. Tax group indicates the taxonomic group (according to NCBI Taxonomy browser). The number of sequences (N Seq), the total pool size (in base pairs), average sequence length (Avg Seq Lgt) and GC content (% GC) are shown. Average coverage (± SD), minimum and maximum coverage, along with the enzyme combination resulting in the deepest cDNA pool coverage for each species are indicated.

Tax Group	Species	Source	N Seq	Total pool size (bp)	Avg Seq Lgt	% GC	Coverage ± SD	Min-Max Cov.	Best Combination
Actinopterygii	*Danio rerio*	ENSEMBL	31841	51017126	1602.25	48.09	67.11 ± 8.90	50.64 - 84.63	MseI - CviAII
Actinopterygii	*Fundulus heteroclitus*	NCBI	4573	3367792	736.45	47.39	48.34 ± 12.03	25.39 - 72.12	MseI - CviAII
Actinopterygii	*Gadus morhua*	NCBI	10792	7919862	733.86	43.2	52.86 ± 13.69	30.47 - 84.51	MseI - CviAII
Actinopterygii	*Gasterosteus aculeatus*	ENSEMBL	27629	45847847	1659.41	55.02	70.69 ± 15.89	39.48 - 89.39	HpaII - CviAII
Actinopterygii	*Oncorhynchus mykiss*	NCBI	25264	21635734	856.39	45.1	50.12 ± 14.27	28.64 - 82.10	MseI - CviAII
Actinopterygii	*Oryzias latipes*	ENSEMBL	24662	38325234	1554.02	52.36	65.66 ± 12.19	44.21 - 82.86	HpaII - CviAII
Actinopterygii	*Pimephales promelas*	NCBI	22442	17900531	797.64	44.3	51.01 ± 12.26	31.59 - 83.62	MseI - CviAII
Actinopterygii	*Salmo salar*	NCBI	29722	22077976	742.82	43.34	44.02 ± 16.83	21.51 - 82.16	MseI - CviAII
Actinopterygii	*Takifugu rubripes*	ENSEMBL	48027	91791931	1911.26	53.96	72.10 ± 14.78	43.41 - 88.88	HpaII - CviAII
Actinopterygii	*Tetraodon nigroviridis*	ENSEMBL	27991	37821073	1351.19	55.1	55.53 ± 13.30	30.89 - 73.81	HpaII - CviAII
Avg. Actinopterygii (N=10)			**25294**	**33770511**	**1194.53**	**48.79**	**57.74 ± 16.50**	**21.51 - 89.39**	
Ascidiaceae	*Ciona intestinalis*	ENSEMBL	19858	29064597	1463.62	41.6	64.88 ± 13.73	39.04 - 90.20	MseI - CviAII
Ascidiaceae	*Ciona savignyi*	ENSEMBL	20359	32691732	1605.76	44.98	71.86 ± 10.99	48.09 - 88.73	MseI - CviAII
Ascidiaceae	*Molgula tectiformis*	NCBI	8534	6725171	788.04	35.42	47.35 ± 17.86	21.69 - 88.73	MseI - CviAII
Avg. Ascidiaceae (N=3)			**16250**	**22827167**	**1285.81**	**40.67**	**61.36 ± 17.66**	**21.69 - 90.20**	
Aves	*Gallus gallus*	ENSEMBL	22291	39792561	1785.14	48.61	61.38 ± 9.22	43.79 - 81.48	CviAII - CviQI

Aves	*Meleagris gallopavo*	NCBI	960	679555	707.87	47.42	38.07 ± 12.05	17.71 - 69.48	CviAII - CviQI
Aves	*Taeniopygia guttata*	NCBI	11227	8347852	743.55	44.55	34.33 ± 15.64	17.67 - 77.69	MseI - CviAII
Avg. Aves (N=3)			**11493**	**16273323**	**1078.85**	**46.86**	**44.59 ± 17.31**	**17.67 - 81.48**	
Coniferopsida	*Picea glauca*	NCBI	17812	13565571	761.6	40.63	45.90 ± 16.11	23.70 - 85.03	MseI - CviAII
Coniferopsida	*Picea sitchensis*	NCBI	15699	11905367	758.35	42.55	48.28 ± 13.53	29.91 - 80.79	MseI - CviAII
Coniferopsida	*Pinus taeda*	NCBI	18938	15068523	795.68	43.97	52.19 ± 12.79	33.39 - 82.41	MseI - CviAII
Avg. Coniferopsida (N=3)			**17483**	**13513154**	**771.88**	**42.38**	**48.79 ± 14.29**	**23.70 - 85.03**	
Insecta	*Acrythosiphon pisum*	NCBI	6557	4044893	616.88	33.09	38.73 ± 15.71	16.03 - 70.95	MseI - CviQI
Insecta	*Aedes aegypti*	ENSEMBL	18061	27616123	1529.05	47.98	74.92 ± 7.17	59.49 - 85.72	HpaII - TaqI
Insecta	*Anopheles gambiae*	ENSEMBL	13133	20879537	1589.85	55.26	78.05 ± 12.71	49.41 - 92.32	TaqI - CviQI
Insecta	*Apis mellifera*	NCBI	9791	13386956	1367.27	37.15	54.04 ± 15.89	28.75 - 79.91	MseI - TaqI
Insecta	*Bombyx mori*	NCBI	9939	7662004	770.9	39.02	56.14 ± 11.90	35.87 - 77.49	MseI - CviQI
Insecta	*Drosophila melanogaster*	ENSEMBL	20909	48315668	2310.76	49.91	84.67 ± 6.18	71.79 - 92.33	CviAII - TaqI
Insecta	*Tribolium castaneum*	NCBI	9013	12745306	1414.1	44.63	69.83 ± 7.73	52.41 - 82.41	HpaII - MseI
Avg. Insecta (N=7)			**12486**	**19235784**	**1371.26**	**43.86**	**65.20 ± 18.89**	**16.03 - 92.33**	
Liliopsida	*Hordeum vulgare*	NCBI	22853	20147314	881.6	51.19	63.14 ± 7.96	49.55 - 79.50	CviAII - TaqI
Liliopsida	*Oryza sativa*	NCBI	40742	62731750	1539.73	50.75	72.75 ± 6.63	60.58 - 86.03	CviAII - TaqI
Liliopsida	*Saccharum officinarum*	NCBI	15592	12706205	814.92	50.56	61.23 ± 8.57	44.90 - 77.28	CviAII - TaqI
Liliopsida	*Sorghum bicolor*	NCBI	13984	9709132	694.3	51.83	55.05 ± 9.62	37.25 - 74.96	CviAII - TaqI
Liliopsida	*Triticum aestivum*	NCBI	41358	31737158	767.38	50.47	60.12 ± 7.92	46.51 - 76.64	CviAII - TaqI
Liliopsida	*Zea mays*	NCBI	57495	32228704	560.55	50.58	38.74 ± 4.90	29.81 - 48.70	CviAII - TaqI
Avg. Liliopsida (N=6)			**32004**	**28210044**	**876.41**	**50.9**	**58.51 ± 12.85**	**29.81 - 86.03**	
Mammalia	*Bos taurus*	ENSEMBL	28958	49808680	1720.03	52.5	61.64 ± 7.63	49.56 - 79.20	CviAII - CviQI
Mammalia	*Canis familiaris*	ENSEMBL	27301	42169482	1544.61	51.89	59.50 ± 8.84	46.10 - 80.16	CviAII - CviQI
Mammalia	*Equus caballus*	ENSEMBL	27192	46568281	1712.57	50.03	56.74 ± 8.04	42.77 - 75.27	CviAII - CviQI
Mammalia	*Felis catus*	ENSEMBL	15993	20792059	1300.07	53.89	54.92 ± 9.45	39.87 - 74.44	HpaII - CviAII

Mammalia	*Homo sapiens*	ENSEMBL	48803	125500000	2571.64	49.68	71.73 ± 6.90	61.95 - 85.59	CviAII - CviQI
Mammalia	*Macaca fascicularis*	NCBI	10799	17252467	1597.6	45.93	64.36 ± 11.38	46.16 - 88.40	MseI - CviAII
Mammalia	*Macaca mulatta*	ENSEMBL	38146	70430633	1846.34	50.36	62.24 ± 7.45	52.42 - 78.74	CviAII - CviQI
Mammalia	*Monodelphis domestica*	ENSEMBL	33279	57497869	1727.75	48.1	58.51 ± 11.68	38.49 - 83.06	CviAII - CviQI
Mammalia	*Mus musculus*	ENSEMBL	40959	99678366	2433.61	49.98	71.96 ± 7.36	60.58 – 87.00	CviAII - CviQI
Mammalia	*Ornithorhynchus anatinus*	ENSEMBL	27383	37194655	1358.31	53.33	59.13 ± 10.30	40.07 - 79.33	HpaII - CviAII
Mammalia	*Oryctolagus cuniculus*	NCBI	6517	5377786	825.19	49.96	39.71 ± 8.82	26.21 - 61.49	MseI - CviAII
Mammalia	*Ovis aries*	NCBI	12195	9682040	793.94	50.36	46.76 ± 9.72	32.96 - 67.61	CviAII - CviQI
Mammalia	*Pan troglodytes*	ENSEMBL	34009	78022597	2294.17	49.5	68.47 ± 7.09	59.02 - 83.68	CviAII - CviQI
Mammalia	*Pongo pygmaeus*	ENSEMBL	24431	43871572	1795.73	50.25	58.88 ± 7.50	47.64 - 75.85	CviAII - CviQI
Mammalia	*Rattus norvegicus*	ENSEMBL	34704	60508280	1743.55	51.1	62.60 ± 7.74	51.83 - 81.13	CviAII - CviQI
Mammalia	*Sus scrofa*	NCBI	51706	42874695	829.2	47.29	45.12 ± 10.95	31.94 - 73.95	MseI - CviAII
Mammalia	*Trichosurus vulpecula*	NCBI	11757	9654352	821.16	40.68	36.91 ± 22.28	11.89 - 86.68	MseI - CviAII
Avg. Mammalia (N=17)			**27890**	**48051989**	**1583.26**	**49.7**	**57.60 ± 14.12**	**11.89 - 88.40**	
Streptophyta	*Arabidopsis thaliana*	NCBI	29974	43315662	1445.11	42.16	67.76 ± 14.26	41.39 - 88.45	MseI - CviAII
Streptophyta	*Brassica napus*	NCBI	26287	20322912	773.12	44.99	59.90 ± 11.75	38.83 - 80.12	MseI - CviAII
Streptophyta	*Citrus clementina*	NCBI	6107	6788422	1111.58	44.43	63.58 ± 11.26	44.20 - 88.83	MseI - CviAII
Streptophyta	*Citrus sinensis*	NCBI	9699	7370218	759.89	41.84	48.11 ± 14.69	25.29 - 82.75	MseI - CviAII
Streptophyta	*Glycine max*	NCBI	24518	17344657	707.43	41.21	40.94 ± 16.26	17.90 - 80.96	MseI - CviAII
Streptophyta	*Gossypium hirsutum*	NCBI	16404	12887278	785.62	42.98	51.70 ± 16.22	24.66 - 85.10	MseI - CviAII
Streptophyta	*Gossypium raimondii*	NCBI	3295	2698120	818.85	43.93	53.46 ± 17.15	23.70 - 87.95	MseI - CviAII
Streptophyta	*Helianthus annuus*	NCBI	7969	5407728	678.6	42.8	50.47 ± 13.71	27.42 - 79.57	MseI - CviAII
Streptophyta	*Lactuca sativa*	NCBI	7848	6566967	836.77	42.92	54.32 ± 16.68	27.13 - 86.96	MseI - CviAII
Streptophyta	*Lotus japonicus*	NCBI	13659	7282469	533.16	42.23	33.12 ± 13.89	14.84 - 71.72	MseI - CviAII
Streptophyta	*Malus x domestica*	NCBI	16913	10632914	628.68	44.88	46.35 ± 11.43	27.74 - 70.45	MseI - CviAII
Streptophyta	*Medicago truncatula*	NCBI	17785	12924130	726.69	39.72	43.07 ± 17.13	17.03 - 83.13	MseI - CviAII

Streptophyta	*Nicotiana tabacum*	NCBI	13207	10073670	762.75	41.46	46.96 ± 15.63	21.71 - 80.91	MseI - CviAII
Streptophyta	*Populus balsamifera*	NCBI	11310	8229010	727.59	41.07	44.05 ± 16.84	19.09 - 83.79	MseI - CviAII
Streptophyta	*Populus tremula x tremuloides*	NCBI	7853	4925686	627.24	42.47	41.13 ± 15.10	17.80 - 76.91	MseI - CviAII
Streptophyta	*Populus trichocarpa*	NCBI	14059	10473626	744.98	40.93	44.54 ± 17.14	18.67 - 84.12	MseI - CviAII
Streptophyta	*Prunus persica*	NCBI	7062	4677442	662.34	42.5	41.86 ± 13.31	21.81 - 74.45	MseI - CviAII
Streptophyta	*Solanum lycopersicum*	NCBI	17849	15412230	863.48	40.55	47.90 ± 16.61	20.62 - 81.69	MseI - CviAII
Streptophyta	*Solanum tuberosum*	NCBI	19671	15691567	797.7	40.98	48.51 ± 16.99	21.89 - 83.79	MseI - CviAII
Avg. Streptophyta (N=19)			**14288**	**11738143**	**789.03**	**42.32**	**48.83 ± 17.01**	**14.84 - 88.83**	

Additional file 3 - Duplicate species from ENSEMBL and NCBI databases

Duplicate species from the ENSEMBL and NCBI databases. Average sequence length (Avg Seq Lgt), organismal GC-content (% GC) and the percentage of ambiguous base pairs (% non-ACGT) are indicated. The average pool coverage per enzyme combination, along with maximum and minimum coverage values, are shown.

Database	ENSEMBL							NCBI						
Species	**N Seq**	**Total pool size (bp)**	**Avg Seq Lgt**	**% GC**	**%c Non-ACGT**	**Coverage ± SD**	**Min-Max Cov.**	**N Seq**	**Total pool size (bp)**	**Avg Seq Lgt**	**% GC**	**% Non-ACGT**	**Coverage ± SD**	**Min-Max Cov.**
Aedes aegypti	18061	27616123	1529.1	48.0	0.02	74.9 ± 7.2	59.5 - 85.7	19204	25218464	1313.2	46.4	0.07	72.1 ± 6.5	56.8 - 83.2
Anopheles gambiae	13133	20879537	1589.9	55.3	0.19	78.1 ± 12.7	49.4 - 92.3	21379	15129263	707.7	52.9	0.19	64.6 ± 15.8	35.3 - 84.3
Bos taurus	28958	49808680	1720	52.5	0.01	61.6 ± 7.6	49.6 - 79.2	44106	61853260	1402.4	48.9	0.02	51.5 ± 11.0	37.3 - 79.4
Caenorhabditis elegans	28981	40353676	1392.4	42.3	<0.01	63.3 ± 13.2	34.7 – 84.0	21658	28571833	1319.2	41.7	0.02	62.3 ± 13.8	33.7 – 84.0
Canis familiaris	27301	42169482	1544.6	51.9	<0.01	59.5 ± 8.8	46.1 - 80.2	27781	39172416	1410	49.8	0.21	55.6 ± 9.7	42.2 - 78.5
Ciona intestinalis	19858	29064597	1463.6	41.6	<0.01	64.9 ± 13.7	39.0 - 90.2	3494	2996310	857.6	39.5	0.28	49.6 ± 14.3	25.8 - 80.6
Ciona savignyi	20359	32691732	1605.8	45.0	<0.01	71.9 ± 11.0	48.1 - 88.7	7678	4396714	572.6	39.9	0.21	43.8 ± 14.2	20.4 - 75.0
Danio rerio	31841	51017126	1602.3	48.1	0.07	67.1 ± 8.9	50.6 - 84.6	56561	75435852	1333.7	44.5	0.07	55.9 ± 10.8	40.7 - 86.6
Drosophila melanogaster	20909	48315668	2310.8	49.9	<0.01	84.7 ± 6.2	71.8 - 92.3	17143	31940522	1863.2	48.9	<0.01	76.7 ± 6.6	63.9 - 87.3
Equus caballus	27192	46568281	1712.6	50.0	<0.01	56.7 ± 8.0	42.8 - 75.3	8113	11844488	1459.9	48.9	0.01	56.6 ± 7.9	46.1 - 75.5
Gallus gallus	22291	39792561	1785.1	48.6	<0.01	61.4 ± 9.2	43.8 - 81.5	33589	53084019	1580.4	47.3	0.38	59.0 ± 11.5	41.1 - 83.8
Gasterosteus aculeatus	27629	45847847	1659.4	55.0	<0.01	70.7 ± 15.9	39.5 - 89.4	18965	26081100	1375.2	47.4	1.26	74.4 ± 12.8	47.9 - 92.5
Homo sapiens	48803	125500000	2571.6	49.7	<0.01	71.7 ± 6.9	62.0 - 85.6	123808	147280000	1189.6	46.1	0.11	40.5 ± 13.4	24.3 - 76.8
Macaca mulatta	38146	70430633	1846.3	50.4	0.01	62.2 ± 7.5	52.4 - 78.7	15307	40059048	2617	47.8	0.05	72.0 ± 7.8	59.7 - 87.7
Monodelphis domestica	33279	57497869	1727.8	48.1	<0.01	58.5 ± 11.7	38.5 - 83.1	959	1914395	1996.2	45.5	<0.01	57.4 ± 14.7	35.9 - 84.9
Mus musculus	40959	99678366	2433.6	50.0	<0.01	72.0 ± 7.4	60.6 – 87.0	79607	113180000	1421.8	46.7	0.17	46.3 ± 13.0	29.1 - 78.4
Ornithorhynchus anatinus	27383	37194655	1358.3	53.3	0.01	59.2 ± 10.3	40.1 - 79.3	1688	2073163	1228.2	51.4	0.02	60.2 ± 9.2	41.8 - 77.9
Oryzias latipes	24662	38325234	1554	52.4	0.01	65.7 ± 12.2	44.2 - 82.9	17373	12850714	739.7	47.6	0.21	46.8 ± 12.2	25.6 - 74.7
Rattus norvegicus	34704	60508280	1743.6	51.1	0.01	62.6 ± 7.7	51.8 - 81.1	64373	70355651	1092.9	48.2	0.18	43.6 ± 12.8	27.4 - 75.8
Takifugu rubripes	48027	91791931	1911.3	54.0	<0.01	72.1 ± 14.8	43.4 - 88.9	3757	2475886	659	48.9	0.02	41.4 ± 11.9	19.6 - 66.0
Xenopus tropicalis	27711	45111427	1627.9	46.4	<0.01	62.2 ± 9.9	47.7 - 84.4	42522	45667114	1074	42.6	0.06	46.6 ± 15.5	25.1 - 85.0
Average	**29057**	**52388748**	**1747**	**49.7**	**<0.01**	**66.7**	**34.7 - 92.3**	**29955**	**38646677**	**1296**	**46.7**	**0.17**	**56.0**	**19.6 - 92.5**

Additional file 4 - Influence of database origin on pool coverage

The influence of database origin and enzyme choice on cDNA pool coverage for the 21 species present in both databases. We accounted for variability in coverage resulting from the nesting of species within database and weighted cDNA pool coverage by the number of sequences per pool to account for variation in available sequence data. Denominator degrees of freedom were Kenward-Roger corrected. Partial R-square indicates the proportion of the variation in cDNA pool coverage which is explained by each factor/interaction (Edwards et al. 2007).

Source	Num df	Den df	F	Sig.	Partial R-square
Model	106	129.31	34.44	<0.001	96.58
Database origin	1	17.62	0.00	0.964	0.01
Total pool size (bp)	1	22.66	1.49	0.234	6.18
Average sequence length	1	12.46	197.49	<0.001	94.06
GC content	1	14.68	9.31	0.008	38.81
Non-AGCT content	1	14.36	26.70	<0.001	65.03
Species	20	11.34	21.57	<0.001	97.44
Enzyme combination	27	1055.40	61.44	<.0001	61.12
Database origin * Enzyme combination	27	1055.40	5.68	<0.001	12.69
Enzyme combination * GC content	27	1055.40	9.95	<0.001	20.29

CHAPTER IV: Comparative Transcriptomics of the Male Pregnant Seahorse *Hippocampus abdominalis*

Kai N. Stölting, Marie-Emilie Gauthier, Rémy Bruggmann, Weihong Qi and Anthony B. Wilson

For submission to *BMC Genomics*

Abstract

Background: Male pregnancy is a highly specialized form of reproduction unique to syngnathid fishes. The complexity of this form of reproduction varies across the group, ranging from the simple attachment of eggs to the external surface of the male's body to the completely enclosed pouch of the seahorse, offering an exceptional opportunity to study the evolution of reproductive complexity in a comparative evolutionary framework. Critical to these efforts is the availability of a reference transcriptome for the group. Novel massive parallel sequencing approaches allow for the rapid and cost-effective sequencing of multiple transcriptomes, a method that we applied to the seahorse *Hippocampus abdominalis*, screening gene expression in the transcriptomes of pregnant and non-pregnant individuals.

Results: Our transcriptome sequencing efforts recovered 38,419 cDNA contigs representing more than 30,000 seahorse genes. Functional annotations were obtained for 10,309 contigs (approx 27% of all contigs), 3,500 of which are exclusive to the male brood pouch. After imposing a >5 read cutoff and a minimum 2-fold expression difference, the number of annotated pouch genes is 269, 88 of which are upregulated during pregnancy and 181 of which are downregulated. Annotated genes do not differ substantially among cDNA libraries in their major molecular functions, biological processes or cellular localizations. A comparison of the sequencing depth of normalized and unnormalized cDNA libraries reveals that the normalization of cDNA libraries is essential in studies that aim for a full representation of the transcriptome.

Conclusions: A comprehensive, annotated transcriptome resource has been assembled for the seahorse. Comparative cDNA library sequencing of pregnant and non-pregnant male seahorses has identified hundreds of genes with quantitative expression differences during male pregnancy. The availability of the seahorse transcriptome opens the door for comparative studies investigating the diversification of male pregnancy during the evolution of syngnathid fishes.

Background

Modes of reproduction in fish are highly diverse and range from external fertilization to more derived forms of parental care including mouth-brooding and viviparity (Breder and Rosen 1966). One of the most exceptional forms of reproduction in fish is found in seahorses (syngnathid fishes). Syngnathids reproduce exclusively by male pregnancy and males contribute substantially to the energetic costs of reproduction while carrying the developing offspring (Stölting and Wilson 2007).

Syngnathid fishes are a large family of >250 species, all of which exhibit various forms of morphological specializations for male pregnancy. Two phylogenetically supported subfamilies are recognized in the group, distinguishable by the location of the brooding on the male's body (Wilson et al. 2001, 2003). Brooding structures have increased in complexity in both the Gastrophori (abdominal brooders) and the Urophori (tail brooders, including seahorses) during their evolution, and extant representatives are found for most pouch types (Wilson et al. 2001, 2003). It is thus possible to study the evolution of male pregnancy in a comparative evolutionary framework, identifying the genetic changes associated with functional innovations which have occurred during the evolution of this group.

The brood pouch changes radically in its morphology and function during an extended period of male pregnancy (Carcupino et al. 2002, Laksanawimol et al. 2006). Most apparent are increases in the vascularization of the inner pouch tissues (Carcupino et al. 2002), the osmoregulation of the pouch fluid (Linton and Soloff 1964), and the production of compounds associated with the immune response (Melamed et al. 2005). Hormonal changes also accompany male pregnancy (Boisseau 1967), and there is evidence that the male also provides nutrients to the developing juveniles, at least in species with highly developed brooding structures (Boisseau 1967, Haresign and Shumway 1981).

Seahorses exhibit one of the most derived brood pouch morphologies (Wilson et al. 2001, 2003), and have been the focus of a series of recent studies investigating morphological, physiological and genetic changes during male pregnancy (Melamed et al. 2005, Laksanawimol et al. 2006, Van Look et al. 2007, reviewed in Stölting and Wilson 2007).

The first studies investigating the genetic regulation of male pregnancy (Zhang et al. 2003, Melamed et al. 2005, Harlin-Cognatio et al. 2006) studied gene expression in pouch tissues using EST screens (Zhang et al. 2003, Melamed et al. 2005) and/or methods of differential display (Harlin-Cognatio et al. 2006). While limited in their scope, these earlier studies provided evidence that the genes associated with male pregnancy are highly diverse, ranging from cytoskeletal organization and osmoregulation to immune functions (Zhang et al. 2003, Melamed et al. 2005), and several of these genes also play an important role in mammalian pregnancy (Stölting and Wilson 2007). Detailed knowledge on the transcriptome of male pregnant syngnathids is an essential prerequisite for comparative evolutionary studies, which aim to further our understanding of how changes in the genetic regulation of male pregnancy are associated with functional innovations during its evolution.

Differential display techniques provide a means to identify genes whose expression levels correlate with traits of interest (Liang and Pardee 1992). Subtractive hybridization (Chien et al. 1984) and cDNA-AFLP (Breyne et al. 2003) methods can identify dozens or hundreds of candidate genes associated with phenotypic change (Stölting et al. 2009), but are limited in that usually only a small fraction of the transcriptome is typically covered (Stölting et al. 2009). Microarrays (Schena et al. 1995) are a powerful tool to investigate transcriptome activity, but their application is limited to species for which extensive sequence data are already available. Next generation sequencing approaches have revolutionized the way such questions can be addressed (Margulies et al. 2005, Morozova and Marra 2008), offering the possibility to cost-effectively decipher and compare global transcriptome activity without requiring previous sequence knowledge (Droege and Hill 2008, Morozova and Marra 2008).

While 10,000 or more genes may be active in a given cell, their relative abundance can vary significantly, complicating efforts to obtain the full transcriptome of an organism (Kuznetsov et al. 2002). 10-20 superabundant genes may constitute up to 20% of the total cell mRNA (Zhulidov et al. 2004), while 40-60% of all RNA transcripts in a given cell type are derived from several hundred genes of medium abundance, and the remaining 20-40% of the mRNA consists of rarely expressed genes, each with a low number of transcript copies per cell. Up to 70% of all protein-coding genes may be expressed at low levels, and without for

controlling for differences in expression levels, sequencing efforts aiming at gene discovery are likely to reveal only a relatively small fraction of the transcriptome. Fortunately, the differences in relative transcript abundance in cDNA preparations can be reduced through normalization, and a more comprehensive transcriptome can be generated with the same sequencing effort. Duplex-specific nuclease action (Zhulidov et al. 2004) can be used to reduce excessive transcript copies, and various methods have been proposed to improve the quality of cDNA normalization (Shagin et al. 2002). High throughput parallel sequencing can produce up to a million reads per run, and given the massive scale of this approach, it has been suggested that cDNA normalization may not be necessary, as both high and low expressed genes may be recovered with such a massive sequencing effort (Hale et al 2009).

Given its strengths in quickly providing substantial amounts of data, high-throughput sequencing is now being widely used in many non-model species to characterize transcriptomes and to identify genes involved in traits of interest (e.g. Vera et al. 2008, Alagna et al. 2009, Meyer et al. 2009, Wang et al. 2009, Zagrobelny et al. 2009). Most published studies have used standard 454 sequencing runs, which provide between 300,000 and 600,000 200bp long reads. In most of these studies, between 20–45,000 contigs have been identified. 35–70% of these contigs can be functionally annotated, and annotation success seems to depend on the availability of a high quality reference transcriptome from a closely related species (Vera et al. 2008, Alagna et al. 2009, Meyer et al. 2009, Wang et al. 2009, Zagrobelny et al. 2009).

We report here on the first *de novo* sequenced transcriptomes of the seahorse *Hippocampus abdominalis* and use a comparative sequencing approach to identify and characterize suites of genes correlated to male pregnancy. We analyze and compare the transcriptomes of the male pregnant brood pouch, the non-pregnant brood pouch, and a seahorse reference transcriptome (Figure 1), and identify pouch-specific genes differentially expressed during pregnancy. Our experimental design also allows us to test the impact of normalization on the rate of gene discovery in transcriptome sequencing, a question we investigate through the comparison of normalized and unnormalized cDNA libraries prepared from pregnant and non-pregnant tissues.

Results

Assembly

One plate of 454 titanium sequencing produced more than one million reads (Table 1). After the removal of adaptor and chimera sequences, 854,000 quality-controlled sequences (average length 227 ± 113 base pairs, Table 1) were included in the assembly. Contiguous cDNA sequences (contigs) were assembled in two stages, in order to control for the presence of highly expressed transcripts in the unnormalized data. The first pass used stringent assembly parameters, while the second used settings typical for data produced by Sanger sequencing. 705894 reads (83%) were assembled into 36706 contigs in the first assembly. This dataset provided significant blastx hits (at an e-value cutoff of e^{-3}) for 11,889 of the contigs (32%, Table 1), of which 8,444 (71%) are non-redundant. The secondary assembly successfully assembled 38,419 contigs from 783,592 reads (92% of the complete dataset). Of these secondary contigs, 11,741 provided blastx results (31%), 9,319 of which are non-redundant (79%). The secondary assembly produced more, on average longer (361bp vs. 328bp for the primary assembly) and fewer redundant contigs than the primary assembly (Table 1), and subsequent analyses are based on this assembly. Given the degree of redundancy in the annotated contigs present in our 38,419 contig dataset (21%), our dataset is estimated to contain more than 30,000 different cDNAs.

Annotation

Our dataset of 38419 contigs was functionally annotated using Blast2Go (b2g, Cones et al. 2005, Götz et al. 2008). 10309 (approx. 27%, Figure 2A) contigs were annotated using this approach, allowing the identification of prominent gene functions, biological processes and cellular localization. The number of reads contributing to each contig is highly variable across cDNA libraries (Table 2), and as many of our contigs are represented by only two sequences, many poorly represented transcripts may not have been recovered here. Success of functional annotation is positively correlated with both the number of contributing reads and the contig length (Table 3, Figure 3). A stringent cutoff of a minimum of five contributing reads per contig (methods) was imposed when quantifying expression differences in order to minimize the effects of false positives, resulting in a set of

15300 high-quality contigs, 33% of which (5178, Figure 2B) have functional annotations.

Identification of male pregnancy genes

High-throughput sequencing provides both qualitative (presence/absence) and quantitative expression data. As outlined below, quantitative comparisons are here restricted to the unnormalized libraries, while both normalized and unnormalized data provide presence/absence information. 872 of the 10309 annotated contigs are present in the pregnant tissues but are absent from any other tissue source, while 713 of the annotated contigs are restricted to the non-pregnant brood pouch (Figure 2A). Among the 1915 annotated contigs which are shared among brood pouch libraries, 1196 contigs contain sequencing reads from both unnormalized cDNA libraries and can thus be used for quantitative inference (MID4 and MID5). 623 of these contigs contain at least 5 reads from the unnormalized libraries (n. b. these contigs may contain additional reads from other libraries). When imposing a 2-fold cutoff for the detection of expression differences, 70 of these annotated contigs are upregulated in pregnant tissues, while 141 show reduced levels of expression in pregnant tissues compared to the non-pregnant library.

A similar approach can be taken when analyzing the high-reliability annotated contigs containing a minimum of five reads. 73 of the 5178 annotated high-reliability contigs are specific to the male-pregnant brood pouch (Figure 2B). An additional 55 contigs of this dataset are restricted to the non-pregnant brood pouch, and 754 contigs are found in both brood pouch libraries. 244 of these 754 contigs are found in unnormalized libraries and can thus be analyzed for quantitative information. 15 of these contigs are upregulated by at least 2-fold in the pregnant brood pouch library, while 126 contigs are down regulated in the pregnant library (Figure 2B).

Functional annotation of male pregnancy genes

Functional annotations for both the full dataset and the high-reliability dataset were determined using Blast2go (Table 4), allowing us to associate contigs with their dominant molecular functions, biological processes and their cell localization. The relative representation of annotation categories within each class

(i.e. process, function or cellular component) is largely identical in the two analyses (Table 4). Figure 4 reveals that cellular and metabolic processes dominate the genes differentially expressed in the brood pouch, followed by biological regulation, developmental processes and localization. Few differences exist in the proportion of up- and down-regulated genes contributing to each category of biological process, with the exception of anatomical structure formation, where a larger than expected proportion of transcripts are upregulated (8 upregulated vs. 3 downregulated, Figure 4A, Table 4). The main molecular functions associated with differentially expressed genes are dominated by binding and catalytic activity followed by molecular transducer, transporter and transcription regulation activity (Figure 4B). Dominant among the cellular components are localizations of annotated genes to the cell, its organelles and macromolecular complexes (Figure 4C). However, after controlling for differences in the number of contigs recovered per tissue type, no significant differences are found in the representation of genes of different annotation classes (data not shown).

Reference tissues share 3568 of the 5178 (69%) annotated high-reliability contigs with the brood pouch tissues (Figure 2). This large fraction of shared annotated contigs accounts for numerical similarities in gene functions of contigs shared among brood pouch and reference libraries (Table 4). The only exception from this is – after correction for the number of contigs per tissue type - the presence of more genes which are associated with localization in the synapse in the reference libraries, an observation with is in line with the inclusion of brain tissues in the reference library. Observations for the high-reliability dataset closely match those made for of the full dataset (Table 4).

Effects of normalization

We prepared both normalized and unnormalized cDNA preparations from pregnant and non-pregnant brood pouch tissues, providing an opportunity to directly compare sequence discovery using these two approaches (Table 5). Normalization of a cDNA library significantly increases contig recovery (2-4x more contigs were recovered with the normalized libraries, MID2, 3, Table 5) and a substantial portion of these contigs were not recovered at all in the unnormalized dataset (Table 5, compare private contigs from normalized and unnormalized

libraries). Somewhat counter-intuitively, a large number of unique contigs are restricted to the unnormalized libraries, suggesting that a portion of the transcriptome would also be underrepresented in a fully normalized study of a similar size (Table 5). While some of the differences in recovery success can be attributed to the lower number of sequences generated from the unnormalized pregnant brood pouch library, the normalized library contains proportionately more private contigs (Table 5).

Normalization also affects the length of contigs, with contigs assembled from normalized cDNA libraries being on average 120bp shorter than those produced from unnormalized tissue sources (Table 4). A portion of this difference may be due to the shorter length of reads in the normalized dataset (average of 40-70bp shorter than the unnormalized data)

While unnormalized libraries contain quantitative information, this information is lost during the normalization step. The effect of the normalization on the relative reads recovered can be compared by correlating numbers of contributing reads per contig across our four brood pouch cDNA libraries (MID2-5). These four libraries share a total of 2719 contigs. While the correlation between normalized and unnormalized libraries is low (r^2=0.25-0.35, Table 6), there is however a high correlation in gene expression (measured here as the number of reads contributing to each contig from each library) within the methods: the number of reads recovered in normalized libraries (MID2, 3) is highly correlated (0.866), a pattern similar to that found when comparing unnormalized libraries (MID4, 5, 0.745). Given the lack of correlation between relative gene copy number in normalized and unnormalized libraries, we restrict our quantitative comparisons to the unnormalized dataset.

Discussion

Studies on the physiological, morphological and behavioral changes during male pregnancy have advanced our understanding of the structural modifications that occur during male pregnancy of syngnathid fishes (reviewed in Stölting and Wilson 2007). While the genetic regulation of male pregnancy is a relatively recent area of study, several candidate pregnancy genes have already been identified (e.g. Zhang et al. 2003, Melamed et al 2005, Harlin-Cognatio et al 2006). Investigating the genetic regulation of male pregnancy in a comparative evolutionary context is complicated by the absence of genetic and genomic resources and the relatively deep divergence of syngnathids from other model teleosts. The stickleback *Gasterosteus aculeatus*, likely the most closest related model organism to syngnathids, is separated by more than 50 million years from seahorses and pipefish (Benton 1993).

Our *de novo* transcriptome sequencing efforts have provided a detailed snapshot of the seahorse transcriptome, providing sequence data for more than 30,000 distinct RNA-derived transcripts (based on redundancy in the annotated dataset). Our dataset produced more than 38,000 contigs, of which approximately 31% obtained significant blastx hits and 27% obtained GO annotations. These results are similar to those reported for other recent transcriptome studies (Vera et al. 2008, Alagna et al. 2009, Meyer et al. 2009, Wang et al. 2009, Zagrobelny et al. 2009, but see Kristiansson et al. 2009). Given that our average contig lengths are shorter than those reported in some other studies (e.g. 361bp, Table 1, vs. ~400bp, Kristiansson et al. 2009), and the positive correlation between contig length and annotation success (Table 3), our transcriptome sequencing effort has likely underestimated the number of contigs which will ultimatey be annotated.

We have assembled our adaptor-trimmed and chimera-cleaned sequencing reads in two rounds of assembly, an approach explicitly incorporated into some assembly algorithms (Chevreux et al. 2004). Manual inspection of the primary assembly, including blast-searches of remaining singlets against contigs revealed significant redundancy in the dataset. A secondary assembly of the first assembly contigs with the remaining singletons reduced overall redundancy (Table 1), and 92% of all reads could be assembled as contigs. This fraction of assembled reads in a transcriptome study is highly dependent on the number of reads produced:

smaller studies with fewer reads contain many more unassembled singlets (Alagna et al 2009, Wang et al. 2009) than studies where the size of the screen is larger (data presented here, Vera et al. 2008, Meyer et al. 2009).

Several previous studies have highlighted suites of genes potentially involved in male pregnancy. Melamed and colleagues (2005) identified 165 ESTs from the brood pouch lining of *Hippocampus comes* species. Among those ESTs are three types of lectins with *in vitro* antibacterial activity. Our assembly of the seahorse transcriptome recovered most (88%) of these ESTs (data not shown), including contigs identified as lectins. While Melamed et al. (2005) detected the presence of lectins in the pouch lining of a pregnant *H. comes*, we detected lectin genes in both the non-pregnant and pregnant brood pouch. Interestingly, five lectin-like genes are upregulated in the non-pregnant pouch relative to the pregnant pouch (additional files 1 and 2), corroborating that lectins might indeed be key players in male pregnancy. Melamed et al. (2005) show that expression levels of a lectin compound decrease during male pregnancy in the brood pouch fluid, but have not addressed questions of expression levels within the pouch lining of non-pregnant tissues. The upregulation of lectin genes in non-pregnant pouch tissues detected here might be explained by our sampling of receptive brood pouch lining, a tissue stage not tested by Melamed et al. (2005), which could already express lectins as part of the preparations for pregnancy without releasing these compounds into the pouch fluid.

While many of the previously known male pregnancy associated sequences have been recovered in the present study, a metalloprotease upregulated during male pregnancy in *Syngnathus scovelli* (Harlin-Cognatio et al. 2006) has not been recovered here and 20 of the 165 *H. comes* sequences identified by Melamed et al. (2005) were also not recovered in the present study. While these differences could be caused by species-specific differences differences in gene expression, they may also indicate that our transcriptome survey is incomplete. Despite these differences, interspecific variation in levels of gene expression during male pregnancy may be responsible for structural and physiological differences in male pregnancy across species, and such comparisons are likely a fruitful area for future research (see below).

Our analysis of the seahorse transcriptome focused on gene expression in late–stage pregnancy tissues and the brood pouch of a sexually receptive non-

pregnant individual. Pregnancy involves a series of coordinated changes to male tissues across 3-6 weeks (Laksanawimol et al. 2006), and the restricted nature of our study can only provide a snapshot of a complex process. As different stages of the pregnancy likely involve the expression of different suites of genes, temporal analyses of gene expression differences during seahorse pregnancy may help to better understand the major functional changes which occur during gestation. We have focused our sequencing efforts primarily on brood pouch tissues – the organ of male pregnancy. It is nonetheless quite likely that other tissues (e.g. the pituitary, testes, interrrenal gland, Boisseau 1967) are also involved in the regulation of this process. Furthermore, we have focused here on pouch-specific genes differentially expressed during pregnancy, but it is likely that slight changes in many constitutively expressed genes in both pouch and other tissues may also play a critical role in the pregnancy process. The development of a microarray based on the data generated here will provide an important tool for studying changes in the spatial and temporal expression of genes associated with male pregnancy.

As part of our efforts for gene discovery in the seahorse transcriptome, we normalized our cDNA preparations to remove excessive differences in relative transcript abundance. Given the availability of both normalized and unnormalized data in our study, we are able to explicitly determine the effects of normalization on gene discovery. While Hale and colleagues (2009) argued that the normalization of cDNA libraries should not be required when large numbers of sequences are obtained from a tissue sample, our study suggests that normalized libraries contain more rare transcripts than do unnormalized libraries, stressing the value of normalization in studies aimed at gene discovery. As unnormalized libraries also contain contigs which have not been detected in other cDNA libraries, normalization may produce a biased subset of the transcriptome. One indication for a normalization-related bias are the observed differences in the average read- and contig lengths of unnormalized and normalized cDNA libraries (Table 4). Here, normalized contigs are built from shorter sequencing reads and are on average shorter than normalized contigs. This observation contradicts results provided by the developers of the normalization method (Zhulidov et al. 2004), who showed that normalization should not affect contig length. An alternative explanation may be that the depth of our transcriptome screen is stil

quite low and that differences between gene discovery in normalized and unnormalized libraries may reflect stochastic sampling issues associated with an incomplete dataset. As the scale of next-generation sequencing projects increases, normalization may become less necessary, but our data strongly support the use of this approach for moderately-sized screens.

Conclusion

The first transcriptome of the seahorse has been assembled based on the brood pouch of pregnant and non-pregnant individuals and a suite of reference tissues. Comparative cDNA library sequencing of pregnant and non-pregnant male seahorses has identified hundreds of genes with quantitative expression differences during male pregnancy. A list of male-pregnancy related genes is provided in the appendix. The characterization of the seahorse transcriptome should provide a resource for future comparative studies investigating the evolution of male pregnancy in syngnathid fishes.

Outlook

We have provided the first detailed studies of the pregnant male seahorse transcriptome and have identified and functionally annotated a large suite of genes that are differentially expressed during pregnancy. As the coverage of many transcripts was low, these contigs have been excluded from quantitative analysis, suggesting that a much larger suite of genes are likely involved in the pregnancy process. The data generated here will be used in the construction of a syngnathid microarray, a tool which will provide a means to screen a broader range of tissue types and individuals. Ultimately this resource will be used for the investigation of gene expression differences during male pregnancy in a comparative evolutionary framework.

Methods

Sampling

Pregnant and non-pregnant seahorses were obtained from aquaculture stocks (Seahorse Australia, Tasmania, Australia). Animals were sacrificed under ethical guidelines (permit 180/2006 Federal Veterinary Office, Switzerland). A single pregnant and non-pregnant male provided tissues for the identification of pregnancy genes. The pregnant individual was sampled during late stage pregnancy (equivalent to stage 7 of Ripley and Foran 2006). The non-pregnant individual was reproductively receptive, with a highly vascularized brood pouch lining. Tissues were extracted from RNA-later preserved samples under a dissection microscope and stored separately in RNA-later at -20°C prior to RNA extraction. All embryonic tissues were removed from the pouch wall of the pregnant male, as were the muscular tissues forming the wall of the brood pouch. Underlying muscle tissues were also removed from the non-pregnant individuals. A reference library consisting of gill tissue, brain, testis, liver and kidney from the pregnant individual was prepared, providing a snapshot view of non-pouch-related mRNA products during pregnancy. Total RNA was extracted from each of these tissues separately and the final reference library was produced from equal amounts of cDNA from each tissue after cDNA synthesis.

RNA extraction and purification

All tissues were homogenized prior to RNA extraction in extraction buffer using Eppendorf pestles (Eppendorf, Hamburg, Germany). RNA was extracted using a modified RNA extraction protocol using equilibrated phenol (Chomczynski and Sacchi 1987). Changes to the original protocol involve RNA extraction at neutral pH and the use of lithium chloride to increase the stability of the RNA preparation and the quality of the cDNA synthesis, steps recommended prior to normalization (Evrogen, Moscow, Russia).

RNA preparations were quantified spectrophotometrically (NanoDrop), and 2µg of total RNA was DNA-digested using RQ1-RNAse free DNAse (Promega) according to the instructions of the manufacturer. DNA-digested RNA was re-purified using the RNA extraction protocol. This second extraction step included only a single phenol-chloroform-isoamyl step, while all other steps were identical.

cDNA synthesis

We synthesized cDNA in 40µL reaction volumes using approx. 1µg of DNA-digested and purified RNA preparations and 2µl ImPromII reverse transcriptase (Promega). This reverse transcriptase has properties similar to MMLV reverse transcriptase and can be used for SMART cDNA synthesis (Zhu et al. 2001). The reaction mixture for the cDNA synthesis contained two modified oligos (IIAFwModMmeI and IIAT20ModMmeI, see Table 1) similar to standard SMART cDNA synthesis oligos at a concentration of 2µM each. Here, IIAFwModMmeI was used as the 5' adaptor, while IIAT20ModMmeI served as the 3'-poly-A specific cDNA adaptor. Reactions additionally contained 1x ImPromII reaction buffer, 2µL of 10mM dNTPs and 4.8µL of 25mM $MgCl_2$ in double-distilled water. Using this system - essentially a modified SMART cDNA-synthesis system – full length cDNAs can be produced which contain both adaptor sequences. After annealing oligos to approx. 1µg total RNA, ImPromII was added to the reaction and cDNA synthesis followed the suggestion of the manufacturer. We added to each cDNA reaction 1µL of RNasin Ribonuclease inhibitor (Promega) to reduce RNA degradation during cDNA synthesis. RT-PCR was performed in a Tetrad DNA Engine 2 thermal cycler (BioRad, Hercules, CA, USA) at 42°C for 1 hour, 45°C for 30min, 50°C for 10min and 70°C for 10min. Synthesized cDNA was purified using MilliPore PCR purification plates (MilliPore) and eluted in 40µL double-distilled water. The concentration of the purified cDNA was estimated to be 100ng – 250ng/µL (Nanodrop).

cDNA-amplification and removal of poly-A-tails

Double-stranded cDNA was prepared using the 5'-oligonucleotide used for cDNA synthesis (IIAFwModMmeI) together with a modified 3' primer (IIAT20_Mod_Reamp, Table 7). This modified 3' primer included several mismatches in its poly-T tail, an approach which helps to interrupt the long polyT-tail of the cDNA products, which are known to negatively affect 454 sequencing (Jarvie and Harkins 2008). We amplified cDNA preparations after an initial denaturation step (95°C for 1min) for 20-35 cycles at 95°C for 15 seconds, 65°C for seconds and 68°C for 6min to allow fragment completion.

Synthesized and re-amplified cDNA was quality checked by both electrophoresis and PCR tests. Beta-actin, as well as three lectin genes previously

suggested to be important for in male pregnancy (Type I, II and III, Melamed et al. 2005) were amplified for each cDNA-preparation, and cDNA preparations amplifying all four control genes were used in subsequent steps. Amplifications contained 1M betaine (Sigma, St. Louis, MO, USA), 0.25mM dNTPs (Roche Diagnostics, Mannheim, Germany), 0.5µM of each oligonucleotide (Table 7) and 1 U of Taq polymerase (NEB) in 1x Taq-reaction buffer (NEB). Amplification conditions for all genes tested were identical and consisted of an initial 1 minute long denaturation step at 95°C followed by 40 PCR cycles at 95°C for 1min, 60°C for 1min and 72°C for 2min. Amplified fragments were completed in a 10minute long final extension step at 72°C.

Integration of 5' and 3' adapters during cDNA synthesis was assayed by rapid amplification of cDNA ends (RACE, Frohman et al. 1988) to test for adaptor integration. Reaction conditions for RACE amplifications were identical to those of the control-amplifications listed above (see also Table 7).

Library combination, normalization and sequencing

Our reference cDNA library (MID1) consists of equal quantities of cDNA extracted from gill tissue, brain, testis, liver and kidney. Libraries II and IV contain non-pregnant brood pouch tissue (MID2 and MID4), while libraries III and V contain pregnant brood pouch tissues (MID3 and MID5).

The relative concentrations of individual gene transcripts can vary substantially within each tissue. To avoid systematic bias towards abundantly expressed genes, libraries MID1, MID2 and MID3 were normalized prior to sequencing. Our normalization used the Trimmer Kit (Evrogen) according to the suggestions of the manufacturer. In brief, 1µg cDNA from each library was normalized with 1µL duplex-specific nuclease at 68°C for 25 minutes, heat-inactivated and PCR-amplified. Reagents used in amplification are identical to those described above, with the following changes: Taq-polymerase was replaced by a Taq/Pfu polymerase mixture (10:1) with reduced error rates, and amplified for 20 cycles at 95°C for 7 seconds, 66°C for 20 seconds and 72°C for 4 minutes using the same oligonucleotides as used for reamplification of cDNA (IIAFwModMmeI and IIAT20_Mod_Reamp, see above). Approximately 5µg of both normalized and unnormalized cDNA-libraries were MID-tagged and submitted to pyrosequencing according to the suggestions of the manufacturer.

Contig assembly

A primary contig assembly joined chimera-cleaned and adaptor-trimmed sequence reads using tgicl (http://compbio.dfci.harvard.edu/tgi/software/, Pertea et al. 2003). Sequence reads greater than 40bp were clustered with overlaps of at least 98% identity, and at least 1bp overlap distance from the sequence end. These settings force the assembler to combine only those reads from which all vector or linker information has been removed (Table 1). Blastx-searches of contigs produced during the first assembly identified substantial redundancy. A less stringent secondary assembly was therefore used to reassemble first-assembly contigs and singlets using the default settings of the assembly software, a sequence identity cutoff of 90% for sequences longer than 40bp and a minimum overhang of 20bp.

Annotation

Contigs were GO-annotated in Blast2GO (b2g) using default settings and the results of blastx-searches against local copies of the protein nr database (NCBI). These settings are recommended to maximize the quality of the annotations (Conesa et al. 2005, Götz et al 2008), which we augmented by using the "Annex" annotation augmentation function as suggested for b2g (Götz et al. 2008). We executed blastx searches against a local mirror of the NCBI protein-nr database (as of December 2009). Given the size limitation of b2g for the import of blast results, batches of 500 sequences were submitted for blastx searching and later combined into a single project file for annotation. Table 2 reports on the number of annotated contigs for each library and both assemblies. The analysis of the assembly and annotation results was performed in SAS 9.1.3 (SAS Institute Inc, Cary, USA).

Analyses

Univariate assembly statistics including average sequence length, read counts per contig and per library and median contig length were calculated for both assemblies (Table 1). We also extracted detailed information on contig length and the number of sequences contributing to each contig for the combined secondary assembly (Table 2).

In order to identify whether normalized and unnormalized cDNA libraries can be combined to identify quantitative differences in gene expression, we identified the set of contigs shared in the four brood pouch cDNA-libraries and tested for pairwise correlations in gene number. Poor correlations between the number of contributing reads per contig in normalized and unnormalized libraries indicate that quantitative information has been altered in normalized libraries, and that only unnormalized libraries can be used to extract quantitative data.

A stepwise process was used to identify pregnancy genes. All five libraries were first mined for the presence or absence of each contig. For this analysis, normalized and unnormalized libraries from the same tissue were pooled, and thus only three comparisons (reference tissues vs. pouch-pregnant tissues vs. pouch non-pregnant tissues) were made here (Figure 1). An initial quantitative screen identified genes which were exclusively present in a single tissue type.

Quantitative information (>2-fold expression differences) were also obtained from the two unnormalized cDNA libraries via comparison to the reference library. Here, our analysis was restricted to these genes expressed exclusively in brood pouch tissues. We measured expression levels as the number of reads from each of the unnormalized libraries contributing to each contig. For those sequences with contributing reads from both unnormalized libraries, fold-differences were obtained by calculating the ratio of contributing reads from the non-pregnant library to the pregnant library (downregulated genes, additional file 1) and vice versa for the upregulated genes (additional file 2).

These two approaches provide sets of male pregnancy-related genes for which b2g annotations can be compared. Since read-coverage of contigs in our dataset is highly variable and generally low, we analyzed both the full dataset and a restricted dataset, where each contig was represented by a minimum of five reads. Details on the experimental design are illustrated in Figure 1.

The molecular functions of annotated, differentially expressed pouch genes were collated using b2g. We compared top-level annotations (graph level 2) for the combined quantitative and qualitative datasets split into the classes of reference genes, as well as those upregulated or downregulated in the male pregnant brood pouch (Table 4). Information has been extracted for all annotation classes of differentially expressed genes (Figure 4, Table 4).

Acknowledgements

The authors wish to thank Sirisha Aluri for library-quantification and Marzanna Künzli for the execution of the next generation sequencing run. Funding from the Forschungskredit and the Zoological Museum of the University of Zurich (KNS) and the Stiftung für wissenschaftliche Forschung (ABW) is gratefully acknowledged.

References

Abouheif E. 1999. Establishing homology criteria for regulatory gene networks: prospects and challenges. *Novartis Found Symp* 222:207-221.

Alagna F, D'Agostino N, Torchia L, Servili M, Rao R, Pietrella M, Giuliano G, Chiusano ML, Baldoni L, Perrotta G. 2009. Comparative 454 pyrosequencing of transcripts from two olive genotypes during fruit development. *BMC Genomics* 10:399.

Benton MJ 1993. *The fossil record 2.* London: Chapman & Hall.

Boisseau JP. 1967. Les régulations hormonales de l'incubation chez un vertebré mâle: Recherches sur la reproduction de l'Hippocampe. *PhD Thesis.* Universite de Bordeaux.

Breder CM, Rosen DE. 1966. *Modes of reproduction in fishes.* New York: Natural History Press.

Breyne P, Dreesen R, Cannoot B, Rombaut D, Vandepoele K, Rombauts S, Vanderhaeghen R, Inze D, Zabeau M. 2003.: Quantitative cDNA-AFLP analysis for genome-wide expression studies. *Molecular Genetics and Genomics* 269:173-179.

Carcupino M, Baldacci A, Mazzini M, Franzoi P. 2002. Functional significance of the male brood pouch in the reproductive strategies of pipefishes and seahorses: a morphological and ultrastructural comparative study on three anatomically different pouches. *J Fish Biol* 61:1465-1480.

Chevreux B, Pfisterer T, Drescher B, Driesel AJ, Müller WEG, Wetter T, Suhai S. 2004. Using the miraEST assembler for reliable and automated mRNA transcript assembly and SNP detection in sequenced ESTs. *Genome Research* 14:1147-1159.

Chien Y, Becker DM, Lindsten T, Okamura M, Cohen DI, Davis MM. 1984. A third type of murine T-cell receptor gene. *Nature* 312:31-35.

Chomczynski P, Sacchi N. 1987. Single-step method of RNA isolation by acid guanidinium thiocyanate-phenol-chloroform extraction. *Anal Biochem* 162:156-159.

Conesa A, Götz S, Garcia-Gomez JM, Terol J, Talon M, Robles M. 2005. Blast2GO: a universal tool for annotation, visualization and analysis in functional genomics research. *Bioinformatics* 21:3674-3676.

Droege M, Hill B. 2008. The genome sequencer FLX system-longer reads, more applications, straight forward bioinformatics and more complete data sets. *J Biotechnol* 136:3-10.

Foster SJ, Vincent A. 2004. Life history and ecology of seahorses: implications for conservation and management. *J Fish Biol* 65:1-61.

Frohman MA, Dush MK, Martin GR. 1988. Rapid production of full-length cDNAs from rare transcripts - amplification using a single gene-specific oligonucleotide primer. *Proc Natl Acad Sci USA* 85:8998-9002.

Götz S, Garcia-Gomez JM, Terol J, Williams TD, Neda MJ, Robles M, Talon M, Dopazo J, Conesa A. 2008. High-throughput functional annotation and data mining with the Blast2GO suite. *Nucleic Acids Research* 36:3420-3435.

Hale MC, McCormick CR, Jackson JR, DeWoody JA. 2009. Next-generation pyrosequencing of gonad transcriptomes in the polyploid lake sturgeon (*Acipenser fulvescens*): the relative merits of normalization and rarefaction in gene discovery. *BMC Genomics* 10, 203.

Haresign TW, Shumway SE. 1981. Permeability of the marsupium of the pipefish *Syngnathus fuscus* to ^{14}C-alpha amino isobutyric acid. *Comp Biochem Physiol* 69a:603-604.

Harlin-Cognatio A, Hoffman EA, Jones AG. 2006. Gene cooption without duplication during the evolution of a male-pregnancy gene in pipefish. *Proc Natl Acad Sci USA* 103:19407-19412.

Jarvie T, Harkins T. 2008. Transcriptome sequencing with the genome sequencer FLX system. *Nature Methods* 2008, 5:vi-viii.

Kristiansson E, Asker N, Förlin L, Larsson DGJ. 2009. Characterization of the *Zoarces viviparus* liver transcriptome using massively parallel pyrosequencing. *BMC Genomics* 10:345.

Kuznetsov VA, Knott GD, Bonner RF. 2002. General statistics of stochastic process of gene expression in eukaryotic cells. *Genetics* 161:1321-1332.

Lee JS. 2000. The internally self-fertilizing hermaphroditic teleost *Rivulus marmoratus* (Cyprinodontiformes, Rivulidae) beta-actin gene: Amplification and sequence analysis with conserved primers. *Marine Biotechnology* 2:161-166.

Laksanawimol P, Damrongphol P, Kruatrachue M. 2006. Alteration of the brood pouch morphology during gestation of male seahorses, *Hippocampus kuda*. *Marine and Freshwater Research* 57:497-502.

Liang P, Pardee AB. 1992. Differential display of eukaryotic messenger-RNA by means of the polymerase chain-reaction. *Science* 257:967-971.

Linton JR, Soloff BL. 1964. The physiology of the brood pouch of the male sea horse *Hippocampus erectus*. *Bull Mar Sci Gulf Carib* 14:45-61.

Margulies M, Egholm M, Altman WE, Attiya S, Bader JS, Bemben LA, Berka J, Braverman MS, Chen YJ, Chen Z, Dewell SB, Du L, Fierro JM, Gomes XV, Godwin BC, He W, Helgesen S, Ho CH, Irzyk GP, Jando SC, Alenquer ML, Jarvie TP, Jirage KB, Kim JB, Knight JR, Lanza JR, Leamon JH, Lefkowitz SM, Lei M, Li J et al. 2005. Genome sequencing in microfabricated high-density picolitre reactors. *Nature* 437:376-380.

Melamed P, Xue Y, Poon JFD, Wu Q, Xie HM, Yeo J, Foo TWJ, Chua HK. 2005. The male seahorse synthesizes and secretes a novel C-type lectin into the brood pouch during early pregnancy. *FEBS Journal* 272:1221-1235.

Meyer E, Aglyamova GV, Wang S, Buchanan-Carter J, Abrego D, Colbourne JK, Willis BL, Matz MV. 2009. Sequencing and *de novo* analysis of a coral transcriptome using 454GSFlx. *BMC Genomics* 10:219.

Morozova O, Marra MA. 2008. Applications of next-generation sequencing technologies in functional genomics. *Genomics* 92:255-264.

Pertea G, Huang XQ, Liang F, Antonescu V, Sultana R, Karamycheva S, Lee Y, White J, Cheung F, Parvizi B, Tsai J, Quackenbush J. 2003. TIGR Gene Indices clustering tools (TGICL): a software system for fast clustering of large EST datasets. *Bioinformatics* 19:651-652.

Ripley JL, Foran CM. 2006. Differential parental nutrient allocation in two congeneric pipefish species (Syngnathidae: *Syngnathus* spp.). *J Exp Biol* 209:1112-1121.

Schena M, Shalon D, Davis RW, Brown PO. 1995. Quantitative monitoring of gene expression patterns with a complementary DNA microarray. *Science* 270:467-470.

Shagin DA, Rebrikov DV, Kozhemyako VB, Altshuler IM, Shcheglov AS, Zhulidov PA, Bogdanova EA, Staroverov DB, Rasskazov VA, Lukyanov S. 2002. A

novel method for SNP detection using a new duplex-specific nuclease from crab hepatopancreas. *Genome Research* 12:1935-1942.

Stölting KN, Gort G, Wüst C, Wilson AB. 2009. Eukaryotic transcriptomics *in silico*: Optimizing cDNA-AFLP efficiency. *BMC Genomics* 10, 565.

Stölting KN, Wilson AB. 2007. Male pregnancy in seahorses and pipefish: beyond the mammalian model. *Bioessays* 29:884-896.

Van Look KJW, Dzyuba B, Cliffe A, Koldewey HJ, Holt WV. 2007. Dimorphic sperm and the unlikely route to fertilisation in the yellow seahorse. *J Exp Biol* 10:432-437

Vera JC, Wheat CW, Fescemyer HW, Frilande MJ, Crawford DL, Hanski I, Marder JH. 2008. Rapid transcriptome characterization for a nonmodel organism using 454 pyrosequencing. *Molecular Ecology* 17: 1636-1647.

Wang W, Wang Y, Zhang Q, Qi Y, Guo D. 2009. Global characterization of Artemisia annua glandular trichome transcriptome using 454 pyrosequencing. *BMC Genomics* 10: 465.

Wilson AB, Ahnesjo I, Vincent ACJ, Meyer A. 2003. The dynamics of male brooding, mating patterns, and sex roles in pipefishes and seahorses (family Syngnathidae). *Evolution* 57:1374-1386.

Wilson AB, Vincent A, Ahnesjo I, Meyer A. 2001. Male pregnancy in seahorses and pipefishes (Family Syngnathidae): Rapid diversification of paternal brood pouch morphology inferred from a molecular phylogeny. *Journal of Heredity* 92:159-166.

Woods CMC. 2000. Preliminary observations on breeding and rearing the seahorse *Hippocampus abdominalis* (Teleostei: Syngnathidae) in captivity. *NZ J Mar Freshwater Res* 34:475-485.

Zagrobelny M, Scheibye-Alsing K, Jensen NB, Lindberg Moller B, Gorodkin J, Bak S. 2009. 454 pyrosequencing based transcriptome analysis of Zygaena filipendulae with focus on genes involved in biosynthesis of cyanogenic glucosides. *BMC Genomics* 10:574.

Zhang N, Xu B, Mou CY, Yang WL, Wei JW, Lu L, Zhu JJ, Du JC, Wu XK, Ye LT, Fu ZY, Lu Y, Lin JH, Sun ZZ, Su J, Dong ML, Xu AL. 2003. Molecular profile of the unique species of traditional Chinese medicine, Chinese seahorse (*Hippocampus kuda* Bleeker). *FEBS Letters* 550:124-134.

Zhu YY, Machleder EM, Chenchik A, Li R, Siebert PD. 2001. Reverse transcriptase template switching: A SMART (TM) approach for full-length cDNA library construction. *Biotechniques* 30:892-897.

Zhulidov PA, Bogdanova EA, Shcheglov AS, Vagner LL, Khaspekov GL, Kozhemyako VB, Matz MV, Meleshkevitch E, Moroz LL, Lukyanov SA, Shagin DA. 2004. Simple cDNA normalization using kamchatka crab duplex-specific nuclease. *Nucleic Acids Research* 32 (3), e37.

Table 1 Comparison of primary and secondary assembly

Descriptive statistics for the primary and secondary assembly. Avg = average; SD = standard deviation; max = maximum, min = minimum, bp = base pairs; Redundancy is estimated as the fraction of genes with the same top hit in a blastx search (December 2009, local mirror of NCBI protein nr database).

	Primary assembly	Secondary assembly
uncorrected reads	1023026	1023026
reads passing assembly	853879	853879
average read length	227.13 ± 112.92	227.13 ± 112.92
reads assembled into contigs	705894	783592
singlets remaining	148164	70287
Singlet length ± SD (bp)	209.26 ± 126.21	177.15 ± 131.76
contigs produced	36706	38419
avg. reads/contig ± SD	19.23 ± 253.39	20.40 ± 263.90
max reads/contig	20626	23478
total length contigs (bp)	12041814	13853626
avg contig length ± SD (bp)	328.06 ± 185.66	360.59 ± 207.81
max contig length (bp)	2453	2846
min contig length (bp)	54	45
Contigs with blastx results (nr)	11889	11741
Non-redundant blastx results (nr)	8444	9319
GO annotated contigs	10580	10309
redundancy	29%	21%
redundancy-corrected estimate of genes	>26000	>30000

Table 2 Descriptive statistics for the secondary assembly

Descriptive statistics for the secondary assembly, separated by cDNA library. Avg.= average; SD = Standard deviation; private contigs = contigs unique to a single library

	MID1	MID2	MID3	MID4	MID5	SUM
pregnant	yes	no	yes	no	yes	
tissue	reference	pouch	pouch	pouch	pouch	
Total reads	228082	159579	223094	153899	89255	853879
assembled reads	202627	144134	205910	145721	85200	783592
Avg read length per read ± SD	189.23 ± 104.82	199.78 ± 94.50	235.09 ± 103.71	272.08 ± 119.44	275.51 ± 124.39	227.13 ± 112.92
Avg read length per assembled read ± SD	191.96 ± 101.68	203.94 ± 90.58	238.44 ± 100.07	276.30 ± 115.87	279.87 ± 121.24	231.62 ± 109.97
contigs	24884	20871	23776	10986	6709	38419
avg. reads per contig ± SD	8.14 ± 66.39	6.91 ± 49.09	8.66 ± 66.57	13.26 ± 222.34	12.69 ± 210.00	20.4 ± 263.90
max reads / contig and library	4112	3721	5029	13519	11428	23478
private contigs	5149	2577	2846	706	210	11488

Table 3 T-tests comparing the influence of read number and contig length on annotated and non-annotated sequences.

T-tests comparing 38419 annotated and non-annotated secondary assembly contigs. N = number of contigs; SD = standard deviation of the average; Sig. = p-value for the null-hypothesis of variance equality.

T-tests	Annotated	N	Average ± SD	Sig.
Contributing reads	No	28110	14.50 ± 215.79	p<0.0001
	Yes	10309	36.47 ± 363.62	
Contig length (bp)	No	28110	303.44 ± 162.19	p<0.0001
	Yes	10309	516.43 ± 236.67	

Table 4 Annotation results for the full dataset and contigs >4 reads

Top-level annotations for annotated contigs of the complete dataset (38419 contigs) and subsets of individual libraries. Data are also presented for 15300 high-reliability contigs built from five or more contributing reads. Numbers of observations for each top-level annotation are indicated for biological processes, molecular functions and cellular components (see also Figure 4). Note: Multiple annotations are possible for each contig.

		38419 contig dataset				15300 contigs >4 reads			
		38419 contigs	**Reference**	**Pouch non-pregnant**	**Pouch pregnant**	**15300 contigs**	**Reference**	**Pouch non-pregnant**	**Pouch pregnant**
	Library	MID1-5	MID1	MID2/4	MID3/5	MID1-5	MID1	MID2/4	MID3/5
	Contigs per dataset	38419	24884	24842	25299	15300	12761	12931	13310
	Private contigs	11488	5149	4076	3545	1093	704	320	262
	Annotated contigs (total dataset)	10309	6809	7341	7951	5178	4296	4576	4784
	Annnotated contigs (private dataset)	2046	855	713	872	214	140	55	73
Biological Process	anatomical structure formation	793	540	531	599	396	345	330	357
	biological adhesion	401	264	279	301	192	161	165	175
	biological regulation	3803	2534	2703	2944	1933	1610	1714	1792
	cellular process	6340	4251	4533	4934	3272	2751	2885	3030
	developmental process	2184	1453	1517	1680	1082	903	951	1000
	growth	259	176	183	216	138	115	125	131
	immune system process	395	270	283	308	204	166	178	191
	localization	1996	1351	1386	1524	1009	850	873	926
	locomotion	350	220	245	280	175	145	147	162
	metabolic process	4524	3059	3297	3575	2386	2025	2137	2230
	multicellular organismal process	1995	1356	1337	1494	981	816	851	893
	multi-organism process	245	161	175	201	130	108	118	121
	pigmentation	60	36	42	48	26	21	25	25
	reproduction	301	193	225	233	155	124	142	139
	response to stimulus	1362	940	972	1041	700	590	617	644
	rhythmic process	73	44	54	49	33	23	30	27
	viral reproduction	53	37	38	46	29	26	27	28
Molecular Function	antioxidant activity	33	24	22	22	15	14	14	12
	auxiliary transport protein activity	35	27	23	23	16	13	14	14
	binding	6390	4272	4551	4920	3241	2736	2847	2995
	catalytic activity	3267	2172	2341	2539	1652	1398	1457	1524
	chemorepellent activity	2	1	1	1	2	1	1	1
	electron carrier activity	109	76	68	81	50	41	44	45
	enzyme regulator activity	522	339	379	394	241	203	209	223
	metallochaperone activity	1	0	1	0	1	0	1	0
	molecular transducer activity	703	449	500	524	344	283	301	317
	proteasome regulator activity	2	1	1	1	2	1	1	1
	structural molecule activity	457	335	332	349	266	236	234	243
	transcription regulator activity	682	458	503	536	362	297	325	340
	translation regulator activity	138	97	108	120	90	79	85	86
	transporter activity	562	398	363	397	285	237	240	258
Cellular Component	cell	6832	4603	4880	5291	3503	2949	3097	3252
	envelope	388	282	284	309	213	185	188	197
	extracellular region	487	320	310	355	234	187	183	202
	macromolecular complex	2441	1679	1761	1949	1339	1145	1201	1251
	membrane-enclosed lumen	1305	867	940	1026	661	551	597	619
	organelle	4601	3122	3331	3606	2413	2054	2136	2248
	synapse	211	150	115	126	86	77	65	71
	virion	5	1	2	2	5	1	2	2

Table 5 Effects of normalization

Comparison of normalized and unnormalized cDNA libraries derived from cDNA preparations of non-pregnant (MID2 and 4) and pregnant (MID3 and 5) male brood pouch tissues. The number of assembled sequencing reads within each library, the number of resulting contigs, the number of annotated contigs and the number of private contigs is reported together with basic descriptive statistics (average read number per contig and its standard deviation together with average contig lengths and corresponding standard deviations) for each library. Note that private contigs here refer to those contigs restricted to either the normalized or unnormalized libraries from a given tissue (i.e. these contigs may be present in libraries from the other tissues). Summary information for each tissue is indicated (Combined).

Library	Non-pregnant brood pouch			Pregnant brood pouch		
	Normalized	**Un-normalized**	**Combined**	**Normalized**	**Un-normalized**	**Combined**
	MID2	**MID4**	**MID2&MID4**	**MID3**	**MID5**	**MID3&MID5**
assembled reads	144134	145721	289855	205910	85200	291110
Avg length/read ± SD	203.94 ± 90.58	276.30 ± 115.87	240.30 ± 110.17	238.44 ± 100.07	279.87 ± 121.24	250.57 ± 108.35
# contigs	20871	10986	24842	23776	6709	25299
Private contigs	13856	3971	17827	18590	1523	20113
avg. Reads/contig ± SD	6.91 ± 49.09	13.26 ± 222.34	11.67 ± 165.33	8.66 ± 66.57	12.70 ± 210.00	11.51 ± 144.34
Max reads/contig	3721	13519	14007	5029	11428	12130
Avg contig length ± SD	378.83 ± 228.37	492.69 ± 262.02	389.98 ± 228.10	401.54 ± 220.13	529.84 ± 289.00	402.65 ± 219.91
Avg length of private contig ± SD	308.55 ± 154.45	448.61 ± 217.48	339.75 ± 180.20	356.76 ± 166.52	420.00 ± 215.67	361.54 ± 171.55
Avg reads/private contig ± SD	2.77 ± 3.79	2.63 ± 10.54	2.74 ± 5.99	3.51 ± 6.52	1.69 ± 1.86	3.37 ± 6.02
Max reads/private contig	91	454	454	216	33	216

Table 6 Pairwise correlations between numbers of contributing reads per contig in each library

Normalization may result in the loss of quantitative information. For the set of 2719 contigs with contributing reads from all four pouch libraries (MID2-MID5), pairwise correlations have been calculated to estimate how well the normalized datasets reflect expression levels in their unnormalized counterparts. Normalized (MID2, 3) and unnormalized (MID4, 5) cDNA libraries derived from the same cDNA preparations of non-pregnant (MID2, 4) and pregnant (MID3, 5) male brood pouch tissues are compared, and the significance of each comparison is identified. Below diagonal: correlation coefficients; above: associated confidence limits for Pearson correlation statistics (Fisher's z transformation). All correlations are highly significant at $p<0.0001$.

	MID2	MID3	MID4	MID5
MID2	-	0.856 - 0.875	0.210 - 0.280	0.134 - 0.206
MID3	0.866	-	0.423 - 0.482	0.314 - 0.379
MID4	0.245	0.453	-	0.745 - 0.961
MID5	0.170	0.347	0.745	-

Table 7 Oligonucleotides used for cDNA synthesis and quality assays

Oligonucleotides used in cDNA synthesis and test –amplifications. Oligos are indicated with **name**, base pair **sequence** in **5'-3'** orientation and associated melting temperatures (T_M). The **function** of each oligonucleotide is indicated, as are reaction-concentrations (**Conc.**) and authors responsible for each primer (**Author**).

Name	Seqeunce(5'-3')	T_M	Function	Author
IIAFwModMmeI	TCCAACAAGCAGTGGTATCAACGCAGAGTGCGGGH	69.0	First strand cDNA synthesis	KNS
IIAT20ModMmeI	AAGCAGTGGTATCAACGCAGAGTTCCGACTTTTTTTTTTTTTTTTTTTVN	63.7	Second strand cDNA synthesis	KNS
IIAT20_Mod_Reamp	AAGCAGTGGTATCAACGCAGAGTTCCGACTTTTGTCTTTTGTTCTGTTTVN	67.0	Poly-T suppression	KNS
Type II Lectin F1	CTCCTTTGCGGGATCAGTGG	65.2	control amplifications, RACE	KNS
Type II Lectin R1	TCCTTCATTTGCTGGAGAGATGC	65.0	control amplifications, RACE	KNS
Type I Lectin F1	ACTGCAAAGATGGCATTCGCT	64.3	control amplifications, RACE	KNS
Type I Lectin R1	CCGTTGCAACAACAGGGTGGCAG	72.7	control amplifications, RACE	KNS
Type III Lectin F1	TCCTTTGTGGGATCAGCGGACTG	69.7	control amplifications, RACE	KNS
Type III Lectin R1	TGACAAGCAAACCCCGTTGC	66.5	control amplifications, RACE	KNS
Type II Lectin F2	CTTCAGTCACAATGAAGCTCA	60.6	RACE	KNS
Type II Lectin R2	TTTCCAGGTCACTGTGGATGG	67.1	RACE	KNS
Type I Lectin R2	ATCACGTTGGAAGATGTAACA	59.5	RACE	KNS
Type I Lectin F2	TATGGACCGATGGCACAGTTA	65.0	RACE	KNS
Type III Lectin R2	CAGACACTCTCGGCATCTGCA	69.1	RACE	KNS
Type III Lectin F2	ATGATTGCGTGGAGCTTCGTC	68.5	RACE	KNS
Bactin 5F'	ATGGATGATGAAATTGCCG	50.9	control amplifications, RACE	Lee 2000
Bactin 3R1	AGGTAGTCTGTGAGGTCTCG	54.8	control amplifications, RACE	Lee 2000

Figure 1 Identification of male pregnancy genes

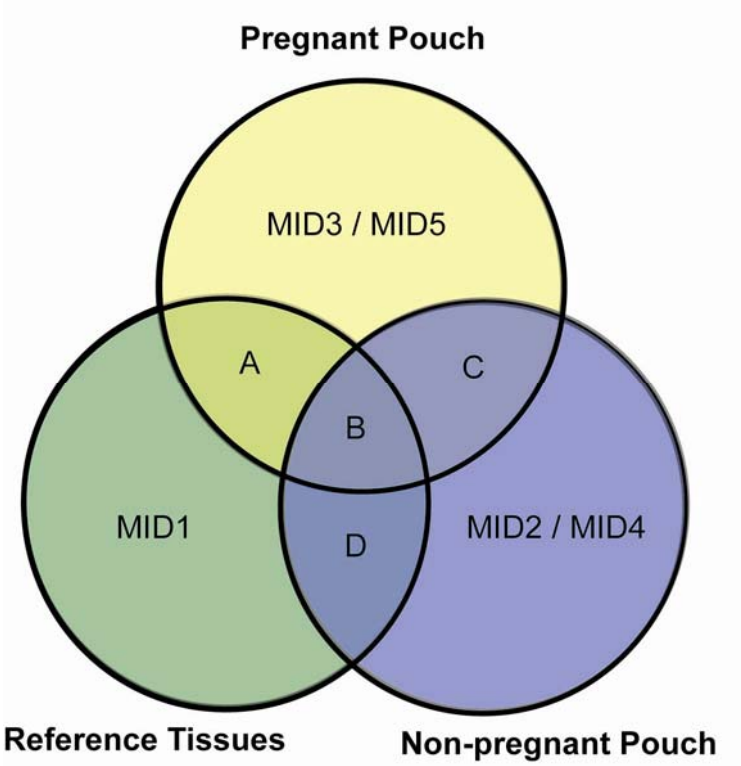

cDNA libraries shown as three pools: Reference genes (green pool), genes from the pregnant pouch (yellow) and genes from the non-pregnant pouch (blue). **A**, genes present in pregnant pouch and pregnant reference tissues, **B**, genes shared by all pools, **C** genes shared between non-pregnant and pregnant pouch tissues and pregnant reference tissues, **D**, genes shared between the non-pregnant pouch and the reference tissues. For unnormalized cDNA libraries, pouch-specific genes are obtained by determining the yellow (non-shared) pouch pregnancy genes, the blue (non-shared) pouch non-pregnancy genes and by extracting quantitative information for the fraction of shared pouch-specific genes for which these data are available. Since quantitative information is not available from normalized libraries (see Table 6), these libraries are used solely for qualitative analyses.

Figure 2: Venn diagrams – distribution of annotated contigs

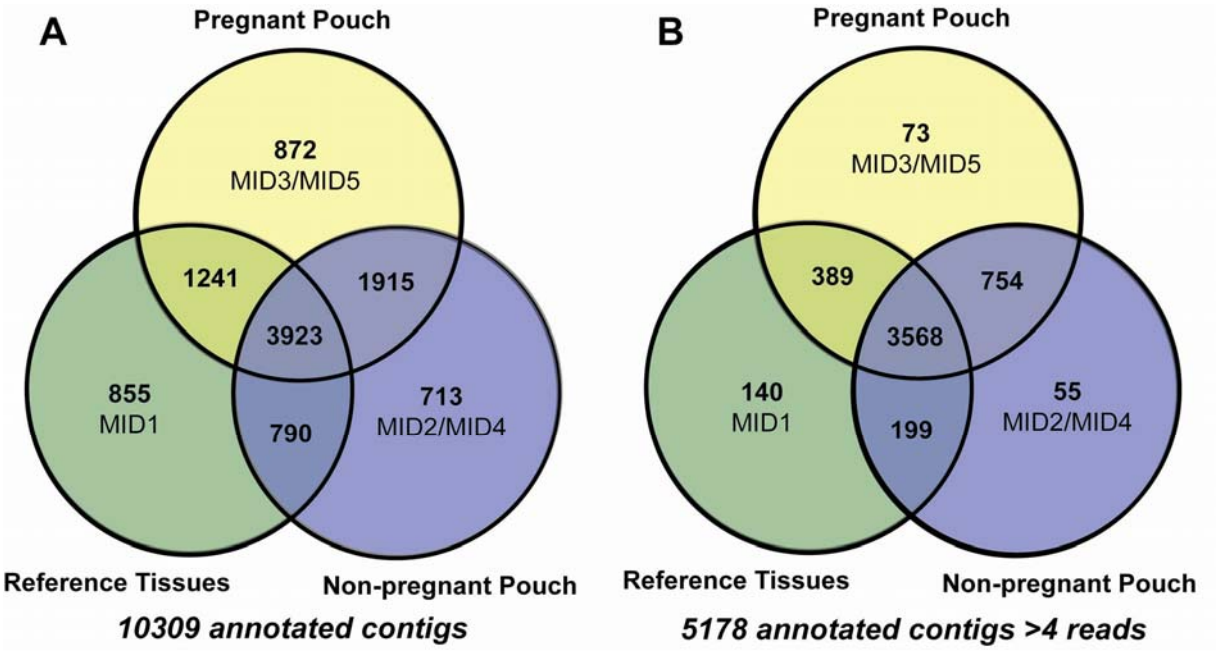

Venn diagrams depicting the number of contigs per cDNA-pool split into shared and non-shared (private) pool fractions. **A** Summary information for all 10309 annotated contigs in the full dataset. **B** Summary information for the 5178 annotated contigs in the dataset of 15300 contigs built from five or more sequencing reads.

Figure 3 Histograms contig-length of annotated and complete datasets

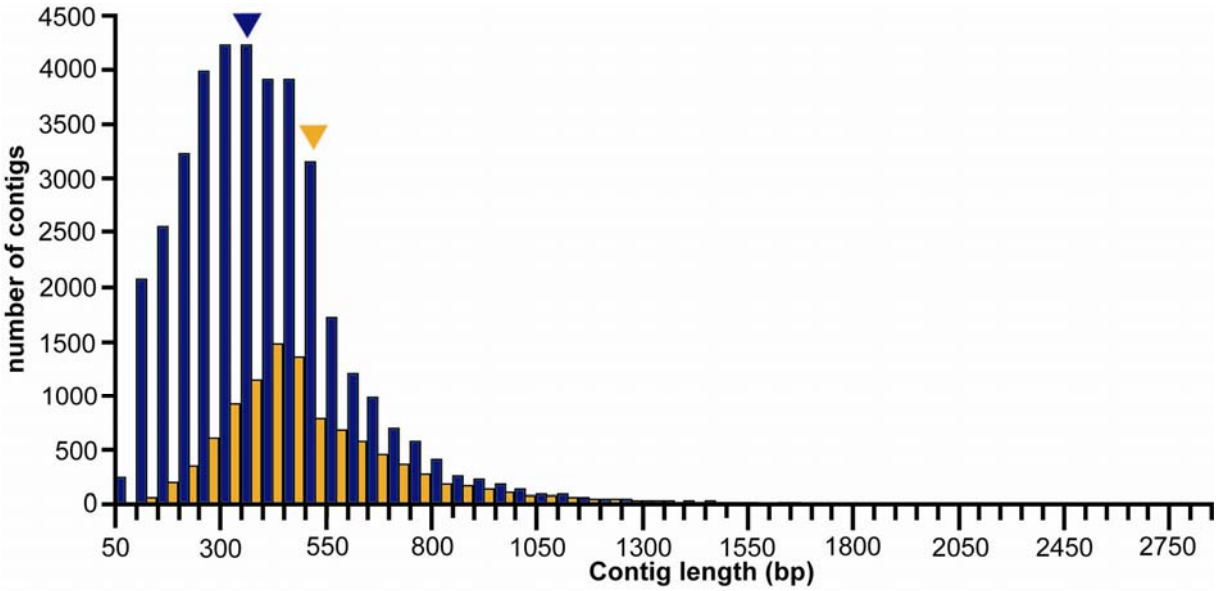

Histogram for secondary assembly contigs, plotting the observed number of contigs against the contig length in base pairs. Dark blue: Full set of 38419 secondary assembly contigs; Yellow: annotated contigs (10309). Arrowheads indicate the average contig length for the full dataset (dark blue) and the subset of annotated contigs (yellow, see also Table 3).

Figure 4 Annotation of pouch-specific pregnancy genes

Annotation of pouch-specific pregnancy genes with five or more contributing reads. Blue: downregulated genes, yellow: upregulated genes. **A** Top level biological processes for all annotated genes, **B** Major molecular functions for all annotated genes, **C** predominant localization of all annotated genes (Table 6 and Methods).

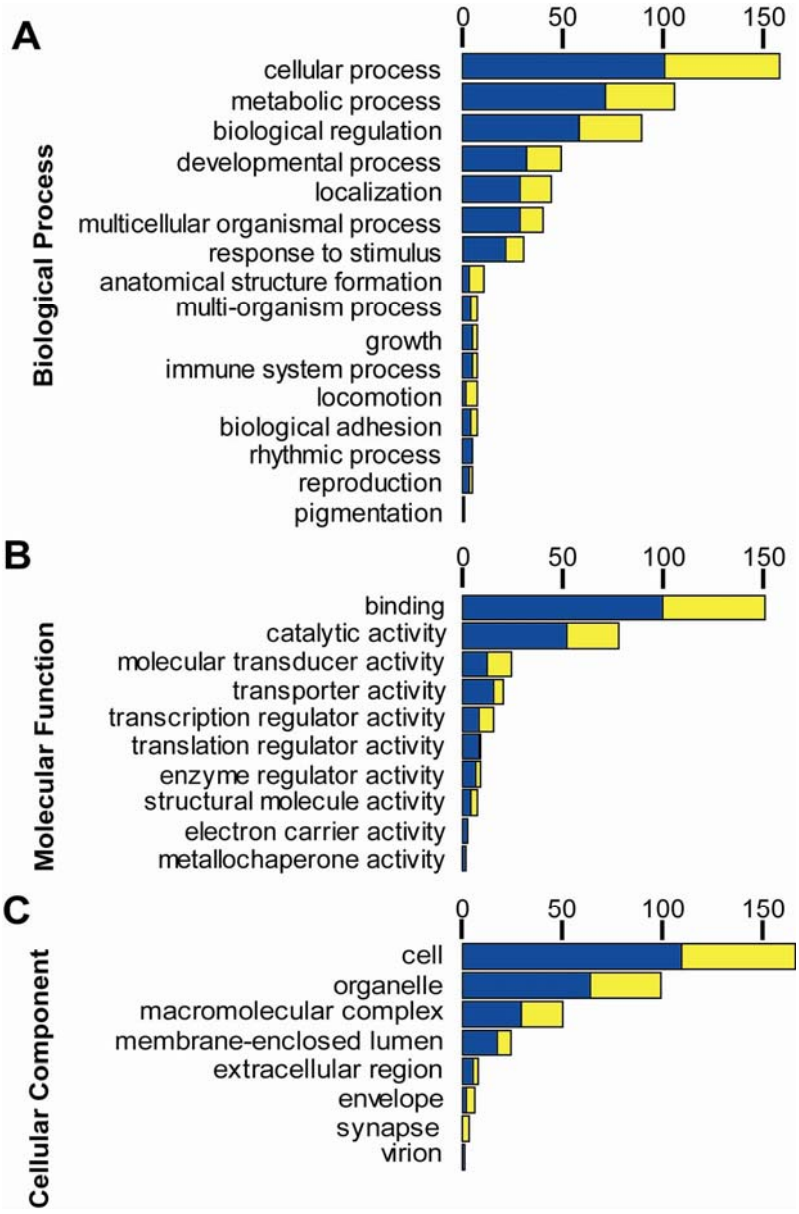

Additional file 1 181 annotated genes which are downregulated or entirely absent from the pregnant brood pouch.

Overview of annotated contigs absent from the pregnant brood pouch or more than two-fold downregulated in the pregnant brood pouch. Contigs are indicated together with their lengths in base pairs and the numbers of contributing reads from the normalized and unnormalized cDNA libraries. Norm= normalized cDNA library, Unnorm= unnormalized cDNA library. PP=pregnant brood pouch tissue, NP=non-pregnant brood pouch tissue. Fold difference reflects expression differences between the unnormalized non-pregnant and pregnant tissues. E-values and sequence descriptions are indicated for the top-blastx hit for each contig together with corresponding GenBank accession numbers. GO annotations are indicated wherever available and the remaining annotations were inferred by blast2go (b2g inferred).

Contig	length (bp)	MID2 Norm/ NP	MID3 Norm/ PP	MID4 Unnorm/ NP	MID5 Unnorm/ PP	Fold difference	evalue	Sequence description	GenBank Accession No.	annotation
Contig8690	793	0	0	5	1	5	4.97E-28	guanine nucleotide binding alpha 11	gi|125850059	GO:0001508
Contig25156	1267	0	1	5	2	2.5	4.63E-79	envoplakin	gi|47214954	GO:0001533
Contig3326	273	6	0	0	0	-	3.96E-33	unc-93 homolog b1 (elegans)	gi|189515413	GO:0002224
CL546Contig3	275	5	0	0	0	-	1.98E-11	sf3b2 protein	gi|194390138	GO:0003676
Contig27446	915	1	1	4	2	2	2.50E-73	regulatory factor 2 (influences hla class ii expression)	gi|47222197	GO:0003677
CL1Contig5434	509	0	1	11	2	5.5	9.62E-76	eukaryotic translation initiation factor	gi|189532710	GO:0003743
CL3723Contig1	412	4	4	5	1	5	4.20E-59	elongation factor 2	gi|28278942	GO:0003746
Contig8455	965	0	9	33	3	11	9.11E-146	a disintegrin-like and metallopeptidase (reprolysin type)	gi|47222514	GO:0004222
Contig6632	483	5	0	3	0	-	1.05E-37	malic enzyme nad(+)- mitochondrial	gi|237681177	GO:0004471
Contig1265	880	2	6	8	4	2	2.08E-94	udp-n-acetyl-alpha-d-galactosamine:polypeptide n-acetylgalacto...	gi|125839743	GO:0004653
CL3455Contig2	658	0	0	4	1	4	1.40E-99	rna guanylyltransferase and 5 -phosphata...	gi|47224366	GO:0004725
CL5253Contig1	1109	1	0	7	0	-	9.62E-90	signal transducer and activator of trans...	gi|224613364	GO:0004871
Contig9207	351	5	0	0	0	-	3.74E-31	hypoxia inducible factor alpha subunit...	gi|56785781	GO:0004871
CL4735Contig1	557	1	4	4	2	2	4.20E-71	tumor necrosis factor receptor member 19	gi|225707736	GO:0004872
Contig27543	850	9	1	6	2	3	1.16E-79	g protein-coupled receptor kinase 5	gi|47228574	GO:0005080

Contig	length (bp)	MID2 Norm/ NP	MID3 Norm/ PP	MID4 Unnorm/ NP	MID5 Unnorm/ PP	Fold difference	evalue	Sequence description	GenBank Accession No.	annotation
Contig25605	973	1	4	11	5	2.2	9.79E-95	rho gtpase activating protein 12	gi|187607956	GO:0005096
Contig4207	1903	3	9	37	12	3.08	0	membrane calcium atpase family member (mca-3)	gi|73984630	GO:0005388
CL8414Contig1	697	0	0	5	0	-	4.95E-32	gag-pro-pol polyprotein	gi|83722645	GO:0005488
CL9583Contig1	565	3	0	2	0	-	8.21E-43	zinc finger protein	gi|47216468	GO:0005488
Contig2281	927	1	0	5	0	-	2.10E-89	muscleblind-like 2	gi|239735526	GO:0005488
Contig25992	561	1	0	4	1	4	2.11E-27	ras-gtpase activating protein sh3 domain-binding protein 2	gi|123703665	GO:0005488
Contig3139	1267	1	3	8	1	8	1.24E-129	ankyrin repeat and btb domain containing 2...	gi|47215237	GO:0005488
CL9103Contig1	313	5	0	0	0	-	6.24E-53	eukaryotic translation initiation factor	gi|223648062	GO:0005515
Contig10583	427	1	0	4	0	-	1.79E-25	hiv-1 induced protein hin-1	gi|47209320	GO:0005515
Contig1070	1085	1	0	18	2	9	2.27E-58	eukaryotic translation initiation factor 3 subunit 6	gi|47209929	GO:0005515
Contig8472	1031	0	3	28	5	5.6	8.30E-92	zinc finger protein 503	gi|82238283	GO:0005515
Contig9732	819	0	0	8	1	8	4.24E-18	solute carrier family 39 (zinc transporter) member 7	gi|146147383	GO:0005515
Contig812	304	1	1	5	2	2.5	3.72E-15	lectin protein type i	gi|34013698	GO:0005529
Contig880	399	1	1	20	3	6.67	2.36E-17	lectin protein type i	gi|34013698	GO:0005529
Contig25542	552	0	0	4	1	4	3.92E-10	senescence-associated	gi|6715146	GO:0005576
Contig10084	740	3	1	12	1	12	2.47E-32	small gtpase ras-dva-3	gi|82617940	GO:0005622
Contig2143	332	1	2	6	1	6	4.67E-42	integral membrane protein 1	gi|148226196	GO:0005624
Contig25785	656	0	0	4	1	4	3.51E-26	transaldolase 1	gi|225706208	GO:0005625
Contig27518	920	2	1	8	3	2.67	2.53E-41	transaldolase 1	gi|226443406	GO:0005625
CL7925Contig1	559	1	0	4	0	-	5.03E-12	phd finger protein 10	gi|225714712	GO:0005634
Contig19735	468	5	0	1	0	-	8.33E-31	c-maf-inducing protein	gi|125843248	GO:0005634
CL9003Contig1	503	0	0	4	1	4	3.05E-71	uba and wwe domain containing 1	gi|189536057	GO:0005730
CL5010Contig1	442	0	2	7	1	7	7.54E-74	lim domain containing preferred transloc...	gi|58801524	GO:0005737
CL6534Contig1	913	1	0	5	1	5	1.58E-98	tumor protein p53 binding 2	gi|47223292	GO:0005737
Contig20232	376	5	0	0	0	-	9.50E-36	rho gdp dissociation inhibitor alpha	gi|47219625	GO:0005737
Contig20356	487	8	0	1	0	-	1.26E-10	copper chaperone for superoxide dismutase	gi|47212233	GO:0005737

Contig	length (bp)	MID2 Norm/ NP	MID3 Norm/ PP	MID4 Unnorm/ NP	MID5 Unnorm/ PP	Fold difference	evalue	Sequence description	GenBank Accession No.	annotation
Contig2385	704	0	0	4	1	4	4.78E-71	casein kinase 1 epsilon	gi|7798595	GO:0005737
Contig26624	436	3	0	2	0	-	1.19E-13	kinesin family member 13b	gi|125841549	GO:0005737
Contig26753	619	1	1	6	2	3	2.95E-53	sh3 and px domains 2b	gi|60649481	GO:0005737
Contig26892	684	0	0	7	1	7	4.47E-89	triple functional domain (ptprf interacting)	gi|47224099	GO:0005737
Contig3254	675	1	3	4	1	4	2.44E-53	asparaginyl-trna synthetase	gi|148231213	GO:0005737
Contig4593	701	1	1	4	1	4	3.17E-18	pleckstrin homology domain family a (phosphoinositide binding	gi|47087415	GO:0005737
Contig4762	637	1	2	4	1	4	2.05E-38	protein cxorf17 homolog	gi|189535889	GO:0005737
Contig7679	648	1	0	5	0	-	5.61E-61	myeloid lymphoid or mixed-lineage leukemia (trithorax drosophi...	gi|55925532	GO:0005737
Contig977	486	0	0	7	2	3.5	1.86E-30	beta-actin	gi|94537157	GO:0005737
Contig929	806	0	1	18	2	9	2.55E-69	nadh dehydrogenase subunit 5	gi|25057953	GO:0005743
Contig26079	892	0	0	4	2	2	3.99E-44	cathepsin f	gi|37903252	GO:0005764
CL1Contig4825	993	0	0	5	1	5	8.39E-36	carboxylesterase 2 (liver)	gi|47219812	GO:0005783
Contig8611	653	2	5	4	1	4	4.04E-75	ergic and golgi 3	gi|157820783	GO:0005789
Contig26544	880	1	5	4	1	4	3.85E-147	eukaryotic translation initiation factor subunit d...	gi|47217933	GO:0005852
Contig25653	645	0	0	5	2	2.5	1.96E-66	beta-actin	gi|157278351	GO:0005856
CL2520Contig2	847	1	0	9	1	9	3.36E-61	claudin 1	gi|49333479	GO:0005887
CL9509Contig1	639	2	0	3	0	-	7.27E-45	solute carrier family (neutral amino aci...	gi|47220869	GO:0005887
Contig1553	433	6	4	23	1	23	3.75E-34	rh type b glycoprotein	gi|123909597	GO:0005887
Contig4760	516	0	3	4	1	4	3.05E-29	rh type c glycoprotein	gi|123886327	GO:0005887
Contig6276	638	1	0	5	0	-	2.04E-44	isocitrate dehydrogenase 1	gi|148232240	GO:0005975
Contig26993	1441	0	1	11	5	2.2	5.02E-110	6-phosphofructo-2-kinase fructose- -biphosphatase 2	gi|41055967	GO:0006007
CL4254Contig3	186	7	0	0	0	-	2.40E-20	spastic ataxia of charlevoix-saguenay	gi|47226310	GO:0006457
Contig6910	982	0	0	7	0	-	8.85E-12	subfamily member 11	gi|77735491	GO:0006457
Contig26046	486	0	1	4	1	4	5.45E-14	vesicle-associated membrane protein 8	gi|209155888	GO:0006461
CL1Contig4615	670	0	0	5	0	-	1.98E-67	methionine adenosyltransferase alpha	gi|47226445	GO:0006556

Contig	length (bp)	MID2 Norm/ NP	MID3 Norm/ PP	MID4 Unnorm/ NP	MID5 Unnorm/ PP	Fold difference	evalue	Sequence description	GenBank Accession No.	annotation
Contig1096	838	0	0	18	0	-	5.53E-13	methionine adenosyltransferase alpha	gi|90076722	GO:0006556
CL1Contig4455	818	0	1	6	3	2	2.21E-22	partial	gi|84579145	GO:0006814
Contig620	401	13	0	0	0	-	3.30E-11	rer1 protein	gi|41053411	GO:0006890
CL1Contig3843	478	0	0	4	1	4	3.04E-20	plastin 3 (t isoform)	gi|224097921	GO:0007015
CL6554Contig1	410	3	0	4	0	-	6.89E-50	eph receptor a2	gi|189536014	GO:0007169
CL3322Contig1	481	0	0	13	3	4.33	9.93E-64	cnksr family member 3	gi|126311220	GO:0007243
Contig7359	669	0	3	7	2	3.5	2.52E-91	plexin b2	gi|47224387	GO:0007275
Contig2834	1049	4	27	19	4	4.75	5.96E-133	hyaluronoglucosaminidase 5	gi|29470175	GO:0007341
Contig22686	495	0	2	4	1	4	1.18E-53	solute carrier family 9 (sodium hydrogen exchanger) member 2	gi|70722630	GO:0008104
Contig26935	640	0	1	5	2	2.5	4.50E-43	protein	gi|13359451	GO:0008134
Contig9835	752	5	0	3	0	-	9.86E-42	kallikrein-related peptidase 15	gi|47212679	GO:0008233
Contig9839	878	19	19	16	2	8	3.01E-81	loc561562 protein	gi|225716632	GO:0008233
Contig2237	323	5	0	0	0	-	2.53E-11	serine arginine repetitive matrix 1	gi|47219559	GO:0008380
Contig2723	977	0	0	8	1	8	5.50E-29	pg1 protein	gi|238855136	GO:0009536
Contig8803	1059	0	0	6	3	2	8.98E-30	clock homolog 3	gi|251747935	GO:0009648
Contig9936	989	0	2	4	1	4	9.35E-85	notch homolog translocation-associated	gi|148725836	GO:0009653
Contig961	890	1	2	48	3	16	2.05E-12	methionine adenosyltransferase alpha	gi|149036421	GO:0009725
Contig18825	927	1	7	5	1	5	1.01E-120	eukaryotic translation initiation factor subunit 2 39kda	gi|126282310	GO:0009749
Contig1041	1539	0	3	98	30	3.27	4.77E-88	ubiquitously transcribed tetratricopeptide x chromosome	gi|122114590	GO:0009952
CL7097Contig1	448	1	0	5	0	-	4.25E-62	adam metallopeptidase with thrombospondi...	gi|47226569	GO:0009986
CL7640Contig1	984	1	0	5	0	-	1.21E-111	transducin -like 3	gi|47218051	GO:0009987
Contig1646	950	1	6	12	2	6	3.16E-48	delta protein	gi|189527777	GO:0009987
Contig17993	1180	1	0	8	1	8	2.74E-90	myeloid lymphoid or mixed-lineage leukemia 2	gi|3540281	GO:0009987
CL3818Contig2	323	5	0	0	0	-	4.94E-18	sec31 homolog a	gi|41054764	GO:0015031
Contig7468	361	10	0	2	0	-	1.23E-18	member ras oncogene family	gi|47211718	GO:0015031
Contig988	866	0	0	6	2	3	1.28E-84	exocyst complex component 5	gi|47230177	GO:0015031

Contig	length (bp)	MID2 Norm/ NP	MID3 Norm/ PP	MID4 Unnorm/ NP	MID5 Unnorm/ PP	Fold difference	evalue	Sequence description	GenBank Accession No.	annotation
CL218Contig7	279	16	0	0	0	-	3.58E-29	rhamnose-binding lectin	gi|58465408	GO:0016020
Contig9256	485	0	0	5	1	5	7.55E-52	cnksr family member 3	gi|47219526	GO:0016020
Contig1151	1669	6	7	35	6	5.83	1.34E-133	solute carrier family member 1	gi|41053617	GO:0016021
Contig17186	418	3	0	2	0	-	5.43E-46	transmembrane channel-like 2	gi|189519780	GO:0016021
Contig4621	1122	0	4	6	3	2	2.01E-137	dispatched homolog 1	gi|118087850	GO:0016021
Contig1038	847	2	6	14	6	2.33	8.74E-46	eukaryotic translation initiation factor 4 2	gi|47230440	GO:0016281
Contig25996	518	0	1	6	1	6	2.31E-42	atg3 autophagy related 3 homolog (cerevisiae)	gi|41053345	GO:0016567
Contig19339	479	5	0	0	0	-	1.72E-12	myotubularin related protein 14	gi|189520682	GO:0016791
Contig26386	762	0	0	22	3	7.33	6.39E-47	atp-binding sub-family c (cftr mrp) member 5	gi|47226181	GO:0017111
CL3541Contig1	845	1	0	10	3	3.33	2.73E-79	arsenic (+3 oxidation state) methyltrans...	gi|47220315	GO:0018872
Contig10231	1114	2	5	8	1	8	8.07E-46	solute carrier family 23 (nucleobase transporters) member 2	gi|189546543	GO:0022891
Contig9911	471	0	3	4	1	4	3.25E-43	adp-ribosylation factor interacting protein 2b	gi|62955267	GO:0030036
CL6282Contig1	645	0	1	4	2	2	8.59E-113	eukaryotic translation initiation factor	gi|164498968	GO:0030154
Contig2165	715	0	0	5	2	2.5	1.60E-116	isoform cra_a	gi|47226311	GO:0030170
Contig2884	823	9	17	8	2	4	2.56E-41	stromal interaction molecule 1	gi|47227834	GO:0030176
Contig9264	327	5	0	0	0	-	5.76E-24	potassium inwardly-rectifying subfamily member 11	gi|89886327	GO:0030315
Contig10375	752	0	2	6	1	6	2.66E-94	atp-binding sub-family a member 1	gi|47212013	GO:0030349
Contig6147	877	6	0	2	0	-	2.92E-92	homolog 1 (coli)	gi|47214710	GO:0031167
Contig2197	785	1	0	4	1	4	1.42E-129	guanine nucleotide binding protein (g protein) alpha inhibitin	gi|169786808	GO:0031821
Contig6373	512	0	1	4	1	4	3.76E-48	phospholipase gamma 2	gi|47221900	GO:0032959
Contig1755	960	2	2	11	1	11	1.16E-105	transferrin receptor	gi|47227995	GO:0035162
Contig21216	804	1	4	4	1	4	5.87E-65	anion exchanger	gi|189525811	GO:0035162
Contig3283	1169	1	3	4	2	2	1.92E-70	tensin like c1 domain containing phosphatase (tensin 2)	gi|189535788	GO:0035264
CL7852Contig1	396	5	0	0	0	-	2.00E-51	enhancer of polycomb homolog 1	gi|47221116	GO:0040008
CL8236Contig1	470	0	0	5	0	-	5.36E-65	tripartite motif-containing 39	gi|47223678	GO:0042802
Contig2231	774	1	0	4	2	2	1.19E-39	dom-3 homolog z	gi|47218017	GO:0042802

Contig	length (bp)	MID2 Norm/ NP	MID3 Norm/ PP	MID4 Unnorm/ NP	MID5 Unnorm/ PP	Fold difference	evalue	Sequence description	GenBank Accession No.	annotation
CL2271Contig2	844	0	2	4	1	4	6.59E-53	supervillin	gi|189525875	GO:0043034
Contig3174	1310	0	3	7	2	3.5	2.51E-65	svil protein	gi|47225200	GO:0043229
Contig6187	881	1	3	8	4	2	4.52E-28	sterol regulatory element binding transcription factor 2	gi|47217021	GO:0043231
Contig2222	580	0	0	5	1	5	1.42E-48	ubiquitin carboxyl-terminal hydrolase l5	gi|47217741	GO:0043234
Contig7307	487	1	8	4	1	4	3.89E-20	nuclear receptor co-repressor 1	gi|158517898	GO:0043565
CL10Contig6	494	3	4	4	2	2	8.32E-29	novel protein	gi|160333557	GO:0044238
CL1Contig3822	583	0	5	58	29	2	5.71E-55	beta-actin	gi|109492380	GO:0044424
Contig26279	484	3	0	4	0	-	5.10E-28	phosphatidylinositol-5-phosphate 4- type alpha	gi|47223480	GO:0046488
CL7566Contig1	244	6	0	0	0	-	2.76E-16	neutral protease	gi|115373991	GO:0046872
Contig8488	608	6	15	10	2	5	9.34E-41	ring finger protein 183	gi|115497842	GO:0046872
Contig9943	993	0	5	17	6	2.83	9.42E-58	establishment of cohesion 1 homolog 1	gi|149411306	GO:0046872
Contig26649	883	1	4	34	10	3.4	7.32E-36	tumor necrosis factor receptor member 26	gi|28875517	GO:0046914
CL8625Contig1	280	5	0	0	0	-	7.18E-38	gdp dissociation inhibitor 1	gi|47229667	GO:0046933
Contig878	1274	3	5	17	4	4.25	2.44E-156	inositol -triphosphate 5 6 kinase	gi|189531088	GO:0047325
Contig566	347	6	0	0	0	-	1.81E-25	dedicator of cytokinesis 7	gi|158253447	GO:0048365
CL8649Contig1	385	2	0	3	0	-	2.24E-54	ring finger protein 14	gi|224613426	GO:0050681
Contig1136	989	6	10	19	6	3.17	4.22E-61	keratin 8	gi|39645432	GO:0050896
CL1Contig3952	524	0	0	5	2	2.5	2.48E-58	rna binding motif protein 47	gi|47209668	b2g inferred
CL1Contig4094	291	0	0	6	1	6	9E-09	lectin protein type i	gi|34013698	b2g inferred
CL1Contig4187	819	0	0	6	1	6	3.08E-24	protein	gi|60687936	b2g inferred
CL1Contig4262	734	0	0	6	1	6	1.38E-22	protein	gi|60687936	b2g inferred
CL1Contig4386	315	0	0	7	3	2.33	7.43E-14	zgc:158463 protein	gi|148357120	b2g inferred
CL1Contig4738	610	0	0	5	1	5	0.0002489	af095770_1pth-responsive osteosarcoma d1	gi|4588085	b2g inferred
CL1Contig5000	921	0	1	4	1	4	2.18E-11	chromosome 17 open reading frame 37	gi|152013691	b2g inferred
CL1Contig5135	479	0	0	4	1	4	2.39E-41	zgc:158463 protein	gi|68226711	b2g inferred
CL3253Contig1	650	0	0	4	2	2	1.49E-17	novel protein vertebrate elongation of v...	gi|115495643	b2g inferred
CL7161Contig1	868	0	0	6	0	-	2.07E-77	solute carrier family member 4	gi|47229374	b2g inferred

Contig	length (bp)	MID2 Norm/ NP	MID3 Norm/ PP	MID4 Unnorm/ NP	MID5 Unnorm/ PP	Fold difference	evalue	Sequence description	GenBank Accession No.	annotation
CL7887Contig1	502	0	1	4	1	4	3.36E-33	novel protein	gi|47224118	b2g inferred
CL7944Contig1	952	1	0	4	1	4	8.64E-39	ankyrin repeat domain 12	gi|220672679	b2g inferred
CL8149Contig1	252	5	0	0	0	-	0.0003143	novel protein vertebrate lps-responsive...	gi|220941667	b2g inferred
CL8277Contig1	458	1	0	4	0	-	7.265E-06	btb domain containing isoform cra_c	gi|119593510	b2g inferred
Contig1004	374	0	0	5	1	5	1.47E-22	zgc:158463 protein	gi|148357120	b2g inferred
Contig1017	443	0	0	5	0	-	7.24E-36	zgc:158463 protein	gi|16930529	b2g inferred
Contig1024	467	0	2	8	4	2	9.60E-19	kiaa1839 protein	gi|16930529	b2g inferred
Contig10241	480	2	3	4	1	4	7.01E-29	mgc80389 protein	gi|194332566	b2g inferred
Contig1068	345	0	0	20	5	4	0.0001034	lectin protein type i	gi|34013698	b2g inferred
Contig1085	549	0	1	6	1	6	1.88E-30	zgc:158463 protein	gi|68226711	b2g inferred
Contig1103	573	0	2	37	19	2	2.62E-07	rrna intron-encoded endonuclease	gi|47155411	b2g inferred
Contig1110	162	0	0	4	2	2	2.698E-05	zgc:158463 protein	gi|148357120	b2g inferred
Contig1175	735	0	0	4	2	2	1.35E-22	protein	gi|60687936	b2g inferred
Contig1188	433	1	0	4	2	2	2.11E-10	zgc:158463 protein	gi|90081018	b2g inferred
Contig1212	1155	0	1	32	15	2.13	1.10E-13	protein	gi|226453528	b2g inferred
Contig1892	948	0	2	5	2	2.5	1.50E-84	family with sequence similarity member h...	gi|113682418	b2g inferred
Contig20291	607	4	0	1	0	-	2.99E-19	lymphocyte antigen 75 precursor	gi|237769789	b2g inferred
Contig25915	465	0	0	4	1	4	4.184E-06	zgc:158463 protein	gi|148357120	b2g inferred
Contig26048	530	9	0	1	0	-	1.19E-11	chromosome 20 open reading frame 116	gi|224050323	b2g inferred
Contig26199	240	0	1	8	2	4	3.168E-06	cell wall glucanase	gi|156357429	b2g inferred
Contig26709	569	1	0	4	0	-	1.26E-06	leukocyte receptor cluster member 8	gi|148236347	b2g inferred
Contig3048	487	4	10	7	2	3.5	3.18E-30	kinesin-like protein	gi|47221202	b2g inferred
Contig4252	635	10	5	29	2	14.5	2.82E-22	nattectin precursor	gi|34013702	b2g inferred
Contig4547	257	5	0	0	0	-	7.187E-06	golgi-associated plant pathogenesis-related protein 1	gi|189519176	b2g inferred
Contig4959	362	4	0	1	0	-	1.415E-06	glutathione s-transferase theta-1	gi|68366260	b2g inferred
Contig594	344	1	0	5	1	5	4.659E-05	6-phosphofructo-2-kinase fructose- -biphosphatase 4	gi|213511877	b2g inferred
Contig6028	1048	1	2	7	1	7	9.89E-122	novel protein	gi|94733339	b2g inferred

Contig	length (bp)	MID2 Norm/ NP	MID3 Norm/ PP	MID4 Unnorm/ NP	MID5 Unnorm/ PP	Fold difference	evalue	Sequence description	GenBank Accession No.	annotation
Contig6384	462	2	0	3	0	-	4.78E-18	semaphorin 7a	gi|189542521	b2g inferred
Contig7051	546	3	8	10	1	10	2.28E-23	carcinoembryonic antigen-related cell adhesion molecule 1	gi|47213151	b2g inferred
Contig7624	507	7	0	0	0	-	2.56E-25	tpa_inf: twist3a	gi|156630558	b2g inferred
Contig7704	392	8	0	0	0	-	2.031E-05	zgc:172136 protein	gi|162287308	b2g inferred
Contig7778	416	6	0	0	0	-	4.08E-07	transcobalamin-2 precursor	gi|47226456	b2g inferred
Contig8426	580	1	0	6	3	2	2.17E-22	tpa: nadph oxidase organizer 1	gi|47218052	b2g inferred
Contig8913	1226	0	2	10	3	3.33	4.73E-111	sec16 homolog a (cerevisiae)	gi|47209224	b2g inferred
Contig9774	1106	3	8	69	20	3.45	3.09E-137	cg31028- isoform partial	gi|47207885	b2g inferred
Contig9777	792	1	1	11	3	3.67	7.75E-14	tumor necrosis factor receptor member 26	gi|28875517	b2g inferred

Additional file 2 88 annotated genes which are upregulated in pregnant brood pouch tissues and/or entirely absent from the non-pregnant pregnant brood pouch libraries.

Overview of annotated contigs absent from the non-pregnant brood pouch or more than two-fold upregulated in the pregnant brood pouch. Contigs are indicated together with their lengths in base pairs and the numbers of contributing reads from the normalized and unnormalized cDNA libraries. Norm= normalized cDNA library, Unnorm= unnormalized cDNA library. PP=pregnant brood pouch tissue, NP=non-pregnant brood pouch tissue. Fold difference reflects expression differences between the unnormalized non-pregnant and pregnant tissues. E-values and sequence descriptions are indicated for the top-blastx hit for each contig together with corresponding GenBank accession numbers. GO annotations are indicated wherever available and theremaining annotations were inferred by blast2go (b2g inferred).

Contig	length (bp)	MID2 Norm/NP	MID3 Norm/PP	MID4 Unnorm/ NP	MID5 Unnorm/ PP	Fold difference	evalue	Sequence description	GenBank Accession No.	annotation
CL1Contig3916	777	0	0	2	5	2.5	5.35E-34	keratin 8	gi|159155987	GO:0005198
CL1Contig4846	219	0	0	2	4	2	2.1E-08	zgc:158463 protein	gi|148357120	b2g inferred
CL1Contig4934	596	0	1	2	6	3	2.77E-28	senescence-associated protein	gi|118392259	GO:0008134
CL2922Contig1	445	0	4	0	1	-	2.99E-57	signal transducing adaptor molecule (sh3...	gi|148725569	GO:0005070
CL3319Contig1	372	0	14	0	2	-	2.73E-16	ctage member 5	gi|41053471	b2g inferred
CL3805Contig2	471	0	3	2	5	2.5	2.49E-46	bcl2 adenovirus e1b 19kda interacting pr	gi|47206353	GO:0008634
CL3960Contig1	344	0	7	0	0	-	8.39E-58	serine threonine kinase ste20 sps1 homol	gi|118093669	GO:0005737
CL5598Contig1	266	0	7	0	0	-	8.14E-13	unnamed protein product [Tetraodon nigro...	gi|47223103	GO:0004714
CL6455Contig1	351	0	6	0	1	-	3.38E-59	pre-mrna processing factor 8	gi|169646741	GO:0005682
CL6617Contig1	538	0	6	0	1	-	4.94E-44	mga protein	gi|5931585	GO:0030528
CL6755Contig1	278	0	6	0	0	-	3.23E-38	lipocalin-interacting membrane receptor	gi|38564425	GO:0016021
CL6784Contig1	549	0	3	0	4	-	6.90E-15	ahnak nucleoprotein isoform 1	gi|189525028	b2g inferred
CL6845Contig1	251	0	6	0	0	-	4.22E-22	riken cdna 1110020p15 variant 1	gi|229366812	GO:0005743
CL7033Contig1	486	0	4	0	1	-	7.07E-57	vesicle transport through interaction wi...	gi|118093013	GO:0005484

Contig	length (bp)	MID2 Norm/NP	MID3 Norm/PP	MID4 Unnorm/ NP	MID5 Unnorm/ PP	Fold difference	evalue	Sequence description	GenBank Accession No.	annotation
CL7521Contig1	299	0	6	0	0	-	5.40E-33	kit ligand	gi|159149094	GO:0016020
CL7760Contig1	327	0	5	0	0	-	2.78E-13	phosphatidic acid phosphatase type 2 dom...	gi|165971070	GO:0016787
CL8009Contig1	407	0	0	2	4	2	1.57E-32	zinc finger	gi|47221021	GO:0005488
CL8028Contig1	427	0	2	0	3	-	2.52E-62	phosphorylase kinase alpha 1	gi|189521695	GO:0005516
CL8211Contig1	462	0	5	0	0	-	1.04E-12	inositol -1(or 4)-monophosphatase 1	gi|62079620	GO:0004437
CL8459Contig1	263	0	5	0	0	-	4E-09	eef1a1 protein	gi|47122516	GO:0003746
CL8760Contig1	265	0	5	0	0	-	1.18E-11	ninein-like protein	gi|189527320	GO:0015630
CL8782Contig1	356	0	5	0	0	-	2.87E-26	caspase recruitment domain member 14	gi|125819589	GO:0001934
CL8982Contig1	434	0	4	0	1	-	4.95E-41	dynamin binding protein	gi|74002322	GO:0035023
CL9119Contig1	453	0	5	0	0	-	3.3E-08	unnamed protein product [Tetraodon nigro...	gi|47214857	GO:0005488
CL9197Contig1	787	0	3	0	2	-	2.63E-118	guanine nucleotide binding protein (g pr...	gi|47218963	GO:0004871
CL9269Contig1	348	0	5	0	0	-	2.80E-13	40s ribosomal protein s12	gi|14903288	GO:0003735
CL9568Contig1	766	0	4	0	1	-	1.73E-103	tyrosine 3-monooxygenase tryptophan 5-mo...	gi|148225538	GO:0001764
CL9588Contig1	313	0	5	0	0	-	1.78E-20	novel protein	gi|189516664	GO:0005488
Contig10181	505	0	6	0	5	-	1.06E-54	glyoxalase 1	gi|197631899	GO:0009438
Contig10416	424	0	0	0	6	-	4.5E-08	glycoprotein a repetitions predominant precursor	gi|47214662	b2g inferred
Contig10568	513	0	5	0	0	-	2.787E-06	gp25l2 [Homo sapiens]	gi|996057	b2g inferred
Contig1057	719	0	0	3	6	2	6.78E-18	protein	gi|60687936	GO:0043565
Contig10679	639	0	5	0	0	-	4.68E-25	novel protein vertebrate nipped-b homolog	gi|47181598	GO:0005634
Contig10686	489	0	5	0	0	-	4.12E-29	heat repeat containing 1	gi|47213370	GO:0005515
Contig10696	439	0	1	0	4	-	1.81E-33	xlfli protein	gi|126327441	GO:0004871
Contig1851	878	1	3	2	4	2	1.34E-81	rho gtpase activating protein 23	gi|189525879	b2g inferred
Contig1871	584	0	2	2	6	3	3.50E-59	tripartite motif-containing 16	gi|47217647	GO:0005737
Contig1916	261	0	11	0	0	-	2.712E-05	motor neuron and pancreas homeobox 1	gi|57770400	b2g inferred
Contig2059	520	0	1	1	6	6	8.48E-27	huntingtin interacting protein 1 related	gi|134133242	GO:0005856

Contig	length (bp)	MID2 Norm/NP	MID3 Norm/PP	MID4 Unnorm/ NP	MID5 Unnorm/ PP	Fold difference	evalue	Sequence description	GenBank Accession No.	annotation
Contig2104	545	0	6	0	0	-	2.18E-10	translocase of inner mitochondrial membrane 50 homolog	gi|45709908	GO:0006915
Contig21307	397	0	5	0	0	-	9.30E-36	type alpha 2	gi|47222238	GO:0005581
Contig2141	472	0	5	0	0	-	1.92E-19	zinc finger protein 512	gi|189535838	GO:0046872
Contig2192	437	0	4	0	2	-	1.04E-33	voltage-gated sodium channel	gi|123913391	GO:0005272
Contig22254	528	0	5	0	0	-	3.59E-60	mitogen-activated protein kinase 1	gi|126324784	GO:0050853
Contig22473	307	0	5	0	0	-	2E-08	glutamine synthetase	gi|25992551	GO:0004356
Contig2262	547	0	5	0	0	-	8.04E-45	ras and rab interactor 1	gi|68397693	GO:0044464
Contig22699	646	0	5	0	0	-	4.64E-90	xrcc6 binding protein 1	gi|209732478	GO:0006303
Contig2278	554	0	5	0	0	-	5.35E-44	microspherule protein 1	gi|47220687	GO:0005737
Contig22925	382	0	5	0	0	-	1.29E-19	centrosomal protein 290kda	gi|47220555	GO:0005829
Contig23174	473	0	4	0	1	-	1.78E-50	chromosome 1 open reading frame 58	gi|47222464	GO:0016020
Contig23737	661	0	5	0	0	-	6.59E-37	hiv-1 rev binding protein 2	gi|224094097	GO:0005732
Contig23773	405	0	7	0	0	-	3.173E-06	PREDICTED: similar to papilin [Acyrthosiphon pisum]	gi|193699971	b2g inferred
Contig2393	393	0	4	0	1	-	4.06E-17	beta-adrenergic receptor kinase 2	gi|197927112	GO:0047696
Contig24238	359	0	5	0	0	-	6E-09	secretory carrier membrane protein 1	gi|56797759	GO:0016021
Contig24249	556	0	5	0	0	-	1.10E-34	procollagen- 2-oxoglutarate 4-dioxygenase (proline 4-hydroxylase)	gi|109089334	GO:0005488
Contig24448	249	0	5	0	0	-	1.55E-13	thyroid hormone receptor associated protein complex component	gi|15020810	GO:0004872
Contig24646	476	0	3	0	2	-	1E-09	orphan 1	gi|51011003	b2g inferred
Contig25082	426	0	6	0	1	-	3.50E-29	centrin-1	gi|189540405	GO:0008026
Contig25216	461	0	2	0	3	-	1.83E-22	laminin isoform a	gi|47209921	b2g inferred
Contig25375	783	0	7	0	0	-	4.93E-39	envoplakin	gi|47214954	GO:0030154
Contig26975	411	0	0	0	5	-	2.32E-25	ring finger protein 38	gi|189514564	GO:0007286
Contig27102	487	0	0	1	4	4	5.82E-16	casein kinase delta	gi|224074484	GO:0009987
Contig27234	997	0	0	2	5	2.5	5.86E-18	senescence-associated protein	gi|13359451	b2g inferred

Contig	length (bp)	MID2 Norm/NP	MID3 Norm/PP	MID4 Unnorm/ NP	MID5 Unnorm/ PP	Fold difference	evalue	Sequence description	GenBank Accession No.	annotation
Contig2908	531	0	31	0	2	-	7.32E-16	ferric-chelate reductase 1	gi|189538290	b2g inferred
Contig3063	611	0	20	0	0	-	1.02E-10	dumpy cg33196-pb	gi|47228008	b2g inferred
Contig3482	558	0	6	0	0	-	7.63E-21	heterogeneous nuclear ribonucleoprotein h3	gi|148233462	GO:0008380
Contig3602	620	0	5	0	0	-	1.20E-54	agrin	gi|47222749	GO:0005604
Contig3664	508	0	4	0	1	-	2.66E-14	aryl hydrocarbon receptor 1b	gi|68299588	GO:0004871
Contig3733	354	0	7	0	0	-	7.04E-22	nuclear oncoprotein skia	gi|6048269	GO:0005488
Contig3753	256	0	5	0	0	-	5.49E-14	thyroid hormone receptor associated protein complex component	gi|15020810	GO:0004872
Contig3938	548	0	6	0	0	-	3.13E-37	slc9a3r2 protein	gi|189529308	GO:0065007
Contig3970	533	0	4	0	1	-	3.67E-23	bai1-associated protein 2-like 1	gi|62955633	GO:0003779
Contig4654	645	0	8	0	1	-	2.97E-22	zinc finger protein 598	gi|213624689	GO:0046872
Contig4797	588	0	8	0	1	-	3.57E-18	high choriolytic enzyme 1 precursor	gi|62122709	GO:0004222
Contig5124	425	0	4	0	1	-	3.62E-34	tuberous sclerosis 1	gi|47212214	GO:0032862
Contig6123	1141	0	4	2	6	3	2.41E-13	solute carrier family 39 (zinc transporter) member 6	gi|47199137	GO:0001837
Contig6149	492	0	5	0	0	-	8.89E-17	growth factor receptor-bound protein 7	gi|47217632	b2g inferred
Contig6199	857	1	1	1	5	5	2E-09	sterol regulatory element binding transcription factor 2	gi|47217021	GO:0030528
Contig6215	734	0	4	0	2	-	5.08E-14	laminin b2	gi|189515983	GO:0043256
Contig6242	269	0	7	0	0	-	1.57E-21	hyaluronoglucosaminidase 4	gi|189537618	GO:0006027
Contig6376	805	0	3	0	3	-	5.49E-103	protocadherin 15	gi|47223231	GO:0001750
Contig6618	751	0	13	0	1	-	1.94E-56	tripartite motif-containing 23	gi|47228454	GO:0008047
Contig7735	378	0	5	0	0	-	3.75E-51	myotubularin related protein 6	gi|47210742	GO:0005737
Contig7751	581	0	5	0	0	-	2.88E-25	dna helicase hel308	gi|189533893	GO:0005488
Contig7752	490	0	5	0	0	-	1.09E-30	all-1 related protein	gi|3540281	GO:0005488
Contig7948	498	0	5	0	0	-	6.89E-27	integrin beta	gi|47217145	GO:0005178
Contig8909	470	0	6	2	4	2	1.46E-51	insulin receptor b	gi|18150106	GO:0006468
Contig956	317	0	1	1	5	5	6.48E-15	calmodulin 2	gi|119577831	GO:0005829

ACKNOWLEDGEMENTS

I am very much indebted to the many that have helped me so much in the past few years. Without your help, support, supervision, care and "being-there" this thesis would never have been possible.

I cordially thank **Prof. Anthony B. Wilson** for thesis supervision and constant support throughout the past four years and my thesis committee members **Prof. Andreas Wagner** and **Prof. Tadeusz Kawecki** for very helpful suggestions and advice over the past years. Special thanks go to **Prof. Sebastian Bonnhoeffer**, who, with his pointed suggestion during the 2005 course of evolutionary biology in Guarda/Switzerland, gave me critical career incentives.

My very deep thanks go to **Sabine Marty** and **Rosemarie Keller-Gruber**. Being constantly helpful and always providing caring support for me and my wife, you made work in the Zoological Museum a pleasure. **Yves Choffat** provided great support from the IT (and coffee- ☺) ends of research, and **Thomas Bucher** helped with the sequencing duties – thanks a million for that!

Work and life in the laboratory would not have been the same without my dear colleagues. My deep thanks go to you (and note the alphabetical order!), **Alexandra Wegman, Angela Fechner, Beat Mattle, Iris Eigenmann, Jasmin Winkler, Lisa Palme, Marie-Emilie Gauthier, Morana Mihaljevic, Pascal Hablützel, Stephan Zehnder, Valeria Fiorella Rispoli** for all the great laughs we had, for the good times and the support when work was piling up. You made the difference!

With research projects ever growing in scale and difficulty, the present work would not have been possible without the help of great colleagues and friends. Thank you for putting up with me, for helping out when it was needed, and for the right suggestions to get projects sorted. My thanks go to **Dr. Christian Wüst, Dr. David Berger, Dr. Erik Postma, Prof. Gerrit Gort, Prof. Luc Bussiere, Prof. Lukas Keller, Marco Demont, Dr. Martin Schäfer, Dr. Peter Wandeler Dr. Stephanie Bauerfeind, Prof Wolf Blanckenhorn.** Of outstanding support were also **Dr. Marzanna Künzli, Dr. Ralph Schlapbach, Dr. Rémy Bruggmann, Dr. Sirisha Aluri** and **Dr. Weihong Qi** from the functional genomics centre in Zurich. Thanks a lot for all your support on the 454 sequencing and associated issues.

Without the right supervisors early on in my studies I would, very likely, not have chosen to follow the bumpy but satisfying road into evolutionary biology. It is due to **Prof. Tomas Hrbek** and **Prof. Izeni Farias** that I did, and I enjoy it a lot. And without **Prof. Michael Arnold** I would not be where I am - Thank you so much for all your support!

Special thanks for their kind friendship, their support and help are due to (almost) twelve fine young men: **Lukas Schreiber, Cedric Laghi, Daniel Wyss, Mehi Satgunarajah, Tobias Bhend, Travis Hood** and **Giuseppe Damiano.**

I would have never reached the place I am at now without my parents, **Ingrid** and **Dr. Siegfried Stölting**. Thank you so much for all you did!

My deepest thanks will as always go to my wife **Meline Nogueira Lucena Stölting**. Thank you for leaving everything behind and being here with me, for your deep care, kind support, your love and understanding.

Lastly, I wish to gratefully acknowledge financial support from the **Forschungskredit der Universität Zürich**, without which the present work would not have been possible.

CURRICULUM VITAE

Name	Stölting
Vorname	Kai Nikolas
Geburtsdatum	12. April1979
Heimatort	Bad Kreuznach/Deutschland

Ausbildung

1991-1998	Niedersächsisches Internatsgymnasium Bad Bederkesa (NIG)
1998	Abitur (Allgemeine Hochschulreife) am NIG
1998-1999	Wehrdienst
1999-2003	Biologiestudium an der Universtät Konstanz, Vertiefungskurse in Evolutionsbiologie, Neurobiologie, Limnologie, Fischökölogie
2003	Diplomprüfung :Tierphysiologie und Limnologie
2004	Diplomarbeit in Evolutionsbiologie bei Prof. Axel Meyer Titel: The Midas Cichlid Species Flock: Incipient Sympatric Speciation?
2005	Forschungsassistent Labor Prof. Axel Meyer, Konstanz
2006-2010	Dissertation am Zoologischen Museum der Universität Zürich unter der Leitung von Prof. Anthony B. Wilson Titel der Dissertation: Male Pregnancy in the Seahorse (*Hippocampus abdominalis*): Investigating the Genetic Regulation of a Complex Reproductive Trait

Publikationen

1. **Stölting KN**, Gort G, Wüst C, Wilson AB. 2009. Eukaryotic transcriptomics *in silico*: Optimizing cDNA-AFLP efficiency. *BMC Genomics*, 10, 565.
2. Bussiere LF, Hunt J, **Stölting KN**, Jennions MD, Brooks R (2008) - Mate choice for genetic quality when environments vary: suggestions for empirical progress. *Genetica*, 134(1), 69-78.
3. Michel C, Hicks BJ, **Stölting KN**, Clarke AC, Stevens MI, Tana R, Meyer A, van den Heuvel MR. 2008. Distinct migratory and non-migratory ecotypes of an endemic New Zealand eleotrid (*Gobiomorphus cotidianus*) - implications for incipient speciation in island freshwater fish species. *BMC Evolutionary Biology*, 8, Article 49.
4. Bleher H, **Stölting KN**, Salzburger W, Meyer A. 2007. Revision of the Genus *Symphysodon* Heckel, 1840 (Teleostei: Perciformes: Cichlidae) based on molecular and morphological characters. *Aqua* 12(4), 133-174.
5. **Stölting KN**, Wilson AB. 2007. Male pregnancy in seahorses and pipefish: Beyond the mammalian model. *BioEssays*, 29, 884-896.
6. Van den Heuvel M, Michel C, Stevens MI, Clarke AC, **Stölting KN**, Hicks BJ, Tremblay LA. 2007. Monitoring the effects of pulp and paper effluents is restricted in genetically distinct populations of common bully (*Gobiomorphus cotidianus*). *Environmental Science & Technology* 41 (7), 2602-2608.
7. Luo J, Lang M, Salzburger W, Siegel N, **Stölting KN**, Meyer A. 2006. A BAC library for the goldfish *Carassius auratus auratus* (Cyprinidae,

Cypriniformes). *Journal of Experimental Zoology B Mol. Dev. Evol*. 306(6), 567-574.

8. Barluenga M, **Stölting KN**, Salzburger W, Muschick M, Meyer A. 2006. Evolutionary biology: Evidence for sympatric speciation? (Reply). *Nature*, 444, E13.
9. Barluenga M*, **Stölting KN***, Salzburger W*, Muschick M, Meyer A. 2006. Sympatric speciation in Nicaraguan crater lake cichlid fish. *Nature* 439, 719-723.***equal contribution***
10. Hrbek T, **Stölting KN**, Bardacki F, Kücück F, Wildekamp RH, Meyer A. 2004. Plate tectonics and biogeographical patterns of the *Pseudophoxinus* (Pisces: Cypriniformes) species complex of central Anatolia, Turkey. *Molecular Phylogenetics and Evolution* 32, 297-308.
11. Hrbek T, Kücück F, Frickey T, **Stölting KN**, Wildekamp R and Meyer A. 2002. Molecular phylogeny and historical biogeography of the *Aphanius* (Pisces, Cyprinodontifomes) species complex of central Anatolia, Turkey. *Molecular Phylogenetics and Evolution* 25, 125-137.

Eingeworbene Fördermittel

1. Forschungskredit der Universität Zürich: ~90,000CHF
2. Internal Grants des Zoologischen Museums der Universität Zürich: 7,500CHF